Distribution Agreement

In presenting this thesis or dissertation as a partial fulfillment of the requirements for an advanced degree from Emory University, I hereby grant to Emory University and its agents the non-exclusive license to archive, make accessible, and display my thesis or dissertation in whole or in part in all forms of media, now or hereafter known, including display on the world wide web. I understand that I may select some access restrictions as part of the online submission of this thesis or dissertation. I retain all ownership rights to the copyright of the thesis or dissertation. I also retain the right to use in future works (such as articles or books) all or part of this thesis or dissertation.

Signature:

_____   _____

David Brandin Weir   Date

**Characterization of cell death in
Casp3-deficient Mouse Embryonic Fibroblasts**

By

David Brandin Weir
Doctor of Philosophy

Graduate Division of Biological and Biomedical Sciences
Cancer Biology

_____
Lawrence H. Boise, Ph.D.
Advisor

_____
Jing Chen, Ph.D.
Committee Member

_____
Andrew Kowalczyk, Ph.D.
Committee Member

_____
Adam Marcus, Ph.D.
Committee Member

_____
Shoichiro Ono, Ph.D.
Committee Member

Accepted:

_____
Kimberly Jacob Arriola, Ph.D., M.P.H.
Dean of the James T. Laney School of Graduate Studies

_____
Date

Characterization of cell death in
Casp3-deficient Mouse Embryonic Fibroblasts

By

David Brandin Weir
B.Sc., McGill University, 2005
M.A., Columbia University, 2008

Advisor: Lawrence H. Boise, Ph.D.

An abstract of
A dissertation submitted to the Faculty of the
James T. Laney School of Graduate Studies of Emory University in partial fulfillment of the
requirements for the degree of Doctor of Philosophy
in the Graduate Division of Biological and Biomedical Sciences
Cancer Biology
2022

Abstract

Caspases are required for the successful implementation of apoptosis. Nonetheless, when apoptosis is not possible, signals that normally trigger apoptosis are still capable of inducing cell death. Caspase-3 is an executioner caspase that is activated downstream of mitochondrial events in intrinsic apoptosis. However, previous work demonstrates that Casp3-deficient mouse embryonic fibroblasts (MEFs) are resistant to mitochondrial-mediated apoptosis and display a delay in the mitochondrial events of apoptosis, including Bax activation, mitochondrial outer membrane permeabilization (MOMP), and cytochrome c release. In the following chapters, we detail work demonstrating that caspase-3 regulates fibronectin secretion, and through this function influences cell morphology, adhesion, migration and the apoptotic threshold of the cell. Furthermore, we show that in the absence of fibronectin, serum withdrawal-induced death occurs by a caspase-independent mechanism. We go on to show that death in this circumstance is autophagy-dependent, and that ablating the cells ability to undergo autophagy results in a blockade of cell death. Taken together our data indicate that Casp3-deficient MEFs are incapable of executing apoptosis triggered by serum withdrawal and are protected from autophagy-dependent death by fibronectin-mediated adhesion. The implications of our research to the cell death field, and consequently diseases involving aberrant cell death, such as cancer, may prove significant. Our work is the first to link autophagy-dependent death to fibronectin adhesion.

Characterization of cell death in
Casp3-deficient Mouse Embryonic Fibroblasts

By

David Brandin Weir
B.Sc., McGill University, 2005
M.A., Columbia University, 2008

Advisor: Lawrence H. Boise, Ph.D.

A dissertation submitted to the Faculty of the
James T. Laney School of Graduate Studies of Emory University in partial fulfillment of the
requirements for the degree of Doctor of Philosophy
in the Graduate Division of Biological and Biomedical Sciences
Cancer Biology
2022

TABLE OF CONTENTS

LIST OF FIGURES

I. Introduction

A. Cell Death

Naturally occurring cell death was first described by Karl Vogt in 1842, when he reported that the notochord and adjacent cartilage of the midwife toad is eliminated by cell death during metamorphosis, thereby facilitating the genesis and development of vertebrae (Clarke and Clarke, 1996;Fuchs and Steller, 2015;Tang et al., 2019). Over 100 papers involving cell death were published in the 19th century, with landmark studies focused on insects, amphibians, fish and mammals (Clarke and Clarke, 1996). Study of cell death continued intensely in the first half of the 20th century. However, for over a century, cell death was thought to be a passive and inevitable phenomenon (Fuchs and Steller, 2015;Galluzzi et al., 2018). This perspective began to shift with a number of studies in the 1960s that indicated cell death during development is genetically "programmed" (Lockshin and Williams, 1964;Saunders, 1966;Tata, 1966;Lockshin, 1969). In 1972, Kerr, Wyllie and Currie published a seminal paper in which they coined the term 'apoptosis' (from the Greek for "falling off"; referring to leaves in Autumn). to described an active, inherently programmed form of cell death involving breakdown of cells into membrane bound apoptotic bodies, under both physiological and pathological conditions (Kerr et al., 1972), in contrast to necrosis, in which cells swell, rupture and die due to overwhelming stress or injury die by (Fuchs and Steller, 2011). This paper led to an explosion of cell death research, and accordingly, our knowledge of cell death has expanded dramatically and become infinitely more detailed (Danial and Korsmeyer, 2004;Fuchs and Steller, 2011;2015;Green and Llambi, 2015;Galluzzi et al., 2018;Tang et al., 2019). Currently, more than a dozen subroutines of cell death are recognized (Galluzzi et al., 2018;Tang et al., 2019). These include intrinsic apoptosis, extrinsic apoptosis, autophagy-dependent cell death (ADCD), necroptosis, ferroptosis, pyroptosis, parthanatos,

mitochondiral permeability transition (MPT)-driven necrosis, entotic cell death, NETotic cell death, lysosomal-dependent cell death (LDCD), immunogenic cell death (ICD), oxeiptosis, and alkaliptosis (Galluzzi et al., 2018;Tang et al., 2019). For the purposes of this dissertation, I will focus on intrinsic apoptosis and autophagy-dependent death.

B. Intrinsic Apoptosis

Apoptosis is the most widely known and well-studied form of cell death (Yuan et al., 1993;Xue et al., 1996;Zou et al., 1997;Earnshaw et al., 1999;Creagh and Martin, 2001;Wei et al., 2001;Danial and Korsmeyer, 2004;Jiang and Wang, 2004;Bao and Shi, 2007;Kumar, 2007;Riedl and Salvesen, 2007;Li and Yuan, 2008;Taylor et al., 2008;Youle and Strasser, 2008;Chipuk et al., 2010;Green and Llambi, 2015;Shalini et al., 2015;Kalkavan and Green, 2018). It is crucial to development and tissue homeostasis, while its dysregulation underlies various pathologies, most notably tumorigenesis (Hanahan and Weinberg, 2011;Elliott and Ravichandran, 2016;Singh et al., 2019). Apoptosis is morphologically characterized by cellular shrinkage, nuclear condensation, DNA fragmentation, and disintegration of the cell into well-preserved membrane-bound structures termed apoptotic bodies, which are subsequently cleared by phagocytic cells (Kerr et al., 1972;Wyllie, 1980;Elliott and Ravichandran, 2016). In contrast, cells that die by necrosis swell, rupture and leak cellular contents, causing inflammation (Fink and Cookson, 2005;Nirmala and Lopus, 2020).

Mutagenic studies in *Caenorhabditis elegans* by Horvitz and colleagues defined much of the core machinery of apoptosis (Ellis and Horvitz, 1986;Hengartner et al., 1992;Yuan and Horvitz, 1992;Yuan et al., 1993). Strikingly, the proteins involved and the central pathway itself are conserved from *C. elegans* to mammals (Ellis and Horvitz, 1986;Yuan et al., 1993;Hengartner

and Horvitz, 1994;Xue et al., 1996;Lamkanfi et al., 2002;Green and Llambi, 2015). *Drosophila melanogaster* and mammalian systems are more complex than that of *C. elegans* (Lamkanfi et al., 2002;Kumar, 2007;Fuchs and Steller, 2015). Egl-1 is similar to proapoptotic BH3-only proteins in mammalian cell, CED-9 is a multidomain Bcl-2 family member, CED-4 is a homolog of APAF-1, CED-3 is an apoptotic caspase orthologue (Hengartner, 2000;Fuchs and Steller, 2011).

Apoptosis consists of two subtypes, extrinsic and intrinsic apoptosis, which are mediated by cell surface receptors and mitochondria, respectively (Danial and Korsmeyer, 2004;Elmore, 2007;Tang et al., 2019). Both extrinsic and intrinsic apoptosis ultimately result in activation of executioner caspases (*C*ysteine-dependent *ASP*artate-specific prote*ASES*), which complete apoptosis (Creagh and Martin, 2001;Elmore, 2007;Taylor et al., 2008). Intrinsic apoptosis can be triggered by a number of different cell-intrinsic death signals, including growth factor deprivation, DNA damage, and endoplasmic reticulum (ER) stress (Cornelis et al., 2005;Roos et al., 2016;Pihán et al., 2017). Upon a death signal, proteins of the Bcl-2 family coordinate the formation of pores in the mitochondrial outer membrane, culminating in mitochondrial outer membrane permeabilization (MOMP) (Fig. 1) (Chipuk et al., 2010;Czabotar et al., 2014). The Bcl-2 protein family consists of proapoptotic (e.g., Bax, Bak, Bad, and Bid) and antiapoptotic (e.g., Bcl-2, Bcl-X_L, and Mcl-1) members, which regulate MOMP via complex interactions (Chipuk et al., 2010;Kale et al., 2018). Ultimately, Bax and Bak oligomerize and are inserted into the mitochondrial outer membrane causing the release of mitochondrial contents, including cytochrome *c* (Korsmeyer et al., 2000;Kuwana et al., 2005;Tait and Green, 2010). Cytochrome *c* is a hemeprotein localized to the mitochondrial intermembrane space (until MOMP occurs), which plays crucial roles in apoptosis and the electron transport chain. Upon release into the cytosol, cytochrome *c* enables formation of the apoptosome, a sophisticated oligomeric signaling platform

consisting of several molecules each of cytochrome *c*, apoptotic protease-activating factor 1 (APAF-1) and the initiator caspase procaspase-9 (Li et al., 1997;Bao and Shi, 2007;Riedl and Salvesen, 2007;Dorstyn et al., 2018). Upon recruitment to the apoptosome, inactive monomeric procaspase-9 molecules dimerize and become activated (Renatus et al., 2001;Boatright et al., 2003;Pop et al., 2006). Importantly, cleavage is not required for the activation of procaspase-9 (Rodriguez and Lazebnik, 1999;Stennicke et al., 1999). Consequently, procaspase-9 activation is reversible, and thereby circumvents adventitious activation (Riedl and Salvesen, 2007). Once activated, procaspase-9 cleaves the zymogens procaspase-3 and procaspase-7, giving rise to the active executioners caspase-3 and caspase-7 (Li et al., 1997;Zou et al., 1997;Srinivasula et al., 1998;Boatright et al., 2003). In contrast to initiator caspases such as procaspase-9, executioner caspases such as caspase-3 and caspase-7 exist as dimers both in their latent forms and catalytically active forms, and are activated by irreversible cleavage (Earnshaw et al., 1999;Riedl and Salvesen, 2007). An executioner caspase typically undergoes two cleavage events, one leading to the release of a short N-terminal prodomain, the other separating the large and small subunits, thereby activating the enzyme (Earnshaw et al., 1999;Fuentes-Prior and Salvesen, 2004). Catalytically active caspase-3 and caspase-7 proceed to dismantle the cell from within via selective proteolysis of hundreds of proteins (Creagh and Martin, 2001;Kumar, 2007;Luthi and Martin, 2007;Dix et al., 2008;Mahrus et al., 2008;McIlwain et al., 2015).
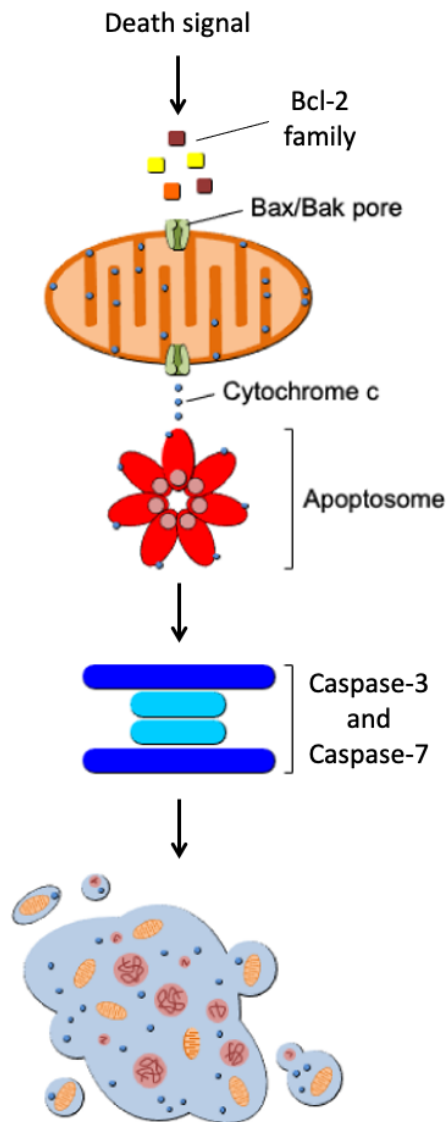
Figure 1. Intrinsic apoptosis. Cell-intrinsic death signals, such as growth factor deprivation, trigger proteins of the Bcl-2 family to coordinate the formation of Bax/Bak pores in the mitochondrial outer membrane. This results in mitochondrial outer membrane permeabilization (MOMP), causing the release of mitochondrial contents, including cytochrome c, which enables formation of the apoptosome, a sophisticated oligomeric signaling platform consisting of several molecules each of cytochrome c, apoptotic protease-activating factor 1 (APAF-1) and the initiator caspase procaspase-9. Upon recruitment to the apoptosome, inactive monomeric procaspase-9 molecules dimerize and become activated. Activated procaspase-9 cleaves the zymogens procaspase-3 and procaspase-7, giving rise to the active executioners caspase-3 and caspase-7 which degrade the cell through proteolysis of hundreds of target proteins.

C. Caspases

Caspases are a highly conserved family of proteases that are inextricably linked to apoptosis in all metazoans (Earnshaw et al., 1999;Creagh and Martin, 2001;Kumar, 2007;Li and Yuan, 2008;Shalini et al., 2015;Julien and Wells, 2017). Caspases are best known for their functions in cell death and inflammation (Tang et al., 2019;Van Opdenbosch and Lamkanfi, 2019;Kesavardhana et al., 2020). The founding member of the caspase family, caspase-1, was initially identified as interleukin-1β-converting enzyme (ICE), the human protease responsible for activating the precursor of interleukin-1β (Cerretti et al., 1992;Thornberry et al., 1992). In 1993, the first study to suggest caspases function in cell death was published (Yuan et al., 1993). In this seminal paper, the protein encoded by the *C. elegans* "cell death gene" CED-3 was cloned and demonstrated to be similar to ICE (Yuan et al., 1993). At least a dozen caspases have been identified in both humans and mice (McIlwain et al., 2015;Van Opdenbosch and Lamkanfi, 2019). Based on functionality and domain architecture, three classes of caspases exist, namely initiator (or apical) apoptotic caspases, executioner (or effector) apoptotic caspases, and inflammatory caspases (Kumar, 2007;Salvesen and Ashkenazi, 2011;McIlwain et al., 2015;Van Opdenbosch and Lamkanfi, 2019). In mice and humans, the initiators are caspase-8, -9, and -10, while the executioners are caspase-3, -6, and -7 (Kumar, 2007;Salvesen and Ashkenazi, 2011;McIlwain et al., 2015;Van Opdenbosch and Lamkanfi, 2019). The latent or zymogen forms of initiator caspases are monomeric, whereas those of effector caspases are dimeric (Salvesen and Ashkenazi, 2011;McIlwain et al., 2015). The active forms of both initiators and executioners are obligate dimers (Degterev et al., 2003;Fuentes-Prior and Salvesen, 2004). However, while initiator caspases require only dimerization to become active, executioner caspases require dimerization as well as cleavage by initiator caspases (Riedl and Salvesen, 2007;Julien and Wells, 2017).

A plethora of evidence indicates that caspases also have numerous critical non-apoptotic, non-inflammatory functions in various contexts, including roles in adhesion, migration, autophagy, tumorigenesis, metastasis, necroptosis, signaling, cell proliferation and tissue regeneration, cell-fate determination and differentiation, neuronal development and plasticity, axon pruning, and progressing neurological disease (Fujita et al., 2008;Janzen et al., 2008;Li and Yuan, 2008;Yi and Yuan, 2009;D'Amelio et al., 2010;Shalini et al., 2015;Unsain and Barker, 2015;Aram et al., 2017;Mukherjee and Williams, 2017;Tsapras and Nezis, 2017). In fact, the term 'caspase-dependent non-lethal cellular processes' or CDPs was recently coined by Aram, Yacobi-Sharon and Arama, to generally refer to nonapoptotic functions of caspases (Aram et al., 2017). Published in 2003, the first paper to show a non-apoptotic caspase function demonstrated that caspase activity and is required for sperm differentiation in *D. melanogaster* (Arama et al., 2003). Furthermore, caspase-8 has been shown to be required for maintained expression of the integrin subunit α5, which is essential for adhesion and migration of proangiogenic endothelial progenitor cells (Scharner et al., 2009). Additionally, in the eye, the enucleation process that epithelial cells undergo during their differentiation into a lens fiber cell is dependent upon caspase-3 activity (Ishizaki et al., 1998). A number of non-apoptotic functions of caspases do not require the catalytic activity of the enzyme (Cheng et al., 2008;Brentnall et al., 2014;Kamber Kaya et al., 2017). For example, active caspase-1 has been shown to regulate unconventional protein secretion, including that of IL-1α, FGF-2 and caspase-1 itself. Interestingly, neither IL-1α nor FGF-2 is a substrate of caspase-1. Instead, caspase-1 physically interacts with both proteins, suggesting a role as a carrier in an ER/Golgi-independent protein secretion pathway (Keller et al., 2008). Additonally, in neuroblastoma, caspase-8 forms a protein complex with Src, and thereby promotes a Src-dependent adhesion phenotype and subsequent activation of the Erk signaling pathway, regardless

of proteolytic activity (Finlay and Vuori, 2007). Caspase-8 also has a non-apoptotic, non-enzymatic role as a scaffold protein for the assembly of a pro-inflammatory "FADDosome" complex that forms upon TRAIL stimulation (Henry and Martin, 2017). Furthermore, hematopoietic stem cell responsiveness to inflammatory cytokines is limited by caspase-3 independently of proteolytic activity (Janzen et al., 2008). Importantly, several non-apoptotic, non-enzymatic functions are performed not by a mature caspase, but by a zymogen procaspase. In dopaminergic neurons, procaspase-3 acts as a regulator of mitochondria biogenesis via TFAM, Nrf-1, and PGC-1a (transcriptional activators of mitochondrial biogenesis) without affecting autophagy (Kim et al., 2018). Furthermore, in the same study, the authors show that lack of procaspase-3 in dopaminergic neurons dramatically reduced electron transport chain complex I, II, and IV activity. Treatment with caspase-3 inhibitor failed to mimic the observed effects, suggesting that caspase-3-dependent mitochondrial biogenesis is independent of its catalytic activity. Procaspase-3 was recently shown to regulate mitochondrial biogenesis activators Tfam and Nrf-1 (Kim et al., 2018). Additionally, it has been demonstrated in fibrosarcoma cells, that when an interaction between procaspase-8 and Src is disrupted, Src activates ERK and JNK and autophagic cell death occurs (Chen et al., 2011). It has been suggested that caspase-1 plays a role in cytoprotective autophagy during hypoxia-induced mitochondrial stress (Sun et al., 2013).

D. Caspase-3

Caspase-3 is activated by caspase-8 or caspase-9, in extrinsic and intrinsic apoptosis, respectively (Kumar, 2007;McIlwain et al., 2015;Tang et al., 2019). During apoptosis, activated caspase-3 cleaves hundreds of specific protein targets, which vary greatly in their functionality (Luthi and Martin, 2007;Dix et al., 2008;Mahrus et al., 2008). For example, it activates caspase-

activated deoxyribonuclease (CAD) through cleavage of its inhibitor (ICAD), which leads to DNA fragmentation characteristic of apoptosis (Enari et al., 1998). Caspase-3 further promotes DNA fragmentation by cleaving poly (ADP-ribose) polymerase (PARP), which is crucial to DNA repair (Nicholson et al., 1995;Tewari et al., 1995;Le Rhun et al., 1998). Caspase-3 also cleaves caspase-9 as part of a feedback mechanism which propagates the caspase activation cascade (Srinivasula et al., 1998;Slee et al., 1999;Walsh et al., 2008). Also, during apoptosis, caspase-3 impacts cell morphology through cleavage of the cytoskeletal protein α-fodrin, the actin-modulating protein gelsolin, and the cytoskeleton regulator Rho-associated protein kinase/ROCK I (Kothakota et al., 1997;Jänicke et al., 1998;Sebbagh et al., 2001). Caspase-3 has been shown to be important in the autophagy pathway, as well, specifically through cleavage of beclin-1 (Cho et al., 2009).

E. Caspase-3 in Cancer

Dysregulation of apoptosis underlies tumorigenesis (Hanahan and Weinberg, 2011). Not surprisingly, defective caspase activation that culminates in insufficient cell death can promote tumorigenesis (McIlwain et al., 2015). Although caspases have crucial functions in cell death, unlike mutations of p53 or members of the PI3K pathway, mutation of CASP genes is not common in cancer (McIlwain et al., 2015).

F. Autophagy

Christian de Duve coined the term autophagy from the Greek for "self-eating" in 1963 (Klionsky, 2008). Three types of autophagy have been described: macroautophagy, microautophagy, and chaperone-mediated autophagy with all three culminating in lysosomal degradation of cellular constituents (Uttenweiler and Mayer, 2008;Kaushik and Cuervo, 2012;Noda and Inagaki, 2015).

Macroautophagy is a highly coordinated pathway that entails sequestration of cytoplasmic components of the cell, such as macromolecules and organelles, through formation of double-membraned autophagosomes, which subsequently fuse with lysosomes to generate autolysosomes capable of degrading cellular cargo (Klionsky and Emr, 2000;Galluzzi et al., 2017a). In contrast, microautophagy does not involve autophagosomes, instead lysosomes directly engulf autophagic cargo for degradation (Uttenweiler and Mayer, 2008;Schuck, 2020). Chaperone-mediated autophagy involves selective degradation of certain proteins, delivered to the lysosome by chaperones and internalized via receptors (Kaushik and Cuervo, 2018). It should be noted that both macroautophagy and microautophagy are capable of cargo selectivity, as well (Sahu et al., 2011;Stolz et al., 2014). Macroautophagy (hereafter referred to as 'autophagy') is conserved in all eukaryotes, is performed at basal levels by virtually all cell types, and is increased by various intracellular and extracellular stimuli (Levine and Kroemer, 2019). Autophagy is essential to cellular homeostasis, and is a crucial prosurvival mechanism under various conditions of stress, including both nutrient and growth factor withdrawal (Levine and Kroemer, 2008;Mizushima and Komatsu, 2011;Levine and Kroemer, 2019). Autophagy promotes cell survival by providing energy and macromolecular precursors through recycling of cellular components such as protein aggregates and damaged mitochondria (Mizushima and Komatsu, 2011;Galluzzi et al., 2017a;Levine and Kroemer, 2019).

Autophagy is best understood in the context of nutrient starvation (Kroemer et al., 2010;Mizushima and Komatsu, 2011). The autophagy pathway can be viewed as a five-step process: (1) initiation, (2) phagophore nucleation, (3) phagophore expansion, (4) autophagosome-lysosome fusion, and (5) lysosomal substrate degradation (Galluzzi et al., 2017b;Galluzzi and Green, 2019). Nonspecific autophagy is inhibited by nutrient-rich conditions (Klionsky and Emr,

2000). The process is initiated by nutrient-sensing mechanisms, for example, when energy in the form of ATP becomes limiting, AMP kinase (AMPK) becomes activated and induces autophagy (Green and Levine, 2014). Similarly, growth factor or amino acid starvation causes inhibition of the mammalian target of rapamycin (mTOR) complex 1 (mTORC1), which, under nutrient-rich conditions, exerts a negative regulatory effect on autophagy via interaction with Unc-51-like kinase 1/2 (ULK1/2) (Klionsky and Emr, 2000;Kroemer et al., 2010;Green and Levine, 2014). ULK1/2 also regulates the lipid kinase activity of the Beclin 1/class III phosphatidylinositol 3-kinase (PI3K) complex, which is required for autophagy (Kroemer et al., 2010). Induction of autophagy leads to the formation of an isolation membrane also known as a phagophore (Kroemer et al., 2010;Galluzzi et al., 2017b). The phagophore can be generated from multiple sources, including the endoplasmic reticulum (ER) (Axe et al., 2008), the mitochondrial outer membrane (Hailey et al., 2010), and the plasma membrane (Ravikumar et al., 2010). Two ubiquitin-like conjugation systems participate in phagophore elongation (Kroemer et al., 2010). The first pathway involves the conjugation of Autophagy related 12 (Atg12) to Atg5, facilitated by the E1-like enzyme Atg7 and E2-like enzyme Atg10 (Kroemer et al., 2010). Atg12-Atg5 then noncolvalently binds Atg16, and this complex enhances the Atg3-mediated conjugation of phosphotidylethanolamine (PE) to microtubule associated protein light chain 3 (LC3). This conjugation converts the un-lipidated form of the protein, known as LC3-I, to its lipidated form (LC3-II), which subsequently enters pre-autophagosomal and autophagosomal membranes (Kabeya et al., 2000;Kabeya et al., 2004). LC3, particularly the LC3B isoform, is commonly employed to monitor autophagy (Mizushima, 2007;Klionsky et al., 2016). LC3B-II is localized to the interior membrane of the mature autophagosome, and subsequently the autolysosome, where it degraded in the same fashion as other protein cargo.

The Autophagy Related 5 (ATG5) gene is required for canonical macroautophagy. Specifically, it is essential to the phagophore expansion stage of autophagosome formation (Klionsky 2016B). A protein complex containing ATG5 is responsible for conjugation of LC3B-I to PE, thereby generating LC3B-II (Otomo et al., 2013). LC3B-II can be elevated by increased autophagy or by decreased degradation. In the later stages of autophagy, the autophagosome fuses with the lysosome forming the autolysosome. Thus, in the newly formed autolysosome, the cargo of the autophagosome, including LC3B-II, is introduced into the acidic environment contributed by the lysosome. In the autolysosome, pH-dependent proteases, including cathepsins, are optimally active and protein degradation, including that of LC3B-II, takes place (Takahashi, Yamashima).

G. Autophagy-dependent Cell Death

Historically, three types of morphologically-defined cell death have been described: Type I (apoptosis), Type 2 (autophagic cell death), and Type 3 (necrosis) (Fuchs and Steller, 2015). Autophagy was first proposed to be cell killing mechanism in 1990 (Clarke, 1990). Whether autophagy directly causes cell death, as opposed to merely accompanying it, has been controversial for quite some time (Debnath et al., 2005;Liu and Levine, 2015). However, more recently, a causative role of autophagy in cell death has been defined in a number of distinct circumstances (Liu and Levine, 2015;Galluzzi et al., 2018).

Autophagy maintains cellular homeostasis through removal of unnecessary or dysfunctional cellular components, such as damaged organelles and protein aggregates (Klionsky, 2008). Under conditions of stress, such as nutrient or growth factor deprivation, for example, autophagy serves as a cytoprotective mechanism providing energy and biosynethetic precursors to cells (Komatsu et al., 2006;Colell et al., 2007;Kroemer et al., 2010;Sun et al., 2013). However, it

can result in autophagy-dependent cell death under certain circumstances (Liu et al., 2013;Liu and Levine, 2015;Bialik and Dasari, 2018;Galluzzi et al., 2018;Denton and Kumar, 2019;Nassour et al., 2019;Tang et al., 2019). Autophagy has been shown to cause cell death when apoptosis is not possible, such as growth factor withdrawal (Lum et al., 2005) or etoposide- and staurosporine-treatment in Bax-/-Bak-/- mouse embryonic fibroblasts (Shimizu et al., 2004;Shimizu et al., 2010), or caspase inhibition in murine fibroblasts (Yu et al., 2004;Yu et al., 2006). There is also a form of non-apoptotic autophagy-dependent death termed autosis, which depends on the cellular NA^+,K^+-ATPase (Liu et al., 2013). Additionally, autophagy can degrade prosurvival proteins related to other types of cell death (Gump et al., 2014;He et al., 2014;Gao et al., 2016;Hou et al., 2016). For example, ferritinophagy, the autophagic degradation of ferritin, promotes ferroptosis (Gao et al., 2016;Hou et al., 2016).

Autophagic degradation of protein tyrosine phosphatase, non-receptor type 13 (PTPN13, also known as FAP1) favors FAS-driven extrinsic apoptosis (Gump et al., 2014). Autophagic degradation of baculoregulator repeat containing 2 (BIRC2, also known as cIAP1) promotes necroptosis (He et al., 2014).

H. Apoptosis and Autophagy

Apoptosis and autophagy have a complex relationship (Maiuri et al., 2007). The two pathways can be triggered by the same stimuli, and even share molecular components(Maiuri et al., 2007;Eisenberg-Lerner et al., 2009). Apoptosis and autophagy are capable of interacting in several distinct ways, with autophagy usually working as a prosurvival response, but sometimes functioning as a cell death mechanism. They can work in collaboration as well as in opposition to one another. Additionally, although autophagy most often serves as a cytoprotective process, it

can also function as a killing mechanism under certain conditions, including when a cell is incapable of performing apoptosis.

I. Statement of Problem

Knowledge of the molecular mechanisms underlying apoptosis has provided crucial insights into the causes of multiple diseases where aberrant cell death regulation occurs, and has revealed new approaches for identifying small drugs for more effectively treating these illnesses (Reed and Tomaselli, 2000). Similarly, a more complete knowledge of the molecular mechanisms underlying autophagy-dependent death will provide insight into diseases involving this type of cell death and corresponding therapies.

Autophagy and apoptosis share a complex relationship that involves extensive cross talk between the two pathways. The two pathways share many of the same upstream triggers, molecular components and regulatory genes. For example, members of the Bcl-2, ATG, and caspase protein family play roles in both autophagy and apoptosis (Shimizu et al., 2004;Luo and Rubinsztein, 2007;Cho et al., 2009;Gross and Katz, 2017). Perturbations of one pathway can have major effects on the other, as well cell fate. They can work in concert with one another, or the two can be diametrically opposed. Autophagy most often functions as a cytoprotective mechanism, however it can also lead to cell death under certain conditions, including when apoptosis is defective. Bax/Bak-deficient MEFs have been found to undergo a non-apoptotic cell death program that is dependent upon autophagic proteins when treated with etoposide (Shimizu et al., 2004). Additionally, bone marrow-derived IL-3-dependent Bax/Bak-deficient mouse cells were shown to activate autophagy and ultimately succumb to cell death, when withdrawn from IL-3 (Lum et al., 2005). Furthermore, zVAD was demonstrated to induce autophagic cell death in L929 cells when

caspase-8 expression was decreased (Yu et al., 2004). However, several gaps in the field remain. Importantly, no work has been done linking autophagy-dependent death to cell adhesion.

In the following chapters, we detail work demonstrating a newly discovered link between autophagy-dependent death and cell adhesion. Specifically, we show that knockdown of fibronectin blocks the ability of Casp3-deficient MEFs to spread in one hour. Having shown this, the adhesion-dependent survival advantage of Casp3-deficient MEFs and that Casp3-deficient MEFs secrete higher amounts of fibronectin, we then went on to demonstrate that fibronectin is required for the survival of Casp3-deficient MEFs following serum withdrawal. Furthermore, in the absence of fibronectin, serum withdrawal results in caspase-independent cell death in Casp3-deficient MEFs. Additionally, cytochrome c release is independent of serum-withdrawal-induced death in Casp3-deficient MEFs. Bcl-X_L blocks both cytochrome c release and death. Crucially, we show that autophagy is increased by serum withdrawal in Casp3-deficient MEFs when FN is silenced. Perhaps most importantly, we demonstrate that ablation of ATG5 expression blocks serum withdrawal-induced death in Casp3-deficient MEFs. These findings shed light on a link between adhesion and autophagy-dependent death, specifically the importance of fibronectin in this arena.

II. Procaspase-3 regulates fibronectin secretion and influences adhesion, migration and survival independent of catalytic function

Matthew Brentnall[1,2], David B. Weir[3], Anthony Rongvaux[4], Adam I. Marcus[1], and Lawrence H. Boise[1]

[1]Departments of Hematology and Medical Oncology and Cell Biology, Winship Cancer Institute of Emory University, Atlanta, GA, [2]Sheila and David Fuente Graduate Program in Cancer Biology, University of Miami Miller School of Medicine, Miami, FL, [3]Cancer Biology Graduate Program, Emory University, Atlanta, GA, [4]Department of Immunobiology, Yale School of Medicine, New Haven, CT

Originally published in Journal of Cell Science, 2014.

My contribution to the manuscript was figure 6 panel E.

Summary:

Caspase-3 is an effector caspase that is activated downstream of mitochondrial outer membrane permeabilization (MOMP) during apoptosis. However, previous work demonstrates that caspase-3-deficient MEFs are resistant to mitochondrial-mediated cell death and display a delay in the mitochondrial events of apoptosis including Bax activation, MOMP and release of cytochrome c. Here we show that caspase-3 regulates fibronectin secretion and impacts cell morphology, adhesion and migration. Surprisingly, the catalytic activity of caspase-3 is not required for these non-apoptotic functions. Moreover, we found that caspase-3-deficient MEFs are not resistant to death induced by anoikis and exogenous fibronectin protects WT MEFs from serum withdrawal-induced cell death. Together, our data indicate that procaspase-3 has a non-apoptotic function, which regulates the secretion of fibronectin and influences morphology, adhesion and migration. Furthermore, this novel procaspase-3 function may alter the apoptotic threshold of the cell.

Introduction:

During stimulation of intrinsic apoptosis, BH3-only proteins regulate the activation of Bax and Bak, which causes mitochondrial outer membrane permeabilization (MOMP) and the release of cytochrome c. This results in the formation of the apoptosome, caspase-9 activation and subsequent activation of effector caspases, including caspase-3 (Danial and Korsmeyer, 2004). The role of these effector caspases during the degradation phase of apoptosis is well characterized and includes activation of DNA fragmentation, cell shrinkage and membrane blebbing (Woo et al., 1998;Shi, 2002). However, previous work shows that caspase-3-deficient MEFs display a delay in the mitochondrial events of intrinsic apoptosis, including Bax activation, MOMP and cytochrome c release, which are thought to occur upstream of caspase-3 activation (Lakhani et al., 2006). These data suggest that caspase-3 either feeds back on the mitochondria after activation or has other novel functions upstream of the mitochondria that influence the apoptotic threshold of a cell.

Classically, caspases are thought to act as cysteine proteases that cleave their substrates at specific aspartic acid residues (Shi, 2002). However, "day jobs" of these caspases that can be distinguished from their catalytic functions have recently been discovered. Caspase-8 has been shown to interact with the p85 subunit of PI3K to promote Rac activation during migration and caspase-11 has been shown to interact with Aip1 and promote actin depolymerization during cell migration (Li et al., 2007;Senft et al., 2007). Therefore we hypothesized that caspase-3 also has a non-apoptotic function and that loss of this function could result in a change in the apoptotic threshold of the cell.

Here we show that caspase-3 regulates cell morphology, adhesion and migration. Interestingly, we found that the catalytic activity of caspase-3 is not required for these novel non-apoptotic functions. Furthermore, we found that caspase-3 regulates fibronectin secretion and by doing so, influences the apoptotic threshold of a cell. Taken together, our data indicate that procaspase-3 has a novel non-apoptotic "day job" that is independent of its role as an executioner caspase, yet can influence the apoptotic threshold upstream of the mitochondrial events of apoptosis.

Results:

While studying the role of caspase-3 in mitochondrial dysfunction during apoptosis, we made the empiric observation that caspase-3-deficient MEFs were difficult to trypsinize from cell culture plates and displayed changes in morphology. This raised the possibility that in addition to its role as an executioner caspase during apoptosis, caspase-3 could have other cellular functions and these novel functions could influence the apoptotic threshold of a cell. Specifically, we hypothesized that caspase-3 was a negative regulator of adhesion and loss of caspase-3 resulted in an increase in adhesion-mediated survival signaling. Therefore, we formally tested the role of caspase-3 on adhesion-associated cellular events. Initially, we measured the effects of loss of caspase-3 on cellular morphology and adhesion. WT MEFs display a small rounded morphology with some cells having a distinct leading edge-lamellipodia structure (Fig. 1A). Casp3$^{-/-}$ MEFs share a similar overall size to WT MEFs (Fig. 1B), however they have more of an elongated morphology (Fig. 1A). WT MEFs have an average cell length of 42.2 μm ± 1.7 μm, while caspase-3-deficient MEFs are nearly two times longer (67.8 μm ± 3.6 μm) (Fig. 1C). These changes were not due to differences in overall size or cell volume of Casp3$^{-/-}$ MEFs (Fig. 1B, D) indicating that caspase-3 influences cell spreading and elongation which are regulated in part through the binding of integrins to the extra-cellular matrix (ECM) (Gumbiner, 1996). Therefore, we next determined whether caspase-3-deficient MEFs are more adherent. We plated an equal number of cells into 96-well plates and allowed cells to adhere for .5, 1, 2 and 4 hours. Medium was then aspirated and adherent cells were fixed and stained with crystal violet to analyze adhesion. Casp3$^{-/-}$ MEFs display a 3-fold increase in adhesion compared to WT MEFs after 30 minutes and at least a 2-fold increase in adhesion through 4 hours (Fig. 1E).

The regulation of actin-cytoskeleton organization and focal adhesion assembly and disassembly are essential for cell migration (Ballestrem et al., 2000;Matthias Krause et al., 2003;Ridley et al., 2003). Since caspase-3 is regulating morphology and adhesion, we next determined its role in cell motility. *In vitro* wound healing assays were performed with WT and Casp3$^{-/-}$ MEFs and percent wound closure was analyzed by time-lapse microscopy. Casp3$^{-/-}$ MEFs are unable to close wounds as efficiently as WT MEFs showing 37.8 % ± 8.2 % and 50.5 % ± 9.4 % wound closure at 9 and 12 hours, respectively, while WT MEFs display 63.8 % ± 4.9 % and 84.0 % ± 7.2 % wound closure at these time points (Fig. 2). Wound closure can be accomplished through

activation of cell migration and/or cell proliferation (Maria B. Witte and Adrian Barbul, 1997;Tseng et al., 2007;Chera et al., 2009;Li et al., 2010). Therefore, we determined the cell proliferation rate in WT and Casp3$^{-/-}$ MEFs through analysis of cell cycle and cell doubling time. In a standard cell cycle assay, the percent of cells in G1, S, or G2 phase of the cell cycle is not significantly different between Casp3$^{-/-}$ and WT MEFs (Fig. 3A). However, this did not represent a wound healing situation where cells are at confluency and then are released from contact inhibition. Therefore, we determined cell cycle distribution while simulating wound healing by growing cells to confluency and then scratching the plates with 8 parallel scratches or a grid of 16 scratches. After 12 hours of migration, analysis indicated no difference in cell cycle distribution under conditions of 8 scratches or 16 scratches (Fig. 3B). WT and Casp3$^{-/-}$ MEFs were also seeded and counted over time to analyze cell proliferation and doubling time. There is no significant difference in the fold change over time of cell number between Casp3$^{-/-}$ and WT MEFs (Fig. 3C). Thus the differences in wound closure are not due to changes in cell proliferation, indicating that caspase-3 regulates cell motility.

Since no differences in proliferation were detected, the two most likely explanations for a defect in wound healing are a decrease in migration velocity or a loss of directional persistence. Therefore, we performed single cell tracking to identify changes in migration that result in inefficient wound closure in Casp3$^{-/-}$ MEFs. Cell tracks show that WT MEFs move further into the wound than Casp3$^{-/-}$ MEFs (Fig. 4A). The cell tracks were analyzed for average cell velocity (distance / time) and meandering index (displacement / distance). WT MEFs have an average velocity of 37.9 μm/h ± 1.7 μm/h, while a significant decrease in average velocity for Casp3$^{-/-}$ MEFs was observed (21.7 μm/h ± 1.2 μm/h) (Fig. 4B). WT MEFs have a meandering index of 0.79 ± 0.02, while Casp3$^{-/-}$ MEFs display a statistically significant albeit marginal, decrease in their meandering index (0.74 ± 0.02) (Fig. 4C). Taken together, our data indicate that caspase-3 regulates adhesion and is required for efficient migration velocity during *in vitro* wound healing.

Our data demonstrate that caspase-3 has non-apoptotic functions in regulating cell morphology, adhesion and migration. Since these MEFs developed in the absence caspase-3, we next determined if these effects were a direct consequence of the absence of caspase-3 or due to

changes in development. Additionally, the changes in morphology and migration are displayed when there is no exogenous apoptotic stimulation suggesting that there is either localized and controlled activation of caspase-3 or these functions are independent of the catalytic activity of caspase-3. In order to test these possibilities, we introduced caspase-3 (Casp3) or a catalytically inactive caspase-3 (Casp3^{C163S}) into the caspase-3-deficient MEFs and determined if the reconstituted MEFs revert to a WT phenotype. Casp3 and Casp3^{C163S} are expressed at similar levels when compared to endogenous expression in WT MEFs (Fig. 5A). Introduction of Casp3^{WT} into the Casp3$^{-/-}$ MEFs restored DEVDase activity comparable to levels in WT MEFs following serum withdrawal, while introduction of Casp3^{C163S} did not (Fig. 5B). Remarkably, we found that both Casp3 and Casp3^{C163S} revert Casp3$^{-/-}$ MEFs to a WT morphology (Fig. 5C, D) and to a WT migration phenotype. Casp3$^{-/-}$ C3 and Casp3$^{-/-}$ C3^{C163S} MEFs close wounds as efficiently as WT MEFs (Fig. 5E) primarily by increasing average velocity which allows cells to move further into the wound during this time (Fig. 5F, G). The modest change in directional persistence observed in Casp3$^{-/-}$ MEFs is also corrected by introduction of Casp3^{WT} or Casp^{3C163S} (Fig. 5H). Taken together, these data indicate that caspase-3 regulates morphology and migration through a mechanism that is independent from its catalytic activity.

Caspase-3-deficient MEFs display increased cell adhesion and elongation along the ECM, and a slower average velocity compared to WT MEFs. These phenotypes could be explained by increased mature focal adhesion complexes, which are required for adhesion and have been shown to be detrimental to migration (Beningo et al., 2001;Totsukawa et al., 2004;Gardel et al., 2010). However, we were unable to detect differences in integrin β-1 protein expression on the cell surface, integrin β-1 mRNA levels, or integrin β-3 protein expression on the cell surface (Fig. 6A and not shown). Alternatively, these phenotypes could be the result of the increased production and secretion of ECM, which is required for adhesion (Gumbiner, 1996;Pankov and Yamada, 2002b). The previous adhesion experiments were performed in serum-containing medium and/or on fibronectin-coated glass, both of which are an exogenous source of components of the ECM. Therefore, to determine if the adhesion phenotype of Casp3$^{-/-}$ MEFs was due to endogenous production of ECM, exogenous factors were removed through a 4-hour serum withdrawal and then an adhesion assay was performed for 1 hour on glass coverslips with or without fibronectin coating. Additionally, to determine the role of secretion of endogenous

ECM, assays were also performed in the presence of the ER-golgi transport inhibitor brefeldin A. Both Casp3$^{-/-}$ and WT MEFs adhere to and spread on fibronectin with some localized FAK activation on the cellular edge, however only Casp3$^{-/-}$ MEFs spread in the absence of a supplied ECM at this time point (Fig. 6B) and addition of brefeldin A blocks the ability of Casp3$^{-/-}$ MEFs to spread. Introduction of Casp3 or Casp3^{C163S} reverts Casp3$^{-/-}$ MEFs to a WT phenotype (Fig. 6B). These data suggest that caspase-3-deficient MEFs are able to produce and/or secrete their own ECM more efficiently than WT MEFs, indicating that procaspase-3 regulates secretion of ECM through a mechanism that is independent of its catalytic activity. To analyze production and secretion of ECM, we repeated the adhesion assay, however cells were fixed without permeabilization and stained with phalloidin (actin) and DAPI (nucleus) as well as with a fibronectin specific antibody. Casp3$^{-/-}$ MEFs spread faster than WT MEFs and have prominent extracellular fibronectin staining after 1 hour of adhesion (Fig. 6C). Some cells were also fixed without permeabilization and stained with phalloidin (actin) and DAPI (nucleus) as well as with an antibody specific for an intracellular protein, P-FAK, to demonstrate that under these conditions, antibodies do not have access to intracellular space (compare P-FAK staining in Fig. 6B to 6C). To demonstrate this in a more quantitative fashion, we also analyzed fibronectin secretion by ELISA after performing an adhesion assay and found that when compared to WT MEFs, Casp3$^{-/-}$ MEFs have a significantly higher level of soluble fibronectin in the medium when normalized to cell number (Fig. 6D). However, intracellular levels of fibronectin are not significantly different between WT and Casp3$^{-/-}$ MEFs (Fig. 6D). Moreover, fibronectin steady state mRNA levels are not different between these cells (data not shown). Taken together, these data suggest that fibronectin production alone cannot account for the increased adhesion of Casp3$^{-/-}$ MEFs. To determine if fibronectin secretion is altered by loss of procaspase-3, we determined the effects of brefeldin A on fibronectin levels in the culture medium and cells. Consistent with the cell spreading data (Fig. 6B), we found that brefeldin A significantly reduces the amount of fibronectin in the culture medium of Casp3$^{-/-}$ MEFs, returning them to the level of WT MEF secretion (Fig. 6D). To directly test the role of fibronectin in the Casp3$^{-/-}$ adhesion phenotype, we next determined the effects of silencing fibronectin in Casp3$^{-/-}$ MEFs. Consistent with an important role for cell adhesion in the survival of these cells (see below) we were unable to stably silence fibronectin in a constitutive fashion (data not shown). Therefore we developed stable lines carrying an inducible fibronectin shRNA (Tet-On). In the absence of doxycycline,

these cells adhered in a similar fashion as cells infected with empty vector (pLKO) (Fig. 6E) or parental Casp3$^{-/-}$ cells (Fig. 6B). However, treatment with doxycycline for 72 hours prior to assaying adhesion resulted in a significant decrease in cellular fibronectin and a reversion to an adhesion phenotype similar to WT cells (Fig. 6E). Importantly, addition of exogenous fibronectin rescues the adhesion phenotype, demonstrating that neither the shRNA nor doxycycline are having off-target effects. Taken together, these data demonstrate that fibronectin secretion is necessary for the Casp3$^{-/-}$ adhesion phenotype.

Previous work has demonstrated that during cell death stimulation, effector caspase-deficient MEFs display delayed Bax activation, MOMP, and cytochrome c release (Lakhani et al., 2006). Based on the current findings, it is possible that the delay in the mitochondrial events of apoptosis in caspase-3-deficient MEFs may be explained by their ability to adhere and signal more efficiently resulting in an increased apoptotic threshold. To test this possibility, we examined the role of adhesion in the cell death of WT and Casp3$^{-/-}$ MEFs. Cells were seeded in the presence or absence of serum in plates coated with or without polyHEMA, which blocks adhesion and results in the induction of anoikis (Munoz et al., 2010). Consistent with previous findings, Casp3$^{-/-}$ MEFs are significantly protected from serum withdrawal-induced cell death when compared to WT MEFs at all time points analyzed (Fig. 7A). After 24 hours of serum withdrawal, WT MEFs are 38.3 % ± 6.6 % annexin V-positive, while Casp3$^{-/-}$ MEFs are only 7.7 % ± 1.2 % annexin V-positive (Fig. 7A, p = 0.01). Caspase-3-deficient MEFs are not completely resistant to serum withdrawal-induced cell death, however after 96 hours of serum withdrawal, WT MEFs are 88.0 % ± 2.5 % annexin V-positive, while Casp3$^{-/-}$ MEFs are still significantly protected yet display 55.7 % ± 4.5 % annexin V-positive cells (Fig. 7A, p = 0.003). In contrast to serum withdrawal, Casp3$^{-/-}$ MEFs are significantly less resistant to cell death induced by anoikis. After 24 hours of anoikis, Casp3$^{-/-}$ MEFs are 29.3 % ± 1.8 % annexin V-positive and by 72 hours loss of caspase-3 offers no significant protection (Fig. 7A). Thus the protective effects of caspase-3 deficiency require cell adhesion. Interestingly, at 24 and 48 hours, the combination of serum withdrawal and anoikis has an additive killing effect on WT MEFs. In contrast, this combination is antagonistic during the first 48 hours in Casp3$^{-/-}$ MEFs. This suggests that serum withdrawal is protective against anoikis when cells lack caspase-3. We hypothesize that this initial protection is from the activation of autophagy by serum withdrawal and this is currently

under investigation. Consistent with this possibility, we observed a similar effect of anoikis and the topoisomerase II inhibitor, etoposide, on the death of WT MEFs. However, etoposide does not confer protection against anoikis in Casp3-deficient MEFs (data not shown). Caspase-3 is the primary executioner caspase during serum withdrawal (Brentnall et al., 2013) and consistent with this observation, the effects of serum withdrawal and anoikis on Casp3/Casp7 DKO MEFs are identical to that seen in Casp3$^{-/-}$ MEFs (Fig. 7B). Taken together, these data indicate that procaspase-3 is regulating adhesion dependent survival signaling upstream of the mitochondria, which alters the apoptotic threshold of the cell and allows the mitochondrial events of apoptosis to happen quickly and efficiently upon cell death stimulation.

Our data indicate that loss of Casp3 protects cells in an adhesion-dependent manner and that these cells secrete approximately twice as much fibronectin as WT MEFs. This would suggest that relatively modest changes in fibronectin secretion could have profound effects on inhibition of cell death. To test this possibility, we performed a serum withdrawal of WT, Casp3$^{-/-}$, Casp3$^{-/-}$ C3 and Casp3$^{-/-}$ C3^{C163S} MEFs on plates coated with a range of fibronectin from 0 – 10 µg/cm^2 fibronectin. WT MEFs display 48.7 % ± 4.4 % cell death in the absence of a supplied ECM, however even at the lowest concentration of fibronectin tested (0.6 µg/cm^2) a trend toward cell protection is observed and significantly less cell death was observed when cells were plated on fibronectin at concentrations of 2.5 µg/cm^2 or greater (Fig. 8). Interestingly, the amount of protection is not statistically different at concentrations greater than 2.5 µg/cm^2. These data suggest that a minimal increase in the concentration of fibronectin is needed to confer protection from serum withdrawal-induced cell death. Casp3$^{-/-}$ MEFs do not significantly die during serum withdrawal and therefore the addition of fibronectin does not protect these cells. However, Casp3$^{-/-}$ C3 MEFs die in a similar fashion to WT MEFs during serum withdrawal-induced cell death and the addition of fibronectin at concentrations of 2.5 µg/cm^2 or greater protects cells (Fig. 8). Introduction of C3^{C163S} did not result in a significant increase in cell death. This is consistent with the lack of DEVDase activity observed in these cells (Fig. 5B) and our previous finding that caspase-3 is the primary executioner during serum withdrawal (Brentnall et al., 2013). Together these data suggest that in the presence of fibronectin, caspase-3 activity is still required for serum withdrawal-induced death.

Discussion:

Cells constitutively express many if not most of the pro-apoptotic proteins required to initiate and execute programmed cell death. This has lead to the concept that all cells are poised to die if and when they encounter a stress signal such as loss of trophic factors (Ishizaki et al., 1995). However, several studies have now demonstrated that pro-death molecules have additional unrelated functions, which they perform in living cells. Importantly, these "day jobs" often do not require the same activity or domains necessary for these proteins to participate in cell death. The first example of a protein having two distinct functions is cytochrome c, where the region required for binding to Apaf-1 in formation of the apoptosome during apoptosis is dispensable for its "day job" in electron transport (Kluck et al., 2000; Yu et al., 2001). More recently, the BH3-only protein Bad was shown to be important in the regulation of glucokinase and insulin secretion (Danial et al., 2003; Danial et al., 2008). Interestingly, the BH3 domain is important for both its pro-apoptotic and metabolic functions, however in the latter case it must be phosphorylated. In these two cases, neither protein has enzymatic activity, therefore separating the "day jobs" from the pro-apoptotic activity must occur in part through inhibition of the pro-apoptotic activity. In the case of cytochrome c this occurs through compartmentalization while for Bad the post-translational modification that is required for regulation of glucokinase inhibits its ability to function as a Bcl-2 antagonist (Danial et al., 2003; Danial et al., 2008). In contrast to these examples, "day jobs" of caspases may or may not involve the same catalytic activity involved in apoptosis. For example, caspase-8 was shown to increase cell motility and metastasis in neuroblastoma cancer cells through Rab5 activation that is independent of its catalytic activity (Torres et al., 2010). The inflammatory caspase, caspase-11, regulates macrophage migration by regulating actin dynamics through an interaction with Aip1 (Li et al., 2007). However, caspase-8 and -10 can also regulate cell survival through catalytic activity. Caspase-8 prevents RIPK-mediated necrosis, while a recent report demonstrated that caspase-10 prevents autophagic death of myeloma cells by cleaving the Bcl2-interacting protein BCLAF1 (Green et al., 2011; (Kaiser et al., 2011) Lamy et al., 2013; Oberst et al., 2011).

Caspase-3 has also recently been shown to have non-apoptotic roles. Low levels of caspase-3 activation were shown to regulate cell differentiation through activation of a DNase, which was controlled by NF-κB signaling to avoid apoptosis (Basu et al., 2012; Larsen et al., 2010). Also, during wound healing, caspase-3 activation in apoptotic cells promotes proliferation of

surrounding cells by activating growth signals through the release of prostaglandin in a process termed "phoenix rising" (Li et al., 2010). Another form of controlled and localized activation of caspase-3 is needed for the removal of neuronal dendrites during pruning ((Williams et al., 2006;Larsen et al., 2010;Li et al., 2010;Basu et al., 2012). Although these are non-apoptotic roles of caspase-3, these functions are dependent on the catalytic activity of the protein and often resemble specialized forms of cellular degradation. We now provide evidence that procaspase-3 also has a non-apoptotic "day job" controlling cell adhesion that is not related to its function in apoptosis or its catalytic activity. Our data demonstrate that procaspase-3 is regulating fibronectin secretion and that fibronectin secretion is required for the cell adhesion phenotype observed in caspase-3-deficient cells. However, we have not ruled out the possibility that the secretion or cell surface expression of additional molecules also contributes to this phenotype. Our data suggests procaspase-3 plays a role in ER/Golgi transport or vesicle trafficking and this is currently under investigation. However, by regulating cellular adhesion, procaspase-3 can indirectly regulate the apoptotic threshold of the cell. Thus a re-evaluation of survival data in caspase-3-deficient cells may be appropriate. Finally, these data also provide new insight as to why caspase-3 is rarely lost or mutated in cancer (Jäger and Zwacka, 2010b). Previously, it was believed that this was due to the lack of selective pressure to lose a protein that functioned "passed the point of no return" in cell death (Ghavami et al., 2009). However, these new findings raise the possibility that caspase-3 is maintained in cancer cells so that they have a motility or migration advantage.

Materials and methods:

Cell Culture. Immortalized mouse embryonic fibroblasts (MEFs) were generated and grown in Dulbecco's Modification of Eagle's Medium (DMEM, Cellgro) supplemented with 10% fetal bovine serum (Cellgro), 1% Penicillin - Streptomycin (Cellgro), 1% L-Glutamine (Cellgro), 1% non-essential amino acids (Cellgro), 1% sodium pyruvate (Cellgro) and 0.001% 2-Mercaptoethanol (Gibco) at 37°C in a humid 5% CO_2 incubator. ΦNX-Ecotropic packaging cell lines (Nolan lab, Stanford University) and 293T cells were grown in DMEM medium (Cellgro) supplemented with 10% fetal bovine serum (Cellgro), 1% Penicillin - Streptomycin (Cellgro), 1% L-Glutamine (Cellgro), 1% non-essential amino acids (Cellgro) and 1% sodium pyruvate (Cellgro) at 37°C in a humid 5% CO_2 incubator. Serum free medium for death assays was made as described without 10% fetal bovine serum. Splitting and harvesting of adherent cells was conducted by washing cells with phosphate buffered saline (PBS, Cellgro) and applying 0.25% Trypsin (Cellgro) for 5-10 minutes.

Morphological studies. Cells were grown on glass coverslips (Fisher) coated with 5 μg/cm^2 fibronectin unless otherwise specified (Chemicon International) and fixed with PHEMO buffer (68 mM PIPES, 25 mM HEPES, 15 mM EGTANa$_2$, 3 mM MgCl$_2$6H$_2$O, 10% DMSO, pH 6.8) supplemented with 3.7% formaldehyde (Fisher), 0.05% glutaraldehyde (Fisher) and 0.5% Triton X-100 (Fisher) for permeabilization when indicated. Actin was labeled by staining with Alexa Fluor 555 phalloidin (Invitrogen) and DNA was stained with 300 nM 4'-6-diamidino-2-phenylinodle, dilactate (DAPI, Invitrogen) for 5-10 minutes in dH$_2$O. Coverslips were then mounted on microslides (Fisher) polyvinyl alcohol mounting medium with DABCO anti-fade (Fluka). Cell morphology was determined by visualizing cells using a point scanning laser confocal microscope (LSM 510 META) and analyzing cell length and cell footprint area using Ziess Image Browser's region of interest tool (ROI).

Cell adhesion. 5 x 10^3 cells were seeded in 96-well plates in triplicate and allowed to adhere for indicated times. Cells were then fixed with PHEMO fixative and stained with crystal violet (Fisher Scientific) in 2% ethanol for 10 minutes. Plates were washed 3x in H$_2$O and then 2% SDS was added for 30 minutes to reconstitute the remaining crystal violet. Absorbance was measured on a 96-well plate reader at 590 nM (Humphries, 2009).

Cell volume analysis. Cells were harvested by trypsinization, resuspended in FACS buffer (PBS with 1% BSA and 0.01% Sodium Azide) and cell volume was measured by forward scatter (FSC) on a FACSCanto II flow cytometer and analyzed with FlowJo software.

Motility analysis. Cells were seeded into 35 mm x 10 mm cell culture dishes (Corning) and allowed to grow until confluent. Initiation of migration was achieved by scratching confluent cells with a p10 pipette tip. Motility was measured on a Ziess Axiovert 200m microscope mounted with a Perkin Elmer Ultraview ERS enclosed in a heated chamber (37°C) with 5% CO_2 injection. Images were acquired every 10 minutes for at least 15 hours (Liang et al., 2007). After image acquisition, Volocity software was used to determine percent wound closure at designated time points and to analyze single cell tracks over time to obtain velocity and meandering index. The meandering index is a direct measure of how straight a cell moves on a scale from 0 to 1, where a meandering index of 1 is a straight line (displacement = distance).

Cell cycle analysis. Cells were seeded in 6-well plates, allowed to grow for 24 hours, harvested and fixed. Cell cycle analysis was performed on a FACSCanto II flow cytometer after staining with PI/RNase staining buffer (BD Pharmingen) for 30 minutes at room temperature (Krishan, 1975).

Motility cell cycle analysis. Cells were seeded in 6-well plates and allowed to grow to confluency. A p10 pipette tip was used to make 8 parallel scratches or an 8 by 8 scratch grid in order to mimic motility assay conditions and the release of cells from contact inhibition. After 12 hours of migration was allowed to occur in a 37°C incubator, the cells were harvested and cell cycle was analyzed as above.

Doubling time analysis. 5×10^4 cells were seeded in 6-well plates and then cells were trypsinized and counted on a hemocytometer at indicated time points.

Retroviral transduction. ΦNX-Ecotropic packaging cell lines (Nolan lab, Stanford University) were transfected with a plasmid (pBabe-puro, Casp3 pBabe-puro or Casp3^{C163S} pBabe-puro)

using Lipofectamine (Invitrogen). Target MEFs were seeded in 6-well plates and allowed to grow for 24 hours. Viral supernatants were collected and filtered through 0.45 μm syringe filters (Pall) at 24, 28, and 32 hours and then replaced with fresh medium. At each time point, viral supernatants were applied directly on target cells for infection using Polybrene Infection / Transfection Reagent (Millipore). After 24 hours viral supernatants were removed from the target cells and replaced with fresh medium for 24-72 hours. Once cells recovered from infection they were selected with 2.5 μg/ml puromycin (Sigma).

Western blot analysis. Cells were harvested, lysed and subjected to western blot as previously described (Johnson and Boise, 1999). Primary antibody to Casp3 (Cell Signaling) was used. Actin (Sigma) was used as a loading control and was visualized as previously described (Johnson and Boise, 1999).

Caspase activity assay. Cells were seeded and allowed to grow for 24 h. Then medium was removed and replaced with complete medium or serum (FBS) free medium and cells were collected after 48 h. Caspase activity was determined using a colorimetric caspase activity assay kit (Invitrogen).

Flow cytometry for integrin expression. Cells were collected and stained with a FITC conjugated integrin β-1 antibody (Molecular Probes) or a FITC conjugated IgG isotype control (BioLegend) in FACS buffer for 15 minutes at 4°C. Cells were then washed, resuspended in FACS buffer and analyzed by flow cytometry.

Cell spreading. Cells were harvested, washed and incubated under serum-free conditions ± brefeldin A at 37°C for 4 hours. Cells were resuspended in Hanks' Balanced Salt Solution (HBSS, Cellgro) ± brefeldin A and seeded onto glass coverslips with or without fibronectin coating. Plates were incubated at 37°C for 1 hour and then cells were fixed, permeabilized when indicated, stained with phalloidin, DAPI and either an antibody for P-FAK (Sigma) or fibronectin (Sigma). Cells were then mounted and visualized as described above.

Fibronectin secretion and production analysis. Cell spreading assays were performed as described above with equal cell numbers that were plated on to plastic petri dishes. Medium was collected for soluble fibronectin secretion analysis by a fibronectin ELISA kit (Abcam) and cells were collected and lysed for intracellular fibronectin production by ELISA.

Lentiviral transduction and fibronectin knockdown. 293T packaging cell lines were cotransfected with a plasmid (pLKO-TET-on, or pLKO-TET-on-shFibronectin) and two helper plasmids using Lipofectamine (Invitrogen). Target MEFs were seeded in 6-well plates and allowed to grow for 24 hours. Viral supernatants were collected and filtered through 0.45 μm syringe filters (Pall) at 24, 28, and 32 hours and then replaced with fresh medium. At each time point, viral supernatants were applied directly on target cells for infection using Polybrene Infection / Transfection Reagent (Millipore). After 24 hours viral supernatants were removed from the target cells and replaced with fresh medium for 24-72 hours. Once cells recovered from infection they were selected with 2.5 μg/ml puromycin (Sigma). Fibronectin knockdown was accomplished by growing cells in 5 μg/ml doxycycline (Sigma) for 72 hours prior to experiments.

Cell death assays. Cells were seeded in 6-well plates and treated as indicated. After the indicated time points, medium and adherent cells were harvested, washed with PBS and stained with annexin V-FITC (Biovision) and propidium iodide (PI, Sigma) as previously described (Johnson and Boise, 1999). Cell death was determined by flow cytometry on a BD FACSCanto II system with FACSDiva software and data was analyzed with FlowJo.

Statistics. Student's t-test was performed using GraphPad Prism software and statistical significance was determined by $p < 0.05$.

Competing interests:

The authors declare no competing interests.

Author's Contributions:

MB designed and performed experiments and prepared the manuscript. DBW designed and performed experiments. AR and AIM helped with data analysis. LHB oversaw project, designed experiments and prepared the manuscript.
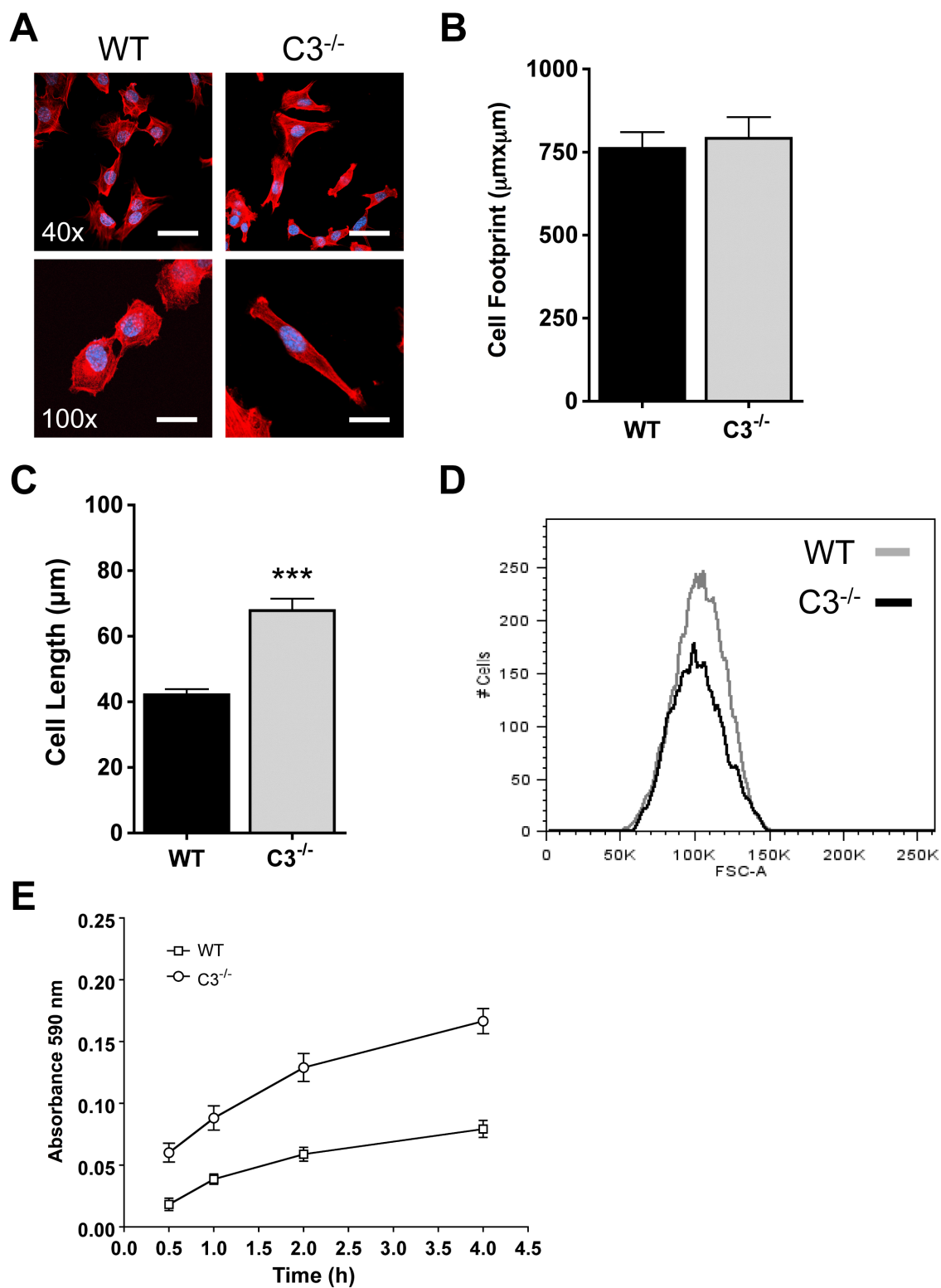
Figure 1. Caspase-3 regulates morphology and adhesion. (A-C) MEFs were grown on fibronectin coated glass coverslips for 24 hours, fixed and stained with phalloidin and DAPI. (A)

Casp3$^{-/-}$ MEFs display an elongated morphology. Cell morphology was determined by confocal fluorescent microscopy. Data representative of at least 3 independent experiments. 40x scale bar 50 μm, 100x scale bar 20 μm. (B) Casp3$^{-/-}$ MEFs have a cell footprint in contact with the ECM that is comparable in size to WT MEFs. Area of contact was quantitated using LSM 510 META software and are presented as mean ± SEM of > 30 individual cells from at least 3 independent experiments. (C) Casp3$^{-/-}$ MEFs have a longer cell length compared to WT MEFs. Cell length was quantified using LSM 510 META software and are presented as mean ± SEM of > 30 individual cells from at least 3 independent experiments. (*** p < 0.0001) (D) Casp3$^{-/-}$ MEFs have the same cell volume as WT MEFs. Cell volume was analyzed by flow cytometry on the FSC channel. Data representative of at least 3 independent experiments. (E) Casp3$^{-/-}$ MEFs adhere at a faster rate than WT MEFs. MEFs were allowed to adhere for indicated times and crystal violet staining was quantitated as described in methods. Data presented as mean ± SEM of at least 3 independent experiments.

A

B
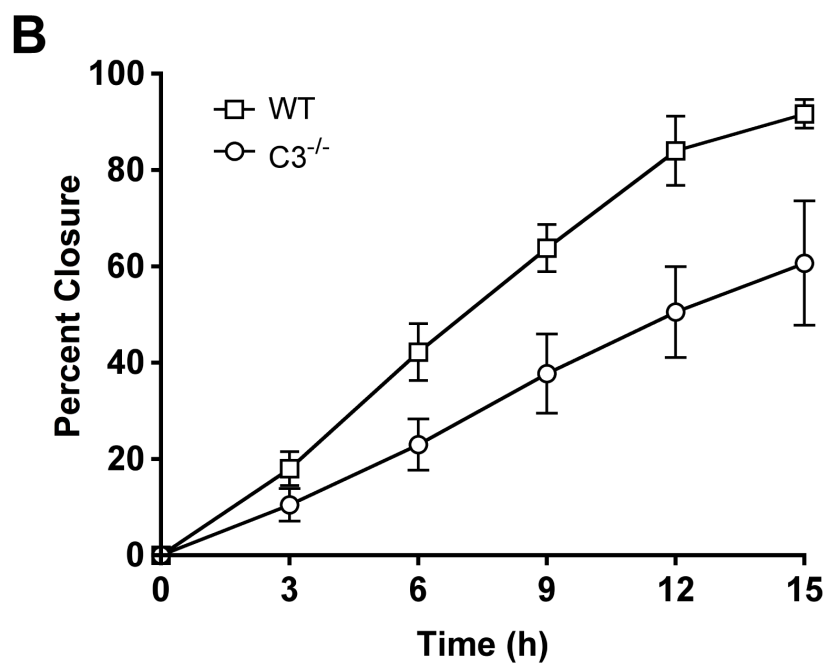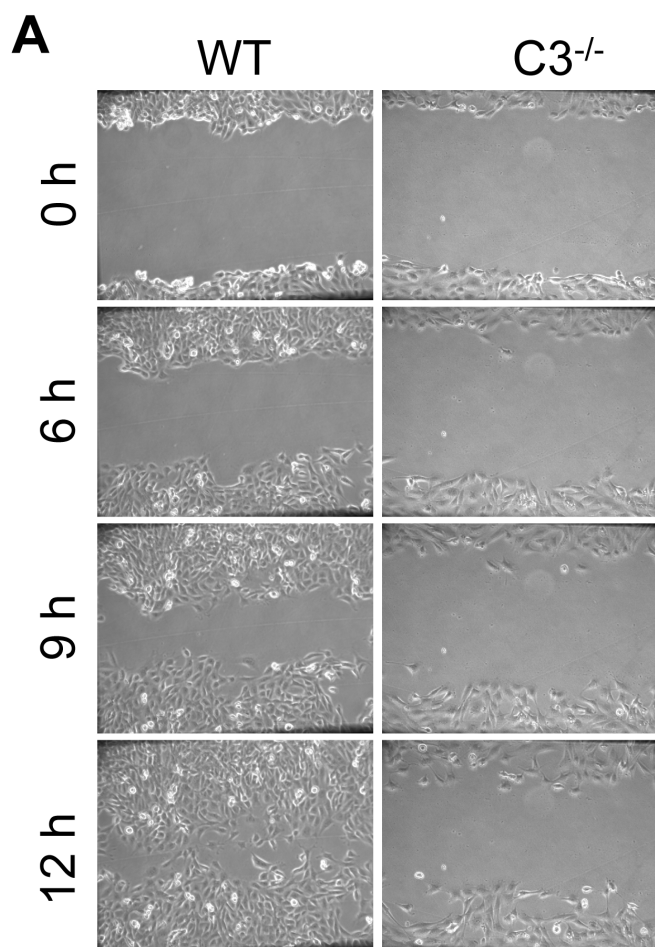
Figure 2. Caspase-3 regulates migration. (A, B) MEFs were grown to confluency, plates were wounded and then analyzed by time-lapse microscopy for at least 15 hours. (A) Casp3$^{-/-}$ MEFs display defective wound closure. Data representative of at least 3 independent experiments. (B) Data quantitated using Volocity software and presented as mean ± SEM of at least 3 independent experiments.

A

B

C
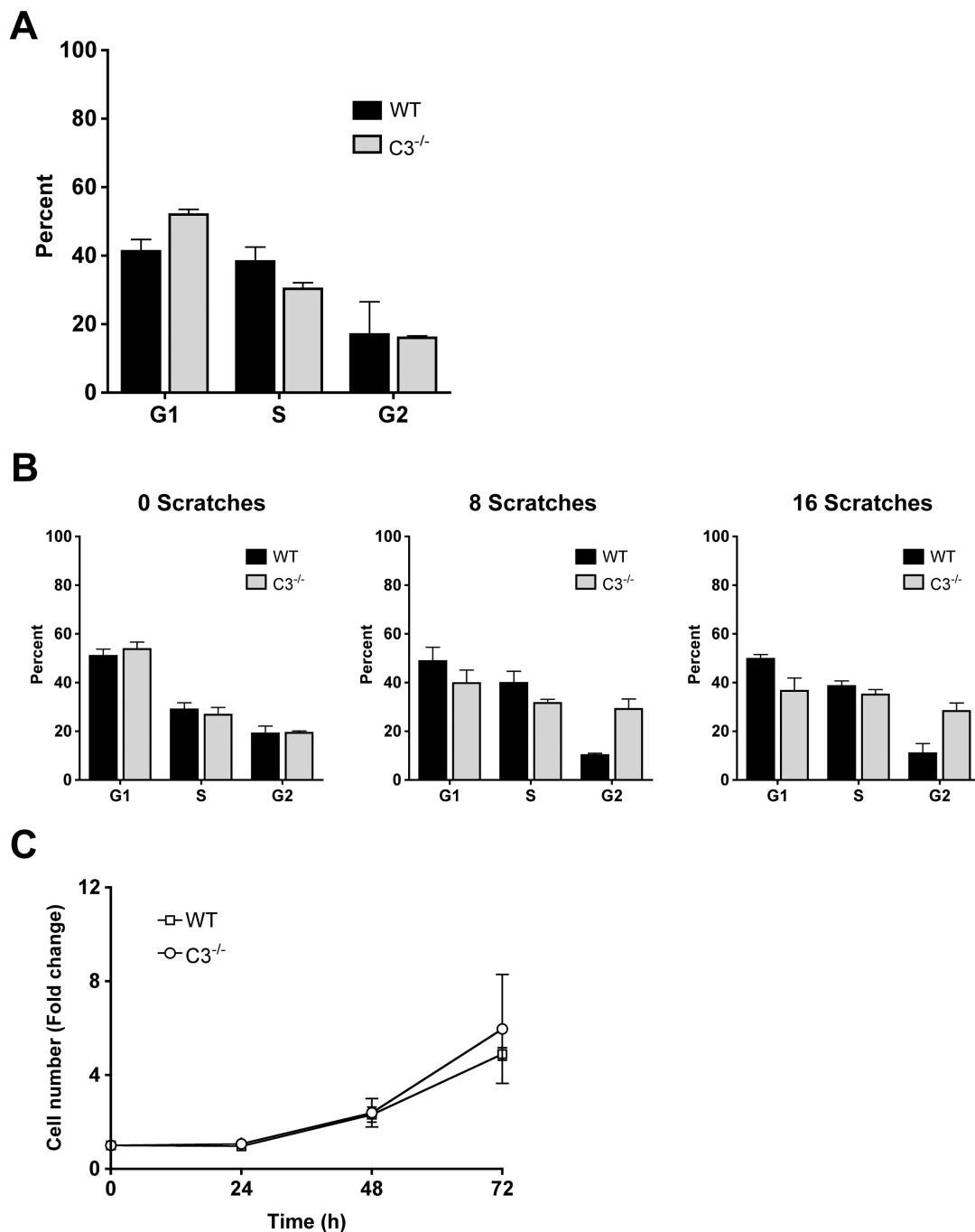
Figure 3. WT and Casp3$^{-/-}$ MEFs have comparable rates of proliferation. (A) MEFs were grown for 24 hours and cell cycle was analyzed by PI staining. Data presented as mean ± SEM of at least 3 independent experiments. (B) Casp3$^{-/-}$ and WT MEFs display comparable amounts of proliferation when migration is stimulated. MEFs were grown to confluency, scratched with 8 parallel scratches or a grid of 16 scratches. After 12 hours of migration, cell cycle was analyzed

by PI staining. Data presented as mean ± SEM of at least 3 independent experiments. (C) Casp3$^{-/-}$ and WT MEFs proliferate at the same rate. Doubling time was analyzed by cell counting at indicated times. Data presented as mean ± SEM of at least 3 independent experiments.
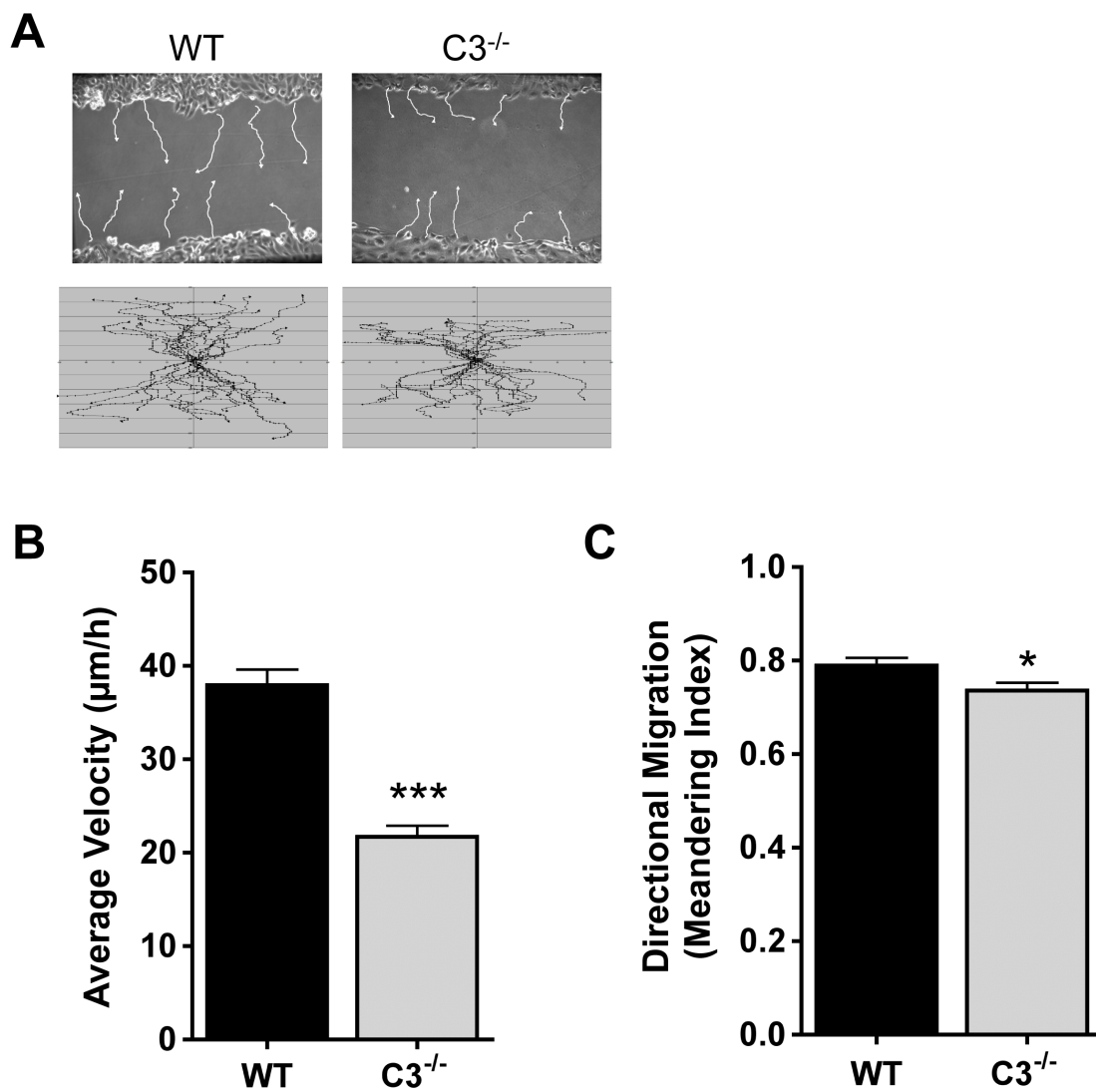
Figure 4. Casp3$^{-/-}$ MEFs display a decrease in average velocity and directional migration. (A) Single cell tracks of approximately 10 hours were analyzed using Volocity software, representative (upper panels) and total (lower panels) tracks are shown. (B, C) Data quantified and presented as mean ± SEM of at least 36 individual cells from at least 3 independent experiments. (* p = 0.03, *** p < 0.0001)
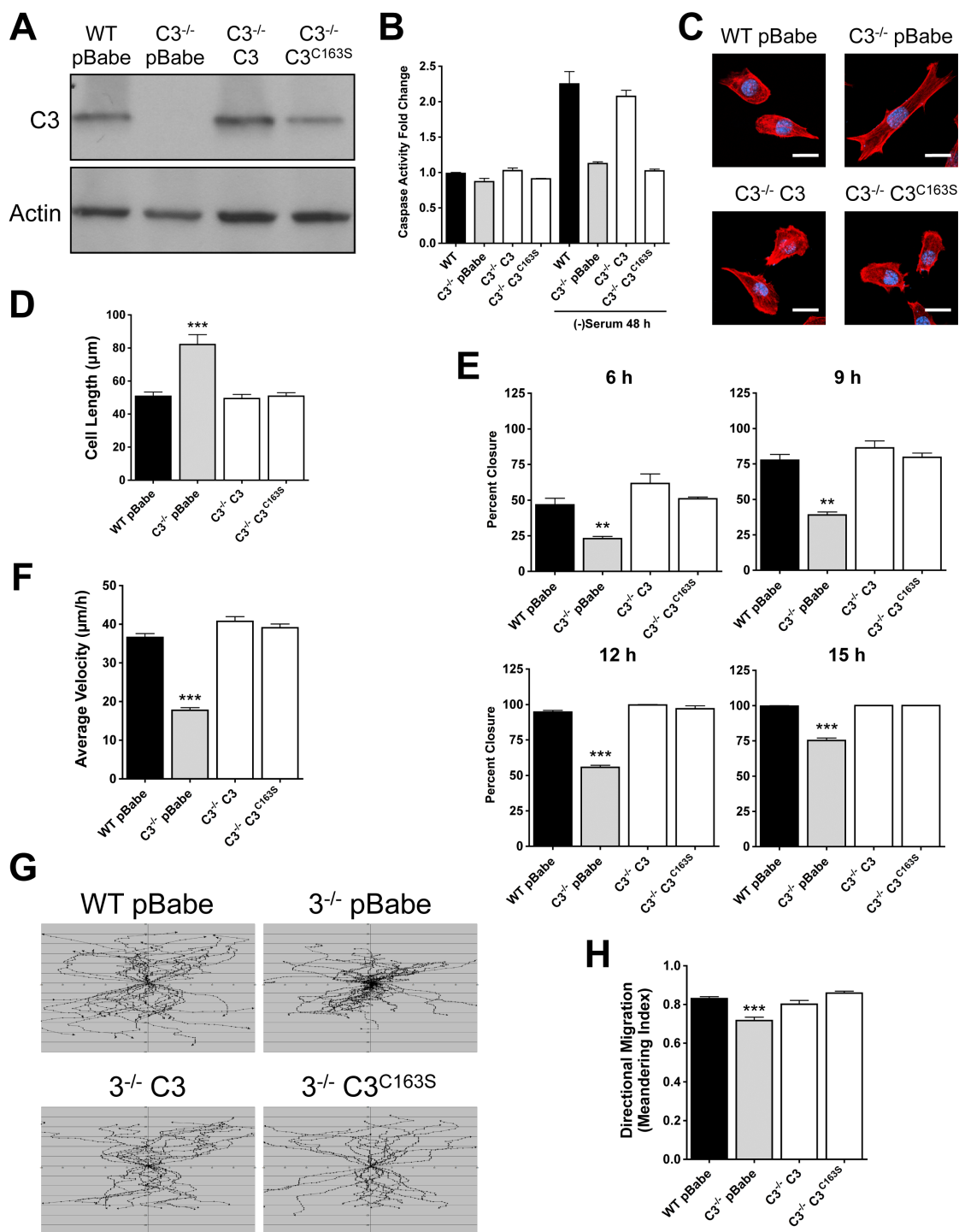
Figure

5. Caspase-3 regulates morphology and migration through a mechanism that is independent of its catalytic activity. (A) Casp3^{-/-} MEFs were reconstituted with Casp3 or Casp3[C163S] and caspase-3 expression was analyzed by western blot. (B) Casp3[C163S] does not function as a catalytic caspase. DEVDase activity was measured after 48 hours of serum withdrawal. Data presented as mean ±

SEM of at least 3 independent experiments. (C, D) Casp3$^{-/-}$ C3 and Casp3$^{-/-}$ C3^{C163S} MEFs revert to a WT morphology. MEFs were fixed, stained with phalloidin and DAPI, scale bar 20 μm. Data quantitated using LSM 510 software and are presented as mean ± SEM of at least 30 individual cells from at least 3 independent experiments. (E) Casp3$^{-/-}$ C3 and Casp3$^{-/-}$ C3^{C163S} MEFs revert to a WT migration phenotype. MEFs were grown to confluency, plates were wounded and then analyzed by time-lapse microscopy for at least 15 hours. Data quantitated using Volocity software and are presented as mean ± SEM of at least 3 independent experiments. (F-H) Casp3$^{-/-}$ C3 and Casp3$^{-/-}$ C3^{C163S} MEFs revert to a WT average velocity and directional migration. Single cell tracks of approximately 10 hours were analyzed using Volocity software, total tracks shown and are presented as mean ± SEM of at least 36 individual cells from at least 3 independent experiments. (** $p < 0.01$, *** $p < 0.0001$)
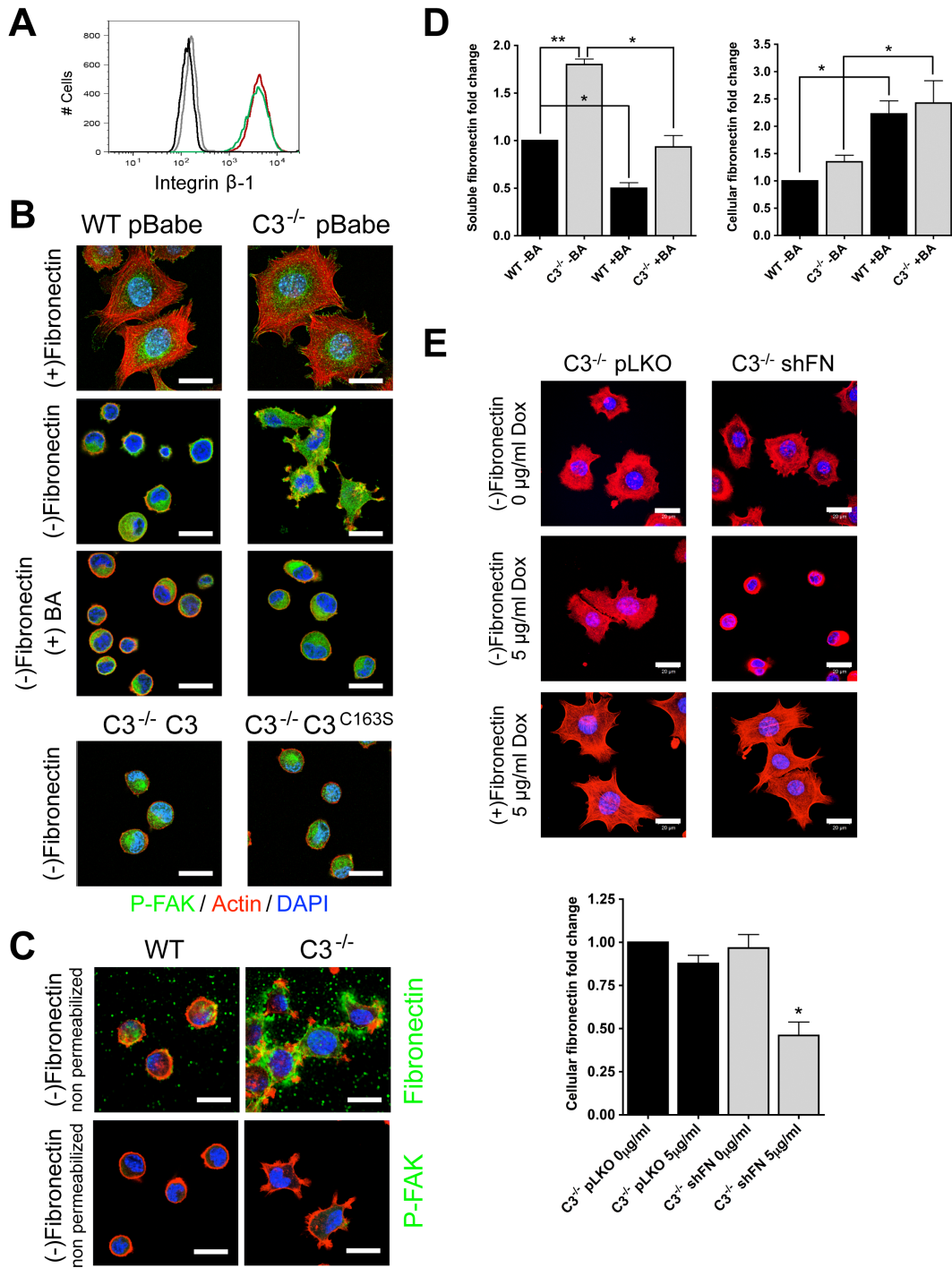
Figure

6. Caspase-3 regulates the secretion of fibronectin. (A) WT and Casp3^{-/-} MEFs have similar levels of cell surface integrin β-1 protein expression. Cells were collected and stained with a FITC conjugated integrin β-1 antibody or a FITC conjugated IgG isotype control and analyzed by flow cytometry. Flow cytometry representative of 3 independent experiments, WT MEFs

isotype control (black), WT MEFs anti-integrin (green), Casp3$^{-/-}$ MEFs isotype control (grey), Casp3$^{-/-}$ MEFs anti-integrin (red). (B, C) Casp3$^{-/-}$ MEFs adhere to and spread on uncoated glass coverslips at a faster rate than WT MEFs. (B) MEFs were subjected to serum withdrawal ± brefeldin A for 4 hours and then allowed to adhere ± brefeldin A for 1 hour. Cells were fixed, permeabilized and stained with phalloidin, DAPI and antibodies for P-FAK. Scale bar 20 µm. (C) MEFs were subjected to serum withdrawal for 4 hours and then allowed to adhere for 1 hour. Cells were fixed without permeabilization and stained with phalloidin, DAPI and antibodies for either fibronectin or P-FAK. Data representative of at least 3 independent experiments. Scale bar 20 µm. (D) Casp3$^{-/-}$ MEFs secrete an increased amount of fibronectin. MEFs were subjected to serum withdrawal for 4 hours ± brefeldin A and then allowed to adhere for 1 hour ± brefeldin A. Supernatants and cells were collected and analyzed for fibronectin by ELISA. Data presented as mean ± SEM of at least 3 independent experiments. (E) Knockdown of fibronectin blocks the ability of Casp3$^{-/-}$ MEFs to spread. Casp3$^{-/-}$ pLKO or Casp3$^{-/-}$ shFN MEFs were treated for 72 hours ± doxycycline. Cells were then trypsinized, subjected to serum withdrawal for 4 hours and then allowed to adhere for 1 hour ± fibronectin coating (upper panel) or were collected and analyzed for fibronectin by ELISA (lower panel). Data presented as mean ± SEM of at least 3 independent experiments. (* $p < 0.05$, ** $p < 0.01$)
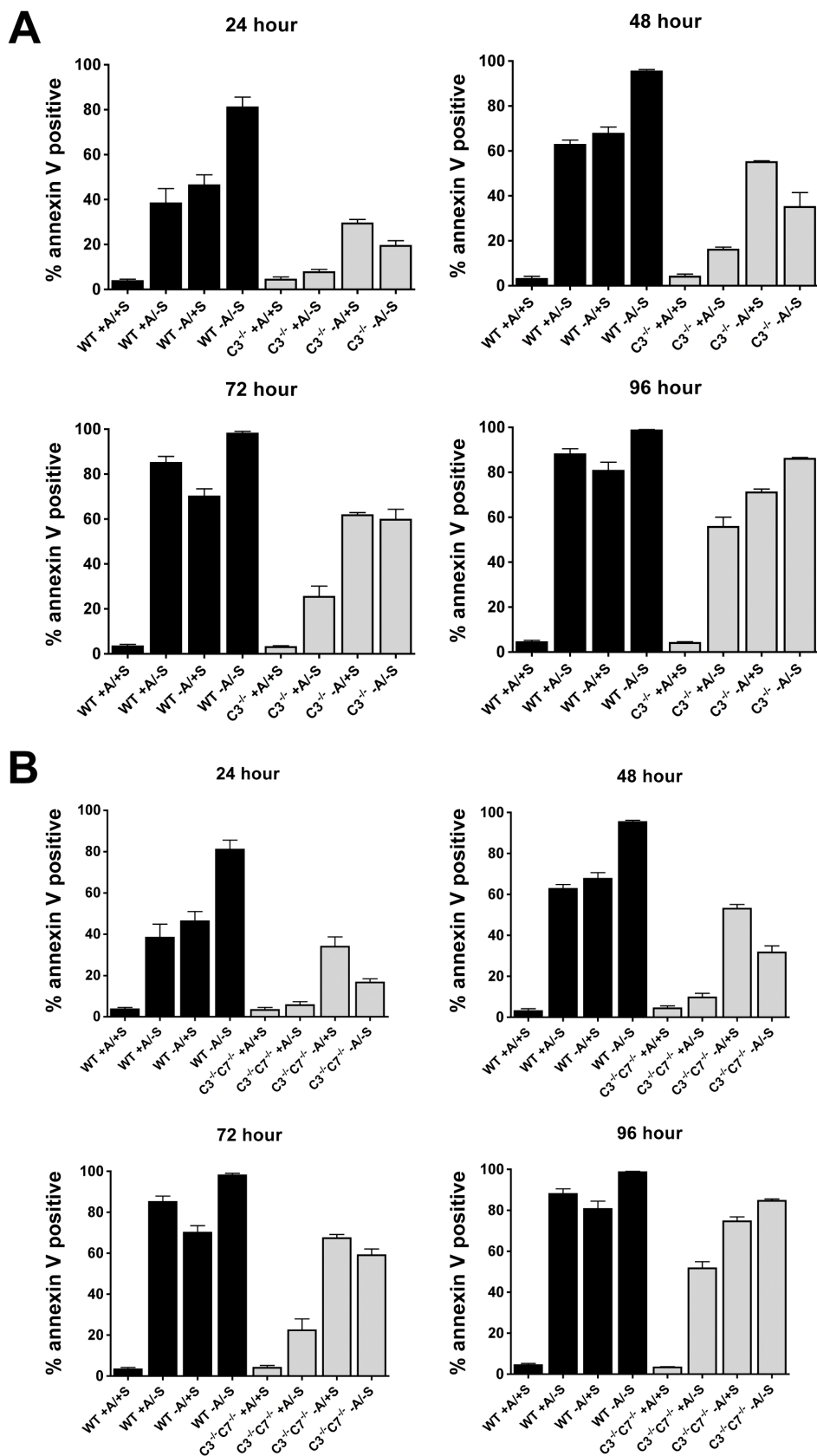
Figure 7. Caspase-3 regulates the apoptotic threshold of cells through adhesion and independent of caspase-7. (A, B) MEFs were seeded into ± polyHEMA coated plates (+/- A) in medium ± serum (+/- S). At the indicated times, cell death was analyzed by annexin V staining. Data presented as mean ± SEM of at least 3 independent experiments. (A) Casp3$^{-/-}$ MEFs are protected from serum withdrawal-induced cell death, however they are not protected from death induced by anoikis. (B) Caspase-3 regulates the apoptotic threshold of the cell through adhesion, independent of caspase-7. C3$^{-/-}$C7$^{-/-}$ MEFs die in a similar manner to C3$^{-/-}$ MEFs during serum withdrawal and/or anoikis.
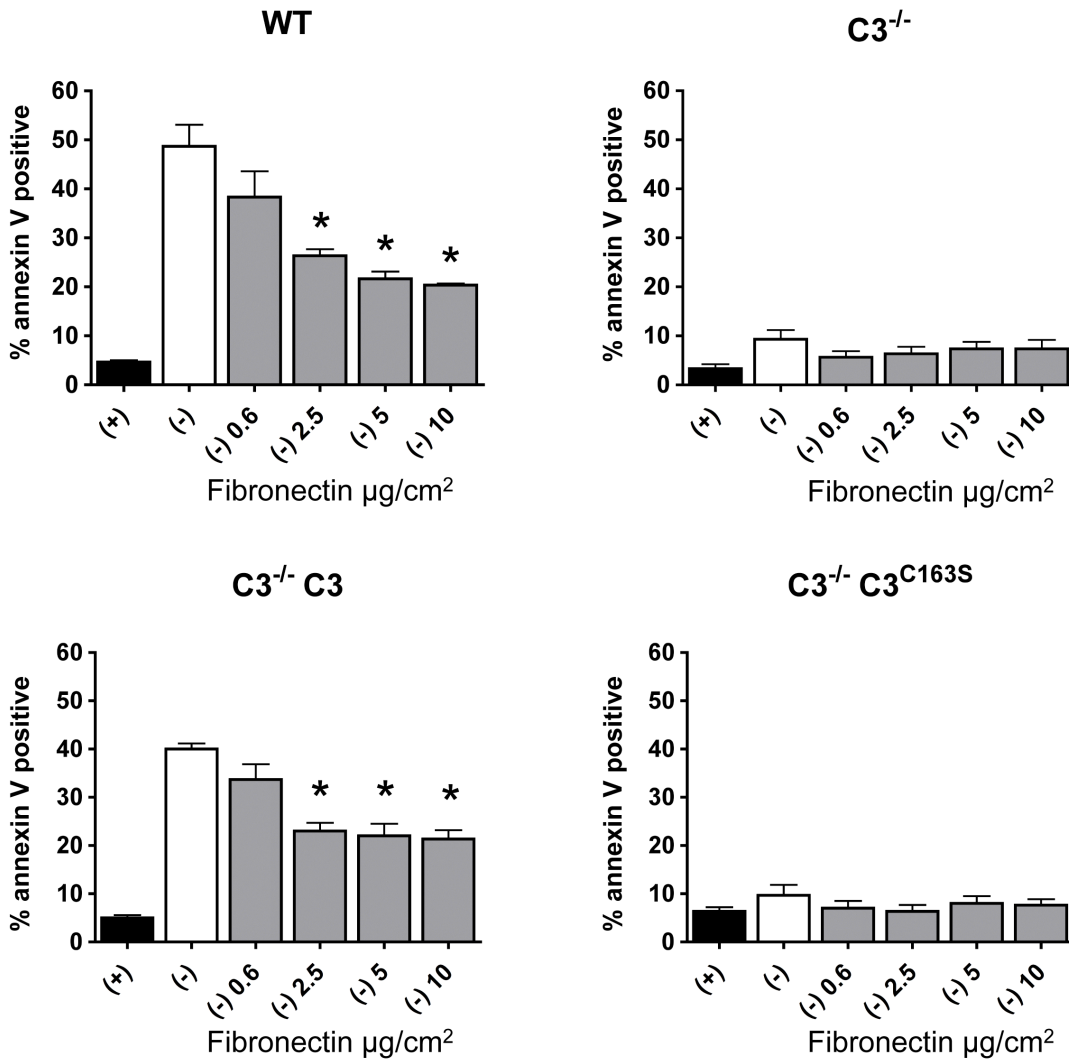
Figure 8. Fibronectin protects WT and C3$^{-/-}$ C3 MEFs from serum withdrawal-induced cell death. MEFs were seeded into plates coated with increasing concentrations of fibronectin in serum free medium. After 24 hours, cell death was analyzed by annexin V staining. Data presented as mean ± SEM of at least 3 independent experiments. (statistics compared to serum withdrawal, * $p < 0.01$)

III. Casp3-deficient fibroblasts require fibronectin for protection against autophagy-dependent death

David B. Weir[1], Lawrence H. Boise[2]*

[1]Cancer Biology Graduate Program, Emory University, Atlanta, GA, USA

[2]Department of Hematology and Medical Oncology, Winship Cancer Institute of Emory University, Atlanta, GA, USA

Abstract

Caspases are required for execution of apoptosis. However, in their absence, signals that typically induce apoptosis can still result in cell death. Our laboratory previously demonstrated that Casp3-deficient mouse embryonic fibroblasts (MEFs) have increased fibronectin (FN) secretion, and an adhesion-dependent survival advantage compared to wild type (WT) MEFs. Here, we show that FN is required for survival of Casp3-deficient MEFs following serum withdrawal. Furthermore, when FN is silenced, serum withdrawal-induced death is caspase-independent. However, procaspase-7 is cleaved, suggesting that MOMP is taking place. Indeed, in the absence of FN, cytochrome c release is increased following serum withdrawal in Casp3-deficient MEFs. Yet death does not correspond to cytochrome c release in Casp3-deficient MEFs. This is true both in the presence and absence of FN. Additionally, caspase-independent death is inhibited by Bcl-X_L overexpression. These findings suggest that Bcl-X_L is not inhibiting death through regulation of Bax/Bak insertion into the mitochondria, but through a different mechanism. One such possibility is autophagy and induction of autophagy is associated with caspase-independent death in Casp3-deficient cells. Importantly, when ATG5 is ablated in Casp3-deficient cells, autophagy is blocked and death is largely inhibited. Taken together, our data indicate that Casp3-deficient fibroblasts are incapable of undergoing canonical serum withdrawal-induced apoptosis and are protected from autophagy-dependent death by FN-mediated adhesion.

1 Introduction

Caspases are a highly conserved family of cysteine-dependent aspartate-specific proteases that are an integral part of apoptosis (Creagh and Martin, 2001;Kumar, 2007;Li and Yuan, 2008;Shalini et al., 2015;Julien and Wells, 2017). The intrinsic apoptotic pathway ultimately results in the activation of executioner caspases, at which point the enzymes complete apoptosis (Danial and Korsmeyer, 2004;Taylor et al., 2008;Fuchs and Steller, 2011;Green and Llambi, 2015;Galluzzi et al., 2018). Upon a death signal, such as growth factor deprivation, Bcl-2 family proteins regulate insertion of Bax/Bak channels into the mitochondria, resulting in mitochondrial outer membrane permeabilization (MOMP) and the release of mitochondrial contents, including cytochrome *c* (Korsmeyer et al., 2000;Wei et al., 2001;Letai et al., 2002;Kuwana et al., 2005). When released into the cytoplasm, cytochrome *c* triggers the formation of the apoptosome, a protein complex composed of multiple molecules each of apoptotic protease-activating factor 1 (APAF-1) and the zymogen procaspase-9. Upon recruitment to the apoptosome, the molecules of procaspase-9 become activated by proximity to one another and cleave the zymogens procaspase-3 and procaspase-7, thereby giving rise to their catalytically active forms (Li et al., 1997;Zou et al., 1997;Srinivasula et al., 1998;Boatright et al., 2003). Caspase-3 and caspase-7 proceed to perform internal demolition of the cell, through the selective proteolytic cleavage of hundreds of proteins (Creagh and Martin, 2001;Kumar, 2007;Luthi and Martin, 2007;Dix et al., 2008;Li and Yuan, 2008;Mahrus et al., 2008;Shalini et al., 2015;Julien and Wells, 2017).

Our laboratory previously demonstrated that in MEFs, procaspase-3 negatively regulates fibronectin (FN) secretion, which impacts cell adhesion, migration, and survival

(Brentnall et al., 2014). FN is an essential component of the extracellular matrix (Johansson et al., 1997;Plow et al., 2000;Pankov and Yamada, 2002a). Adherent cells receive prosurvival signals via integrins bound to FN and depend on integrin-fibronectin binding for survival (Plow et al., 2000;Horton et al., 2015;Kechagia and Ivaska, 2019). Procaspase-3 regulation of FN secretion is distinct and independent from the executioner function of caspase-3 in apoptosis. Furthermore, we determined that cell survival in the absence of Casp3 occurred in an adhesion-dependent manner (Brentnall et al., 2014). However, it remains unclear whether FN is necessary for this cell survival.

Here we show that FN is required for survival of Casp3-deficient cells in the absence serum. Additionally, we demonstrate that cells lacking Casp3 die following serum withdrawal through a caspase-independent mechanism when FN is absent. Furthermore, we show that this caspase-independent death involves induction of autophagy and is blocked by inhibition of autophagy. Taken together, these data indicate that when serum withdrawal-induced apoptosis is inhibited by loss of Casp3, cells become more dependent on FN-mediated adhesion that blocks an autophagy-dependent death pathway.

2   Results

Fibronectin is required for survival of Casp3-deficient cells following serum withdrawal

Our previous study demonstrated that Casp3-deficient (Casp3$^{-/-}$) mouse embryonic fibroblasts (MEFs) secrete higher levels of FN than wild type (WT) MEFs, and that their survival advantage following serum withdrawal is dependent on cell adhesion (Brentnall et al., 2014). However, we never tested if this dependence is mediated by FN. Therefore, to determine the role of FN in the survival of cells lacking Casp3, we examined the effect

of FN silencing on serum withdrawal-induced death in WT and Casp3$^{-/-}$ MEFs. Specifically, we employed a doxycycline (Dox)-inducible shRNA expression system (shFN) to knockdown FN, as previously described (Brentnall et al., 2014) followed by serum withdrawal. A schematic of the experimental design is provided in Figure 1A. Dox-induced FN knockdown was confirmed by western blot in both WT and Casp3$^{-/-}$ (Fig. 1B). Cell death was analyzed via annexin V-propidium iodide (PI) staining and flow cytometry, and was defined as annexin V+, and/or PI+, (Fig S1). WT pLKO MEFs (control cells containing empty vector) exhibited baseline cell death of 5.31%±1.13% when seeded in medium containing serum (Fig. 1C). Death significantly increased following serum withdrawal (32.52%±2.47%) (Fig. 1C). Serum withdrawal-induced death was partially inhibited when exogenous FN was supplied (22.12%±1.87%) (Fig. 1C). Dox administration had no effect on serum withdrawal-induced death in WT pLKO MEFs in the absence or presence of exogenous FN (Fig. 1C). Importantly, serum withdrawal-induced death was nearly identical in WT shFN MEFs when Dox was not administered, consistent with a tightly regulated inducible system. However, Dox-induced FN silencing led to significantly increased death due to serum withdrawal in WT shFN MEFs (48.36%±2.22%) (Fig. 1C). This change is due to an on-target effect, as the death phenotype was significantly inhibited by exogenous FN (Fig. 1C). Casp3$^{-/-}$ pLKO MEFs displayed baseline death of 2.22%±0.22% when cultured in medium containing serum (Fig. 1D). Consistent with our previous findings with Casp3$^{-/-}$ MEFs (Brentnall et al., 2013;Brentnall et al., 2014), Casp3$^{-/-}$ pLKO MEFs are more resistant to serum withdrawal-induced death than their WT counterparts, and addition of exogenous FN resulted in a minimal, yet statistically significant decrease in death (Fig. 1D). Administration of Dox

had no effect on cell death in Casp3$^{-/-}$ pLKO MEFs, and again in the absence of Dox, shFN had no effect. However, silencing resulted in a significant increase in serum withdrawal-induced death for Casp3$^{-/-}$ shFN MEFs, reaching 26.62%±0.97% (Fig. 1D). Thus, FN knockdown ablates the resistance of Casp3$^{-/-}$ MEFs to serum withdrawal. Importantly, when FN was knocked down and exogenous FN was supplied, the protection from cell death seen in Casp3$^{-/-}$ MEFs was restored, with death reduced to baseline serum withdrawal levels (Fig. 1D). Therefore, FN is required for the protection from serum withdrawal seen in Casp3-deficient MEFs.

In the absence of fibronectin, serum withdrawal-induced death is caspase-independent in Casp3-deficient MEFs

Since we determined that cell survival in the absence of Casp3 is dependent upon FN, we wanted to further delineate the mechanism of cell death and whether this cell death is caspase-dependent. To this end, we included the pan-caspase inhibitor Q-VD-OPh (10μM) or a DMSO control in 24hr serum withdrawal experiments (Fig. 2). WT and Casp3$^{-/-}$ MEFs containing the Dox-inducible shFN were seeded in media with or without serum, in the absence or presence of Dox, and in the absence or presence of Q-VD-OPh. WT shFN MEFs displayed baseline death of 5.32%±0.94% when grown in the presence of serum (Fig. 2A). Death rose to 39.48%±2.14% following serum withdrawal (Fig. 2A top panel). Death due to serum withdrawal was blocked by Q-VD-OPh, dropping to 20.58%±3.87% (Fig. 2A). In agreement with previous findings, serum withdrawal-induced cell death increased to 62.10%±3.44% when FN was knocked down. Death decreased to 26.30%±4.56% with the addition of Q-VD-OPh (Fig 2A). These data are consistent with a role for caspases in serum

withdrawal-induced apoptosis. In contrast, caspase inhibition had no effect on death due to serum withdrawal in Casp3$^{-/-}$ MEFs both with and without endogenous FN (Fig. 2B). Casp3$^{-/-}$ MEFs grown in medium containing serum exhibited baseline death of 4.40%±1.06% (Fig. 2B). Death increased to 16.80%±0.74% following serum withdrawal and was unaffected by addition of Q-VD-OPh (Fig. 2B). In the absence of FN, cell death was increased following serum withdrawal. However, in contrast to WT cells this was unaffected by Q-VD-OPh, suggesting that death is caspase-independent. To assure caspase activity was inhibited, we performed western blot analysis of caspase-3 and caspase-7 in the absence and presence of Q-VD-OPh (Fig. 2C). As expected, in WT shFN MEFs that were not administered Dox, cleavage of both procaspase-3 and -7 was evident under serum withdrawal (Fig. 2C left panel). Cleavage of both procaspase-3 and -7 was significantly inhibited when Q-VD-OPh was added under these conditions (Fig. 2C left panel). The amount of procaspase-3 and -7 cleavage under serum withdrawal increased when FN was knocked down, as compared to control (Fig. 2C left panel). This cleavage was also significantly inhibited in the presence Q-VD-OPh (Fig. 2C left panel). Casp3$^{-/-}$ shFN MEFs displayed procaspase-7 cleavage when serum starved, and cleavage was reduced by Q-VD-OPh administration (Fig. 2C right panel). Like WT shFN MEFs, Casp3$^{-/-}$ shFN MEFs exhibited an increased amount of procaspase-7 cleavage due to serum withdrawal when FN was knocked down. Cleavage was inhibited by Q-VD-OPh when FN was knocked down as it was when FN was at baseline (Fig. 2C right panel). These data indicate that Casp3$^{-/-}$ MEFs subjected to FN knockdown and serum withdrawal die in a caspase-independent manner. They are also consistent with our previous findings that caspase-7 is

dispensable for serum withdrawal-induced death (Brentnall et al., 2013;Brentnall et al., 2014).

Caspase-independent death following serum and fibronectin withdrawal results in the induction of MOMP and is inhibited by Bcl-X$_L$

Cleavage of procaspase-7 in Casp3-deficient MEFs subjected to serum withdrawal when FN is silenced implies that mitochondrial outer membrane permeabilization (MOMP) is occurring. To explore this possibility, we examined how MOMP inhibition affects caspase-independent cell death by overexpressing Bcl-X$_L$, a prosurvival member of the Bcl-2 protein family, in WT and Casp3-deficient MEFs. Cell lines containing a Bcl-X$_L$ expression vector or empty vector were generated (Fig. 3A) and seeded into media with or without serum, in the absence or presence of Dox (Fig. 3B,C,D). To measure the degree of MOMP in each set of conditions, we employed a flow cytometric cytochrome *c* release assay (Ryan et al., 2016). Representative flow cytometric plots are included in figure 3B. Briefly, following permeabilization, staining, and fixing, intact cells were sorted by light scatter characteristics, and changes in cytochrome *c* staining intensity were detected. Both serum withdrawal-induced cell death and cytochrome *c* release were measured in vector control (pBABE) cells (Fig. 3C) and Bcl-X$_L$ overexpressing cells (Fig. 3D). The antibiotic alamethicin was used as a positive control for cytochrome *c* release. Under all conditions, WT shFN pBABE cells displayed corresponding death and cytochrome *c* release. These data are consistent with activation of the intrinsic apoptotic pathway following serum withdrawal with inhibition of FN secretion resulting in increased intrinsic apoptotic signaling. In contrast, in Casp3$^{-/-}$ cells, death did not mirror cytochrome *c* release. In fact,

there was no difference between cytochrome *c* release in WT and Casp3$^{-/-}$ cells, while significant differences were observed in cell death. This suggests that all of the differences between the WT and Casp3$^{-/-}$ cells occurs downstream of MOMP, a finding consistent with loss of an effector caspase. However, when Bcl-X$_L$ was introduced into the cells, it was able to block both cytochrome *c* release and cell death regardless of caspase-3 expression (Fig. 3D). Together, these findings suggest that in the absence of caspase-3, the caspase-independent death that is observed is inhibitable by Bcl-X$_L$. One possibility is that the death is due to MOMP itself. However, when FN is present, MOMP levels were high yet death was low (Fig. 3C). Therefore, we investigated the role of an alternate Bcl-X$_L$-inhibitable pathway, autophagy.

Induction of autophagy is associated with death in Casp3-deficient cells

To determine whether autophagy is occurring in Casp-3-deficient MEFs subjected to FN knockdown and serum withdrawal, we measured lipidated-LC3B (LC3B-II) via western blot (Fig. 4). Serum withdrawal resulted in an increase in LC3B-II in both WT (Fig. 4A,C) and Casp3$^{-/-}$ (Fig. 4B,D) cells and this was enhanced by FN silencing. Additionally, LC3B-II accumulation was blocked by Bcl-X$_L$ overexpression. To assure that LC3B-II induction was due to an increase in autophagy and not a decrease in autophagic flux, we repeated the experiment in Casp3-deficient cells containing empty vectors (Casp3$^{-/-}$ shFN pBABE LCv2 MEFs; defined below) and added bafilomycin A1 (Baf) (100nM) or a DMSO control for the final 4 hours to block autophagosomal protein degradation. Baf addition resulted in further increase in LC3B-II (Fig. S2A,B), indicating that the serum withdrawal-induced changes were due to an increase in autophagy. LC3B-II was not observed in cells lacking

ATG5 (Casp3^{-/-} shFN ATG5^{-/-} 1 MEFs; defined below) under any conditions tested (Fig. S2A). Baf administration had no effect on cell death in serum withdrawal experiments (Fig. S2C). We next quantified the change in LC3B-II as per recommended methods (see Materials and Methods) across several experiments. Interestingly, the increase in LC3B-II, and by inference the induction of autophagy, was greater in the Casp3-deficient cells following serum withdrawal both in the presence and absence of endogenous FN (Fig. 4).

To verify induction of autophagy, autophagic vacuolization was measured in WT and Casp-3-deficient MEFs subjected to FN knockdown and serum withdrawal using transmission electron microscopy (TEM) (Fig. 5). TEM images were captured and autophagosomes, or early autophagic vacuoles, and autolysosomes, or late autophagic vacuoles, were enumerated together and generally termed "autophagic vacuoles" (AVs). Early autophagic vacuoles typically have a double membrane and intact cargo, while late autophagic vacuoles typically have only one membrane and contain cargo at various stages of degradation (Klionsky et al., 2021). AVs can be seen at baseline levels, as well as under conditions of serum withdrawal, both with and without FN knockdown (Fig. 5). Consistent with levels of LC3B lipidation, serum withdrawal resulted in elevated numbers of autophagic vacuoles (AVs) per cell in both WT and Casp-3-deficient MEFs (Fig. 5A,B). In medium containing serum, WT and Casp-3-deficient MEFs had 5.00±1.10 and 6.20±0.73 AVs/cell, respectively (Fig. 5A,B). Under conditions of serum withdrawal, WT MEFs displayed 14.60±1.70 and Casp-3-deficient MEFs showed 30.00±4.90 AVs/cell (Fig. 5A,B). The number of AVs was further increased to 57.80±7.50 by FN knockdown in Casp-3-deficient MEFs subjected to serum withdrawal, which also corroborates with LC3B lipidation data (Fig. 5A,B) The trend of increased autophagy due to FN knockdown

under serum withdrawal appears in WT MEFs, with 19.80±1.32 AVs/cell, but there is not a statistically significant difference compared to serum withdrawal without FN knockdown (Fig. 5A,B). Taken together, these data are consistent with the concept that autophagy is limited by the induction of apoptosis and suggests that autophagy is unchecked in the Casp3-deficient MEFs. This raised the possibility that the caspase-independent death that occurs under these conditions is due to excess autophagy.

Autophagy inhibition blocks death in Casp3-deficient cells

Since we had demonstrated that both cell death and the amount of autophagy induced by serum withdrawal in Casp-3-deficient MEFs increase significantly when FN is knocked down, we investigated whether autophagy is required for cell death under conditions of FN knockdown and serum withdrawal. In order to test this, we used CRISPR-Cas9 to knock out Autophagy Related Gene 5 (ATG5) (Fig. 6A). A single cell clone containing the empty vector (Casp3$^{-/-}$ shFN pBABE LCv2 MEFs) was used as a control. Additionally, a single cell clone that received the vector containing a single guide RNA (sgRNA) but did not have ATG5 knocked out (Casp3$^{-/-}$ shFN pBABE ATG5$^{+/+}$) was used as an additional control. Two single cell clones that received the same sgRNA as the Casp3$^{-/-}$ shFN pBABE ATG5$^{+/+}$ MEFs but lost ATG5 (Casp3$^{-/-}$ shFN pBABE ATG5$^{-/-}$ 1 and Casp3$^{-/-}$ shFN pBABE ATG5$^{-/-}$ 2 MEFs) were tested to determine the effect of ATG5 knockout on serum withdrawal with and without endogenous FN. Consistent with Figure 4, following serum withdrawal, Casp3-deficient MEFs that retained ATG5 showed patterns of LC3B-II consistent with induction of autophagy (Fig. 6B,C). In contrast, in both ATG5-deficient

clones, serum withdrawal-induced autophagy was completely blocked as evidenced by a complete block in LC3B lipidation (Fig. 6B). Importantly, ATG5 loss and autophagy induction resulted in a complete block of cell death in FN-silenced cells following serum withdrawal (Fig. 6D). To ensure that loss of the autophagic function, and not an alternate function, of ATG5 is responsible for blockade of cell death, we separately used CRISPR-Cas9 to knock out a second gene required by the autophagy pathway, Autophagy Related Gene 7 (ATG7). A population of cells that grew out following infection and selection as a bulk culture containing the empty vector (Casp3$^{-/-}$ shFN pBABE LCv2 Bulk MEFs) was used as a control, and a similarly selected population of ATG7 knockout cells (Casp3$^{-/-}$ shFN pBABE ATG7$^{-/-}$) were tested. Following serum withdrawal, Casp3-deficient MEFs expressing ATG7 displayed LC3B-II levels corresponding to autophagy induction (Fig. S3A,B). Conversely, in ATG7 knockout cells, serum withdrawal-induced autophagy was almost completely blocked, as indicated by a nearly total loss of LC3B lipidation (Fig. S3A,B). In agreement with results from ATG5 knockout experiments, death in FN-silenced cells following serum withdrawal was inhibited by ATG7 knockout (Fig. S3C). Taken together, these data indicate that death due to serum withdrawal in Casp3-deficient MEFs with diminished FN secretion requires autophagy.

3   Discussion

Apoptosis and autophagy have a complex connection (Maiuri et al., 2007;Eisenberg-Lerner et al., 2009;Fuchs and Steller, 2015;Tsapras and Nezis, 2017). The two pathways share molecular components, can be triggered by the same stimuli, and are capable of interacting in several distinct ways (Maiuri et al., 2007;Eisenberg-Lerner et al., 2009;Fuchs and Steller, 2015;Song et al., 2017;Tsapras and Nezis, 2017). They can work in collaboration

(Espert et al., 2006;Ravikumar et al., 2006;Scott et al., 2007;Pan et al., 2020), as well as in opposition to one another (Boya et al., 2005;Yousefi et al., 2006;Zhu et al., 2010;Tiwari et al., 2011;Pagliarini et al., 2012;Fitzwalter et al., 2018). Additionally, although autophagy most often serves as a cytoprotective process (Komatsu et al., 2006;Colell et al., 2007;Sun et al., 2013), it can also function as a killing mechanism under certain conditions, including when a cell is incapable of performing apoptosis (Shimizu et al., 2004;Yu et al., 2004;Lum et al., 2005;Pattingre et al., 2005;Yu et al., 2006;Lamy et al., 2013;Kim et al., 2018;Denton and Kumar, 2019;Nassour et al., 2019;Zhou et al., 2019). Bax/Bak-deficient MEFs were found to undergo a non-apoptotic cell death program that is dependent upon autophagic proteins when treated with etoposide (Shimizu et al., 2004). Additionally, bone marrow-derived IL-3-dependent Bax/Bak-deficient mouse cells activate autophagy and ultimately succumb to cell death, when withdrawn from IL-3 (Lum et al., 2005). Furthermore, zVAD was demonstrated to induce autophagic cell death in L929 cells when caspase-8 expression was decreased (Yu et al., 2004). In this study, we demonstrate that cells lacking Casp3 become dependent on FN for survival following serum withdrawal, and cells undergo non-apoptotic, autophagy-dependent death.

Our laboratory previously showed that procaspase-3 is a negative regulator of FN secretion and impacts adhesion, migration and survival independent of catalytic function (Brentnall et al., 2014). Introduction of WT or a catalytically inactive mutant caspase-3 reversed the adhesion and migration phenotypes seen in Casp3 deficient MEFs (Brentnall et al., 2014). Additionally, we showed that casp3-deficient MEFs have an adhesion-dependent survival advantage over WT MEFs following serum withdrawal (Brentnall et al., 2014). However, introduction of a catalytically inactive mutant caspase-3, had no effect

on survival of Casp3 deficient MEFs following serum withdrawal (Ponder and Boise, 2019). These data indicate that loss of caspase-3, and not the effects on increased FN secretion were primarily responsible for increased cell survival. The change in FN secretion due to procaspase-3 loss was only a two-fold change (Brentnall et al., 2014). In the current study we investigated the effect of loss of FN on the survival of Casp3-deficient MEFs. Here, we show that in Casp3-deficient MEFs, FN is required for protection from caspase-independent death following serum withdrawal. These findings agree with previous data showing that caspase-7 is dispensable for this death mechanism (Brentnall et al., 2013). Following serum withdrawal, autophagy is induced in Casp3-deficient cells, and cells survive. Interestingly, when FN is silenced, autophagy increases significantly, and death occurs. This raises the possibility that death is contingent upon autophagy. Importantly, blocking autophagy inhibits serum withdrawal-induced death in Casp3-deficient cells, indicating that death is indeed autophagy-dependent.

In WT MEFs, serum withdrawal triggers MOMP, as well as autophagy signaling. MOMP leads to activation of caspase-3, which in turn both inhibits autophagy and completes apoptosis. Inhibition of autophagy by caspase-3 is well documented (Norman et al., 2010;Zhu et al., 2010;Pagliarini et al., 2012). Therefore, it is reasonable to postulate that loss of caspase-3 not only blocks apoptosis, but releases constraints on autophagy. Our model (Fig. 7) posits that serum withdrawal of Casp3-deficient MEFs stimulates MOMP and induces an increased amount of autophagy. However, these cells survive serum withdrawal, primarily because they cannot complete canonical apoptosis due to their lack of caspase-3. Importantly, in the absence of FN, serum withdrawal induces still more autophagy, and under these conditions cell death occurs. Thus, in Casp3-deficient

fibroblasts, FN blocks death that results if autophagy proceeds unhampered.

In WT MEFs, increased autophagy is observed under conditions of serum withdrawal in the absence of FN compared to serum withdrawal in its presence, It might be predicted from our model that increased activated caspase-3 under these conditions would result in the opposite. However, there is evidence that autophagy induction occurs when integrin-mediated cell attachments to ECM are lost (Fung et al., 2008;Chen and Debnath, 2013;Vlahakis and Debnath, 2017). Furthermore, autophagy has been demonstrated to be protective against detachment-induced apoptosis (Fung et al., 2008;Vlahakis and Debnath, 2017). Therefore, it stands to reason that the increase in autophagy observed in serum withdrawn WT MEFs lacking FN compared to those retaining FN is being contributed by a subpopulation of cells that are surviving.

These findings open up several important questions. For example, how exactly are Casp3-deficient cells in the absence of FN dying following serum withdrawal? Cells may be undergoing autophagy-dependent cell death, but not death directly caused by autophagy itself. Autophagy may be activating another death pathway that ultimately kills the cell. Evidently, cells are not dying via necroptosis, as death was not blocked by RIPK3 inhibition (data not shown). Furthermore, a lack of membrane disruption is observed under these experimental conditions (Fig. S4). Although we have not ruled out ferroptosis or pyroptosis, based on this finding, it is unlikely that either is involved.

Additionally, how does FN protect Casp3-deficient cells from death? Perhaps Casp3-deficient cells are resistant to loss of one prosurvival signal, i.e., serum or FN signaling, but are not capable of withstanding the loss of both signals. Excessive autophagy may result when both survival signals are lost. Alternatively, FN signaling via integrins

may modulate the cellular response to serum withdrawal. Crosstalk between integrins and growth factor receptors are important signaling mechanisms (Brooks et al., 1997;Schneller et al., 1997;Mattila et al., 2005). Coupling integrin signaling and growth factor receptor signaling is crucial for cultivating the appropriate cellular response for a given context (Brooks et al., 1997;Schneller et al., 1997;Mattila et al., 2005). The autophagy signal received by cells due to the absence of growth factors may be dampened by FN signaling. Possible signaling pathways involved include Ras-Raf-MEK-ERK and PI3K/Akt. In contrast, the level of autophagy induced by serum withdrawal in the absence of FN may be the same as in its presence, but the signal is never turned off, resulting in excessive autophagy. Furthermore, although the prosurvival signal arising from FN is almost definitely mediated by integrins, it is not clear which integrins are involved. At least a dozen integrin dimers bind FN (Plow et al., 2000). We have previously shown that Casp3-deficient MEFs have cell surface expression of integrins β_1 and β_3 (Brentnall et al., 2014). Whether an individual integrin dimer or a combination of integrin dimers binds FN under experimental conditions is yet to be determined.

Taken together, our data demonstrate that loss of Casp3 results in cellular dependence on FN for protection from autophagy-dependent death. This may have implications in disease settings, such as cancer, where adhesion, autophagy and cell death all play crucial roles. It would be expected that cancer cells would lose caspase-3, as a means of evading apoptosis, yet this is rarely the case (Jäger and Zwacka, 2010a). In fact, caspase-3 expression has been found to be elevated in a number of cancer types (Yoo et al., 2002;O'Donovan et al., 2003;Patel et al., 2015). Perhaps losing caspase-3 would leave cells vulnerable to excessive autophagy. Autophagy has complicated and sometimes

diametrically opposed roles in cancer (Boya et al., 2005;Degenhardt et al., 2006;Yousefi et al., 2006;Karantza-Wadsworth et al., 2007;Levy et al., 2017). A number of studies suggest autophagy serves as a barrier against oncogenesis (Takamura et al., 2011;Belaid et al., 2013;Rosenfeldt et al., 2013;Dou et al., 2015;Wang et al., 2016). Conversely, compelling evidence supports a role for autophagy in survival of established cancer cells (Boya et al., 2005;Degenhardt et al., 2006;Karantza-Wadsworth et al., 2007;Altman et al., 2014;Masui et al., 2016;Kun et al., 2017). Genes encoding central components of the autophagy pathway are generally not lost or mutated in cancer (Lebovitz et al., 2015;Amaravadi et al., 2016;Yang and Klionsky, 2020). However, these types of mutations do occur in specific cancer types (Liang et al., 1999;Qu et al., 2003;Lebovitz et al., 2015). Heterozygous deletion of beclin 1 is found in 40-75% of sporadic breast, ovarian and prostate cancer (Liang et al., 1999;Qu et al., 2003). Three core autophagy genes, RB1CC1/FIP200, ULK4, and WDR45/WIPI4, were found to be under positive selection for somatic mutations in endometrial carcinoma (Lebovitz et al., 2015). This is also true of ATG7 in clear cell renal carcinoma (Lebovitz et al., 2015). Frameshift mutations in ATG2B, ATG5, ATG9B, and ATG12 were found in more than a quarter of gastric and colorectal cancers with microsatellite instability (Kang et al., 2009). The significance of these recurrent mutations in certain cancer types is yet to be determined. Perhaps restricting autophagy in tumor cells where autophagy is already very high provides protection from death. It has been suggested that autophagy might cause cancer cell death (Baehrecke, 2005). Additionally, a number of cancer therapies induce autophagy (Bursch et al., 1996;Kanzawa et al., 2004;Opipari et al., 2004;Shao et al., 2004;Eum and Lee, 2011;Natsumeda et al., 2011). When administered low doses of estrogen agonists, MCF-7

breast cancer cells, one of the few cancer cell lines lacking caspase-3, were shown to have extensive autophagosome formation and die by a nonapoptotic mechanism (Bursch et al., 1996). We tested these cells and determined that they also induce autophagy upon serum withdrawal. However, in contrast to the MEFs used in this study, they also die under these conditions (data not shown). It remains to be determined if this is a difference due to transformation or cell differentiation state. If it is related to cell transformation, it may provide insight into the therapeutic window that exists for the use of autophagic inducers in the treatment of cancer.

4   Materials and Methods

Cell culture

MEFs, ΦNX-ecotropic, and HEK293T (American Type Culture Collection) cells were cultured and split as previously described (Brentnall et al., 2014).

Retroviral transduction and generation of stable cell lines

ΦNX-ecotropic packaging cells were transfected with pBABE-hygro (Addgene plasmid # 1765; empty or Bcl-X$_L$) using Lipofectamine 2000 (Invitrogen). Target MEFs were retrovirally transduced as previously described (Brentnall et al., 2014). Once cells recovered from infection, they were selected through hygromycin B (Calbiochem) selection.

Lentiviral transduction and generation of stable cell lines

HEK293T packaging cells were co-transfected with lentiCRISPR v2-Blast (Addgene plasmid # 83480; empty, ATG5-specific sgRNA [AAGATGTGCTTCGAGATGTG; designed using crispr.mit.edu], or ATG7-specific sgRNA [GAACGAGTACCGCCTGGACG; designed using crispor.tefor.net]), psPAX2 (Addgene plasmid # 12260), and pMD2.G (Addgene plasmid # 12259) using jetPRIME transfection reagent (Polyplus) according to the manufacturer's instructions. Fresh medium was added, and cells were incubated for 48hr at 37°C in a humid incubator under 5% CO_2. Target MEFs were seeded on six-well plates and allowed to grow for 24 hours. Viral supernatents were collected and filtered through 0.45μm syringe filters (Pall), at 48 hours. Viral supernatents were applied directly to target MEFs for infection using Polybrene Infection/Transfection Reagent (Millipore). After 24 hours, viral supernatents were removed and replaced with fresh medium. Once cells had recovered from infection, they were selected with blasticidin (Thermo Fisher).

Western blot analysis

SDS/PAGE and western blot analysis were performed as previously described (Morales et al., 2008). Primary antibodies against Caspase-3 (Cell Signaling #9662), Caspase-7 (Cell Signaling #9492), Fibronectin (Abcam ab2413), Bcl-X$_L$ (Cell Signaling #2764), LC3B (Sigma L7543), ATG5 (Cell Signaling #12994), ATG7 (Cell Signaling #8558) and actin (Sigma A1978) were used.

FN knockdown and coating

To perform FN knockdown, 100 thousand MEFs were seeded in a 100mm cell culture dish and cultured for 24 hours. Subsequently, where indicated, cells were administered 5μg/ml doxycycline (Sigma) for 48hr, then media and dox were replaced with fresh media and dox, and cells were incubated for another 24hr (for a total administration period of 72hr). FN coating was accomplished by adding phosphate buffered saline (PBS, Cellgro) and human plasma fibronectin (Millipore) to six-well plates (Corning). Plates were incubated for 4 hours at 37°C in a humid incubator under 5% CO_2. PBS was removed immediately prior to experiments.

Cell death assays

Cells were trypsinized for 5 minutes. Trypsin was inactivated using medium containing serum. Cells were washed three times with serum-free medium, resuspended in serum-free medium, counted, and 250 thousand cells were seeded into six-well cell culture plates, treated as indicated and placed in cell incubator. After 24 hours, the cell supernatant and floating cells were collected. Adherent cells were washed once with PBS, which was also collected and combined with cell supernatant. Adherent cells were trypsinized for 5 minutes. Trypsin was inactivated using medium containing serum. Trypsin-medium mixture containing cells was collected and combined with cell supernatant-PBS mixture. Total mixture was centrifuged for 5 minutes, supernatant was discarded, and cells were stained with annexin V-FITC (BioVision) and propidium iodide (PI, Sigma), as described previously (Johnson and Boise, 1999). Cell death was determined by flow cytometry on a BD FACSCanto II system with FACSDiva software, and data was analyzed with FlowJo.

Cell death was defined as annexin V+, PI+, or annexin V+/PI+ (i.e., both types of single positives, as well as double positives, are all considered dead; see Fig. S1).

Caspase inhibition assays

Inhibition of caspases was accomplished through administration of the pan-caspase inhibitor Q-VD-OPh (BioVision) at a concentration of 10μM.

Cytochrome *c* release assay

After serum withdrawal, cells were collected, subjected to digitonin (0.001%) treatment, fixed, stained with an Alexa Fluor 488 anti-cytochrome *c* antibody (BD #560263), and analyzed via flow cytometry. Where indicated, cells received alamethicin (15μM) treatment concurrent with digitonin (0.001%) treatment, and served as positive controls. Cytochrome *c* release was determined by flow cytometry on a BD FACSCanto II system with FACSDiva software, and data was analyzed with FlowJo.

Densitometry and LC3B-II/actin quantification

LC3B-II/actin quantification and comparison were accomplished via methods widely used to monitor autophagy (Klionsky et al., 2016). Briefly, Fiji software was used to calculate OD values for LC3B-II and actin for each condition of three different western blots from independent sets of lysates. The ratio of LC3B-II to actin (LC3B-II/actin) was expressed as a fold change normalized to negative control cells.

Lysosomal acidification inhibition assay

Acidification of the lysosome was inhibited through administration of the V-ATPase inhibitor Bafilomycin A1 (Cell signaling) at a concentration of 100nM.

Necroptosis assay

MEFs were grown for 24 hours and subsequently administered doxycycline (Sigma) for 72 hours, as indicated. Cells were then trypsinized for 5 minutes. Trypsin was inactivated using medium containing serum. Cells were then washed three times with serum-free medium, seeded into six-well plates, and treated as indicated, including treatment with a necroptosis-inducing cocktail consisting of the SMAC mimetic BV6 (0.5µM; Calbiochem), TNFα (25ng/ml; Peprotech) and zVAD-fmk (25µM; Enzo). SYTOX Green (Invitrogen) was included in all conditions as an indicator of necroptosis. Necroptosis was determined by live-cell imaging on an IncuCyte Zoom system (Essen), data was analyzed with IncuCyte Zoom software (Essen).

Transmission Electron Microscopy

Serum withdrawal was performed as described above (cell death assay section) up to but not including centrifugation before annexin V-PI staining. Instead, cells were transferred to a 1.5ml microcentrifuge tube and spun at 300rcf for 5 minutes. The supernatant was discarded, cells were washed once in PBS, and spun again at 300rcf for 5 minutes. The PBS wash was discarded and the cell pellet was fixed in a mixture of 2.5% glutaraldehyde and 2% paraformaldehyde in 0.1 M cacodylate buffer at 4°C for 24 hours. After washing with 0.1 M cacodylate buffer, cells were post-fixed with 1% osmium tetroxide for an hour, washed with distilled water, and en bloc stained with 2% uranyl acetate for 30 minutes.

The pellets were dehydrated in an ascending ethanol series ending in two changes of 100% dry ethanol followed by two changes of propylene oxide. Cells were infiltrated with epoxy resin starting with 1:1 mixture of epoxy resin and propylene oxide overnight, followed by two changes of 100% resin over a day, then polymerized at 60°C for two days. The blocks were thin sectioned (70 to 80 nm) using a diamond knife (Diatome, Hatfield, PA) and a Leica Ultracut S ultramicrotome (Leica Microsystems Inc., Buffalo Grove, IL), and collected onto 200 mesh copper grids. The sections were post stained in 5% Uranyl Acetate and Reynold's Lead Citrate. The sections were imaged using a JEOL JEM-1400 transmission electron microscope (TEM) (Tokyo, Japan) at 80kV. The images were acquired at magnifications of 800X, 1200X, 5,000X and 10,000X, using a Gatan US1000 CCD camera (Gatan, Inc., Pleasanton, CA). Images of 5 cells from each of 8 conditions were captured. Autophagic vacuoles (AVs) were enumerated by eye in each of these 40 cells. Images were coded before analysis, allowing for blinded enumeration. Autophagic vacuoles (AVs) were counted manually. AVs were defined as circular structures enclosed by at least one limiting membrane, containing cytoplasmic material and/or organelles at various stages of degradation.

Statistics

Ordinary one-way ANOVA with Šidák's multiple comparison testing was used to analyze data from at least three independent experiments. Statistical analyses were used to compare serum withdrawal conditions only (i.e., conditions including serum were not included in analyses). Data are represented as mean ± standard error of the mean.

5   Acknowledgements

Fig. 1. FN is required for the survival of Casp3-deficient MEFs following serum withdrawal. (A) Schematic of experimental design. (B) Cell lysates were analyzed via western blot. (C) WT pLKO and WT shFN, and (D) Casp3$^{-/-}$ pLKO and Casp3$^{-/-}$ shFN

MEFs were seeded in medium with or without serum, in the presence or absence of Dox (5μg/ml), and incubated for 24 hr. Plates were coated with exogenous FN as indicated. Cell death was analyzed via annexin V-PI staining and flow cytometry, and was defined as annexin V+, PI+, or annexin V+/PI+ (Fig S1). Data are represented as mean ± s.e.m. All data are from at least three independent experiments. Ordinary one-way ANOVA of WT pLKO: $F = 7.297$, $p = 0.0027$; of WT shFN: $F = 41.24$, $p < 0.0001$; of Casp3$^{-/-}$ pLKO: $F = 8.135$, $p = 0.0016$; and of Casp3$^{-/-}$ shFN: $F = 188.7$, $p < 0.0001$. Šidák's multiple comparisons: *$p \leq 0.0360$, **$p = 0.0028$, ****$p < 0.0001$.
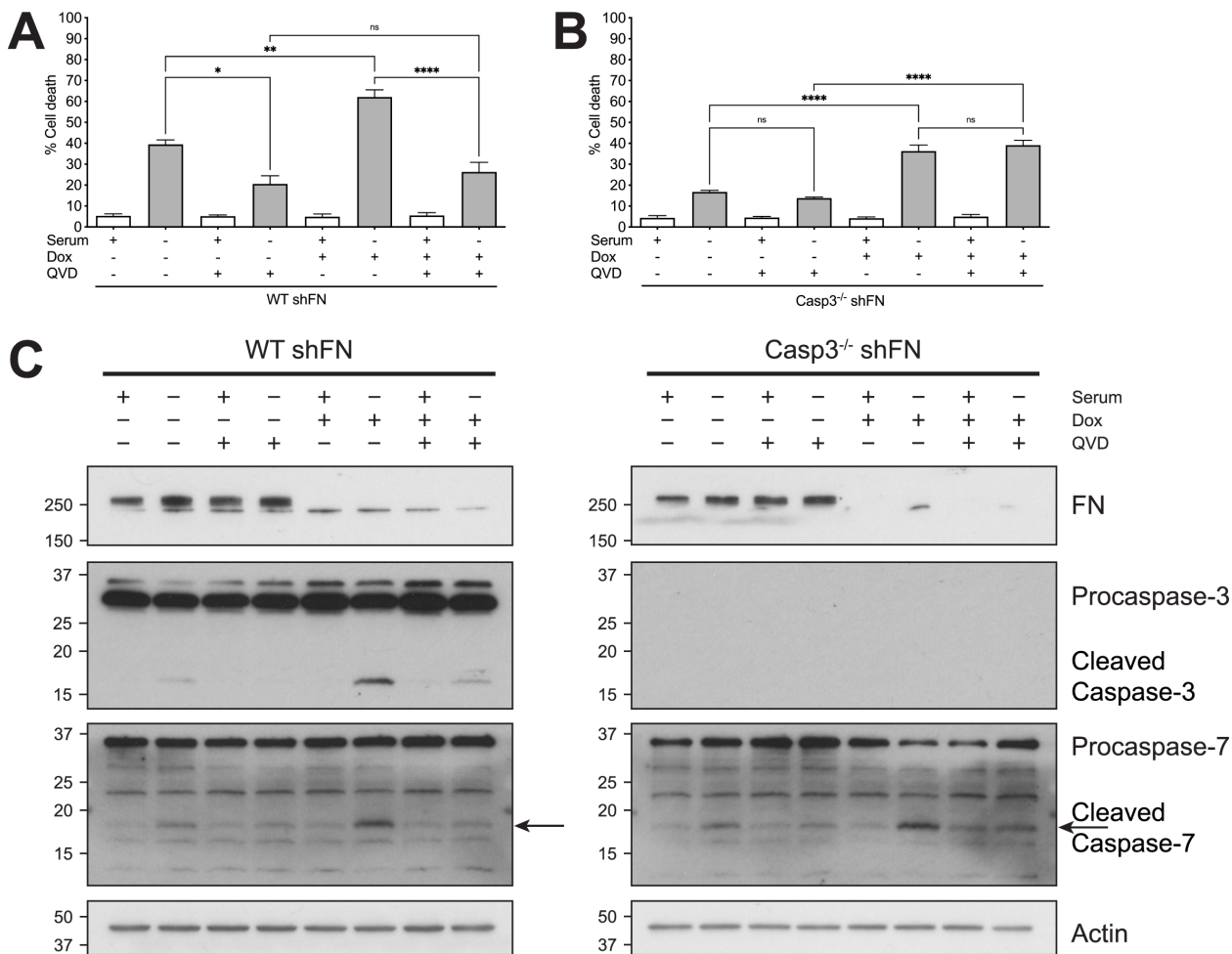
Fig. 2. In the absence of FN, serum withdrawal results in caspase-independent cell death in Casp3-deficient MEFs. (A) WT shFN and (B) Casp3$^{-/-}$ shFN MEFs were seeded in medium with or without serum, in the absence or presence of Dox (5μg/ml), in the absence or presence of Q-VD-OPh (QVD, 10μM), and incubated for 24hr. Cell death was analyzed via annexin V-PI staining and flow cytometry. (C) Cell lysates were analyzed via western blot. Data are represented as mean ± s.e.m. All data are from at least three independent experiments. Ordinary one-way ANOVA of WT shFN: F = 26.08, p < 0.0001; of Casp3$^{-/-}$ shFN: F = 46.92, p < 0.0001. Šidák's multiple comparisons: *p = 0.0121, **p = 0.0033, ****p < 0.0001.
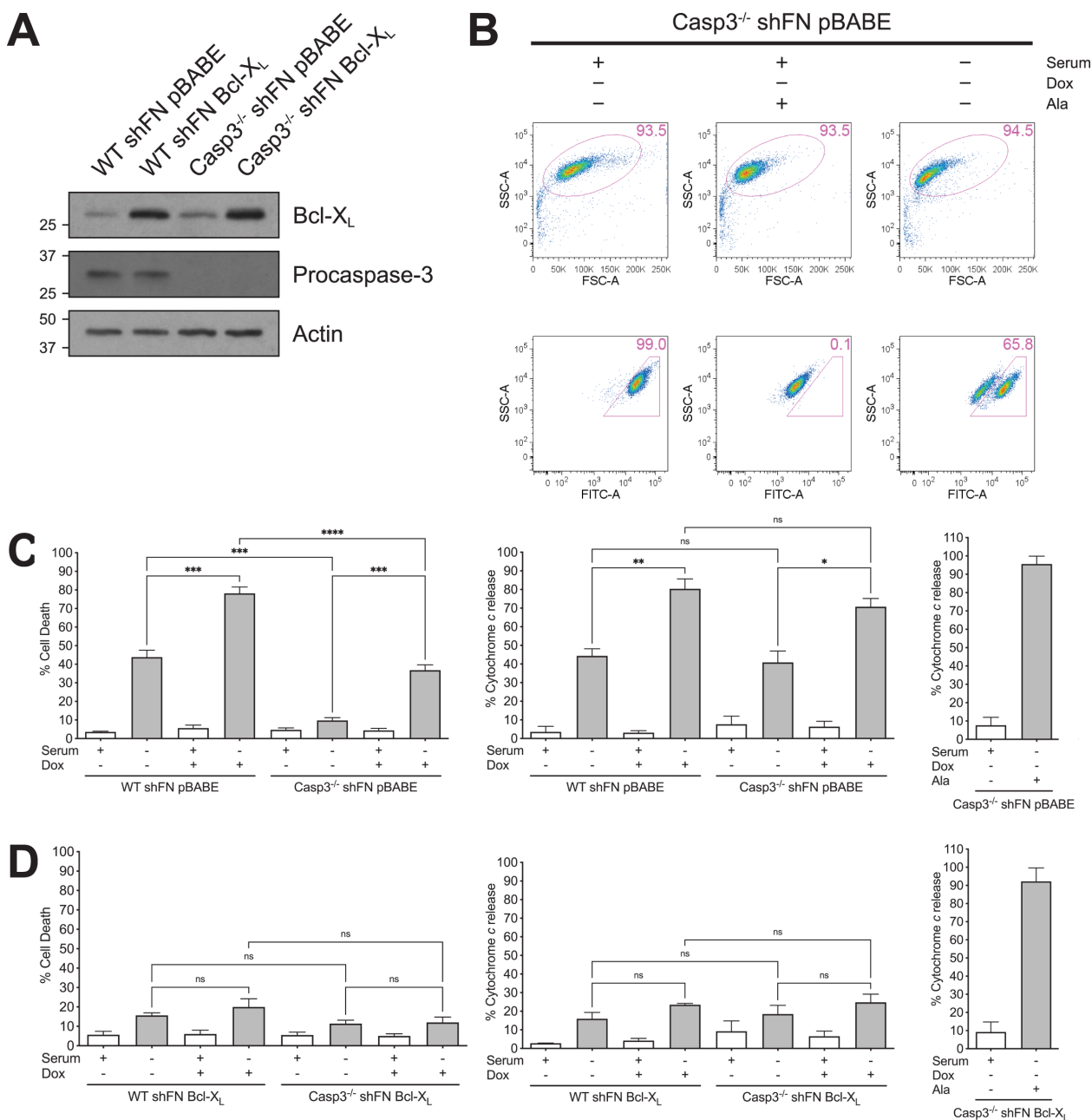
Fig. 3. **Cytochrome *c* release is independent of serum withdrawal-induced death in Casp3-deficient MEFs.** (A) WT shFN and Casp3$^{-/-}$ shFN MEF cell lines with empty expression vector pBABE-hygro (pBABE) or vector containing Bcl-X$_L$ were generated (WT shFN pBABE, WT shFN Bcl-X$_L$, C3$^{-/-}$ shFN pBABE, and C3$^{-/-}$ shFN Bcl-X$_L$). Cell lysates were analyzed via western blot. (B) Representative flow cytometry plots from

cytochrome *c* release assay. (C, left panel) WT shFN pBABE and C3$^{-/-}$ shFN pBABE, and (D, left panel) WT shFN Bcl-X$_L$ and C3$^{-/-}$ shFN Bcl-X$_L$ MEFs were seeded in medium with or without serum, in the absence or presence of Dox (5μg/ml), and incubated for 24hr. Cell death was analyzed via annexin V-PI staining and flow cytometry. (C center and right panels) WT shFN pBABE and C3$^{-/-}$ shFN pBABE, and (D center and right panels) WT shFN Bcl-X$_L$ and C3$^{-/-}$ shFN Bcl-X$_L$ MEFs were treated as indicated, permeabilized, stained with a cytochrome *c* antibody conjugated to Alexa Fluor 488, and analyzed via flow cytometry. Data are represented as mean ± s.e.m. All data are from at least three independent experiments. Ordinary one-way ANOVA of Fig. 3C left panel: F = 87.89, p < 0.0001; of Fig. 3D left panel: F = 2.085, p = 0.1806; of Fig. 3C right panel: F = 15.21, p = 0.0011; and of Fig. 3D right panel: F = 1.305; p = 0.3380. Šidák's multiple comparisons: *p = 0.0115, **p = 0.0037, ***p ≤ 0.0009, ****p <0.0001.
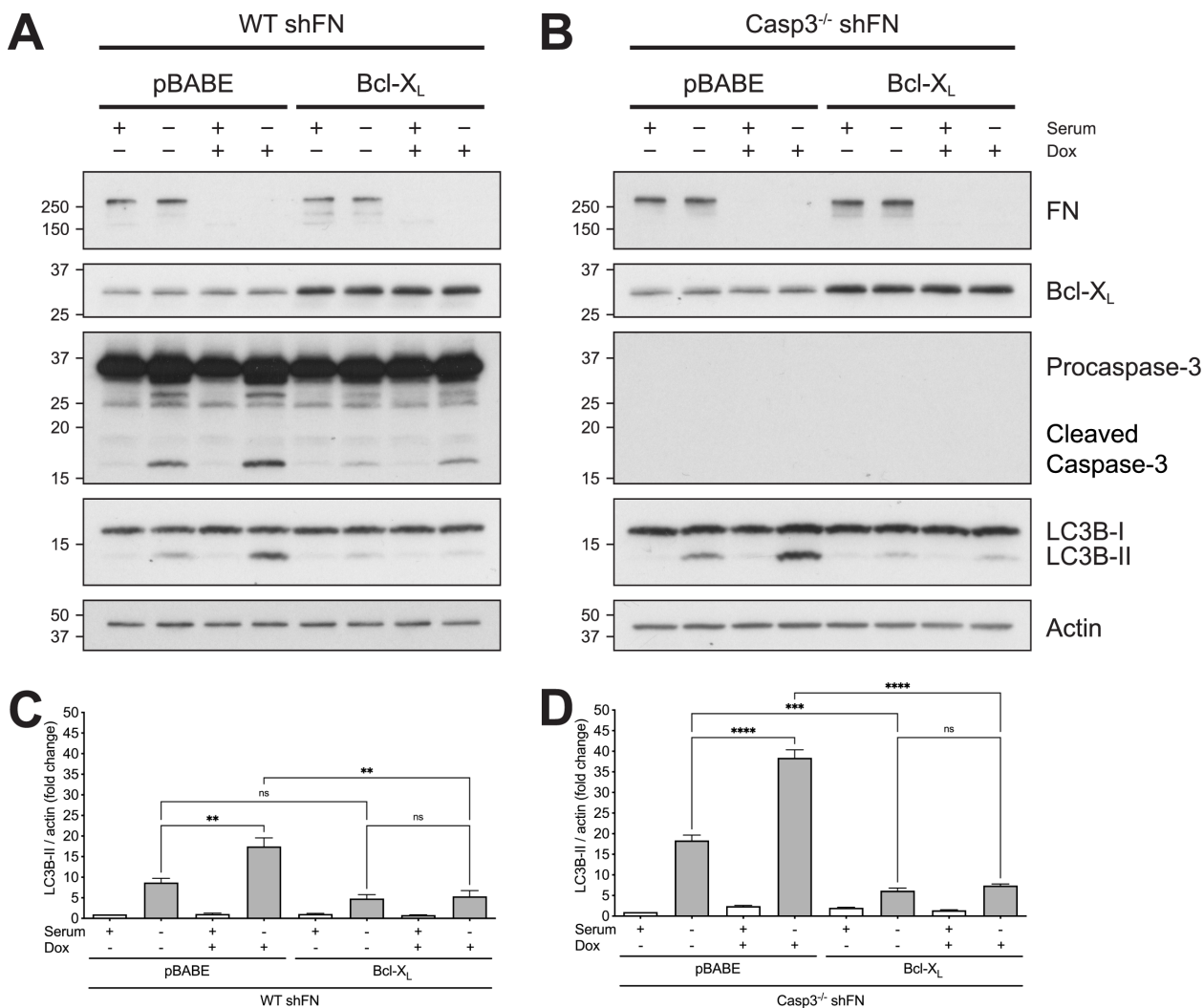
Fig. 4. Autophagy is increased by serum withdrawal in Casp3-deficient MEFs when FN is silenced. Cell lysates from subsets of (A) WT shFN pBABE and WT shFN Bcl-X$_L$, and (B) Casp3$^{-/-}$ shFN pBABE MEFs and C3$^{-/-}$ shFN Bcl-X$_L$ MEFs in Figure 3 were analyzed via western blot. (C,D) Quantification of LC3B-II in panels A and B, respectively. Data are represented as mean ± s.e.m. All data are from at least three independent experiments. Ordinary one-way ANOVA of Fig. 4C: F = 17.03, p = 0.0008; of Fig. 4D: F = 149.4, p < 0.0001. Šidák's multiple comparisons: **p ≤ 0.0095, ***p = 0.004, ****P ≤ 0.0001.

A

WT shFN

+	−	+	−	Serum
−	−	+	+	Dox

whole cell

detail

Casp3$^{-/-}$ shFN

+	−	+	−	Serum
−	−	+	+	Dox

whole cell

detail
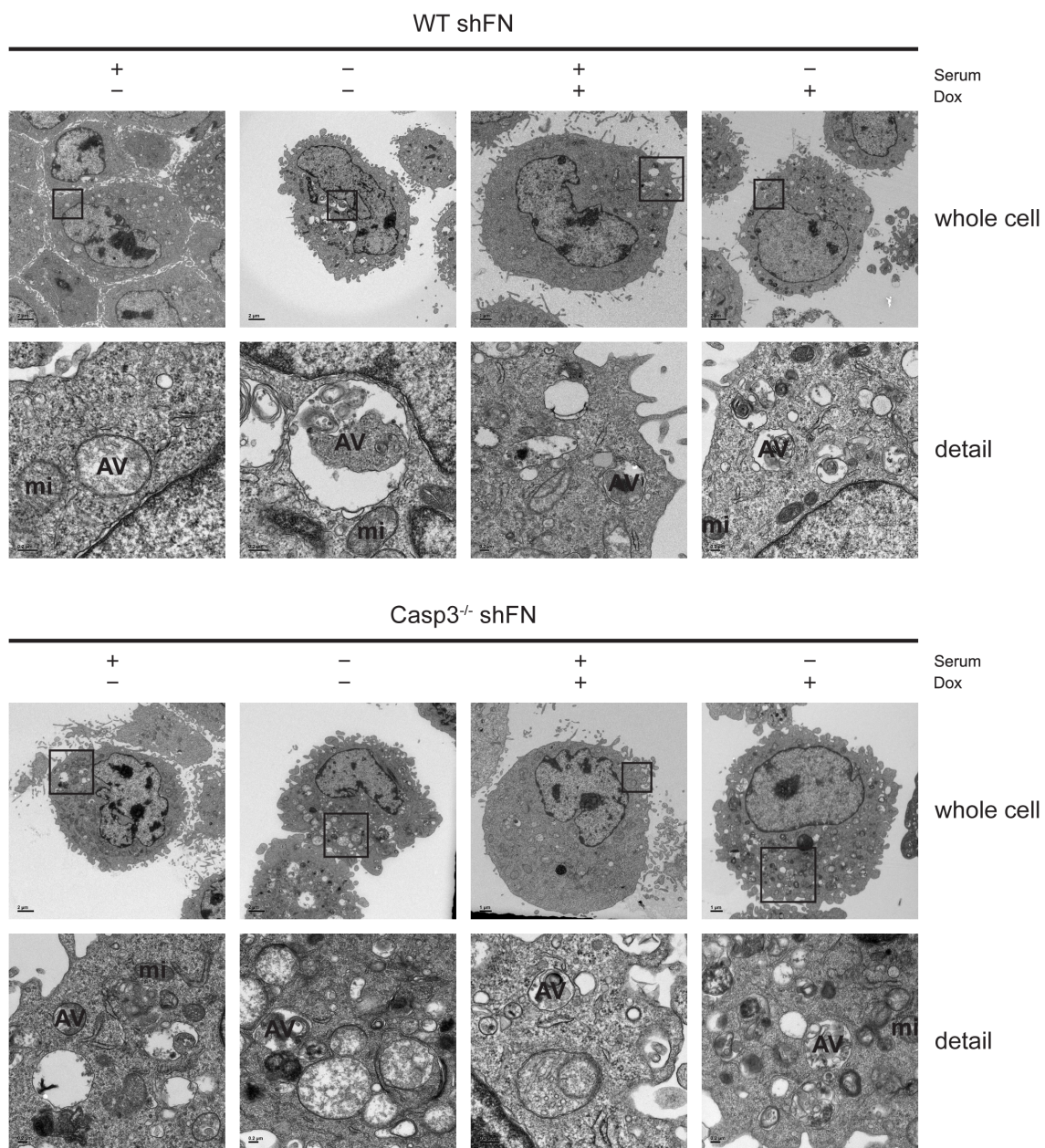
B
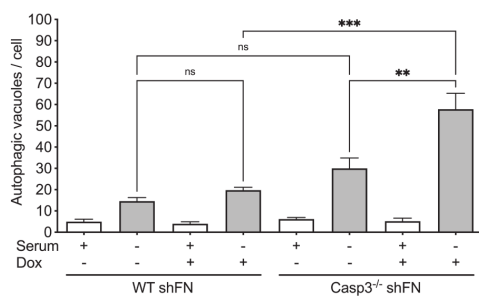
Fig. 5. Number of autophagic vacuoles is increased by serum withdrawal in Casp3-deficient MEFs when FN is silenced. (A) WT shFN and (B) C3$^{-/-}$ shFN MEFs were seeded in medium with or without serum, in the absence or presence of Dox (5μg/ml), and incubated for 24hr. Cells were subsequently trypsinized, fixed and imaged via transmission electron microscopy (TEM). Images were captured of 5 cells from each set of conditions. Images were coded before analysis, allowing for blinded enumeration. Autophagic vacuoles were defined as circular structures enclosed by at least one limiting membrane, containing cytoplasmic material and/or organelles at various stages of degradation, and were counted manually. Representative autophagic vacuoles are labeled (AV), as are mitochondria (mi). Boxed areas in upper panels are enlarged in lower panels. Scale bars (left to right) top row: 2μm, 2μm, 1μm, 2μm; 2nd row: all 0.2μm; 3rd row: 2μm, 2μm, 1μm, 1μm; bottom row: all 0.2μm; Ordinary one-way ANOVA: F = 17.49, p < 0.0001; Šidák's multiple comparisons: **p = 0.0024, ***p = 0.0001.
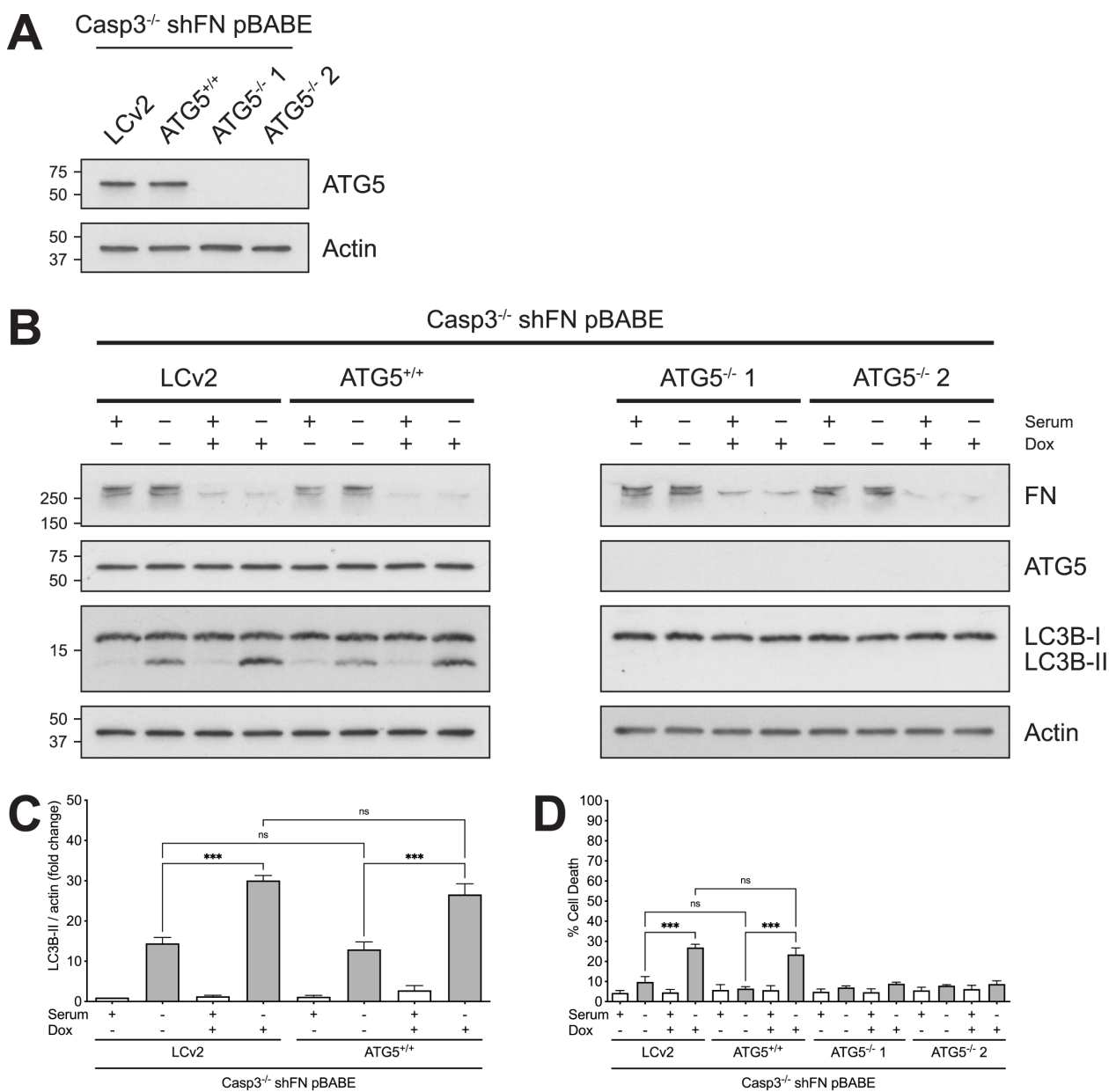
Fig. 6. Ablation of ATG5 expression blocks serum withdrawal-induced death in Casp3-deficient MEFs. (A) Single cell clones with functional ATG5 (Casp3$^{-/-}$ shFN pBABE LCv2 and Casp3$^{-/-}$ shFN pBABE ATG5$^{+/+}$) and single cell clones with loss of ATG5 expression (Casp3$^{-/-}$ shFN pBABE ATG5$^{-/-}$ 1 and Casp3$^{-/-}$ shFN pBABE ATG5$^{-/-}$ 2) were generated. Cell lysates were analyzed via western blot. (B) Casp3$^{-/-}$ shFN pBABE LCv2, C3$^{-/-}$ shFN pBABE ATG5$^{+/+}$, Casp3$^{-/-}$ shFN pBABE ATG5$^{-/-}$ 1, and Casp3$^{-/-}$ shFN

pBABE ATG5$^{-/-}$ 2 MEFs were seeded in medium with or without serum, in the absence or presence of Dox (5µg/ml), and incubated for 24hr. Cell lysates were analyzed via western blot. (C) Quantification of LC3B-II in Casp3$^{-/-}$ shFN pBABE LCv2 and C3$^{-/-}$ shFN pBABE ATG5$^{+/+}$ MEFs in panel B. (D) Cell death was analyzed via annexin V-PI staining and flow cytometry. Data are represented as mean ± s.e.m. All data are from at least three independent experiments. Ordinary one-way ANOVA of Fig. 5C: F = 20.94, p < 0.0001; of Fig. 5D: F = 19.42, p < 0.0001. Šidák's multiple comparisons: ***p ≤ 0.001.
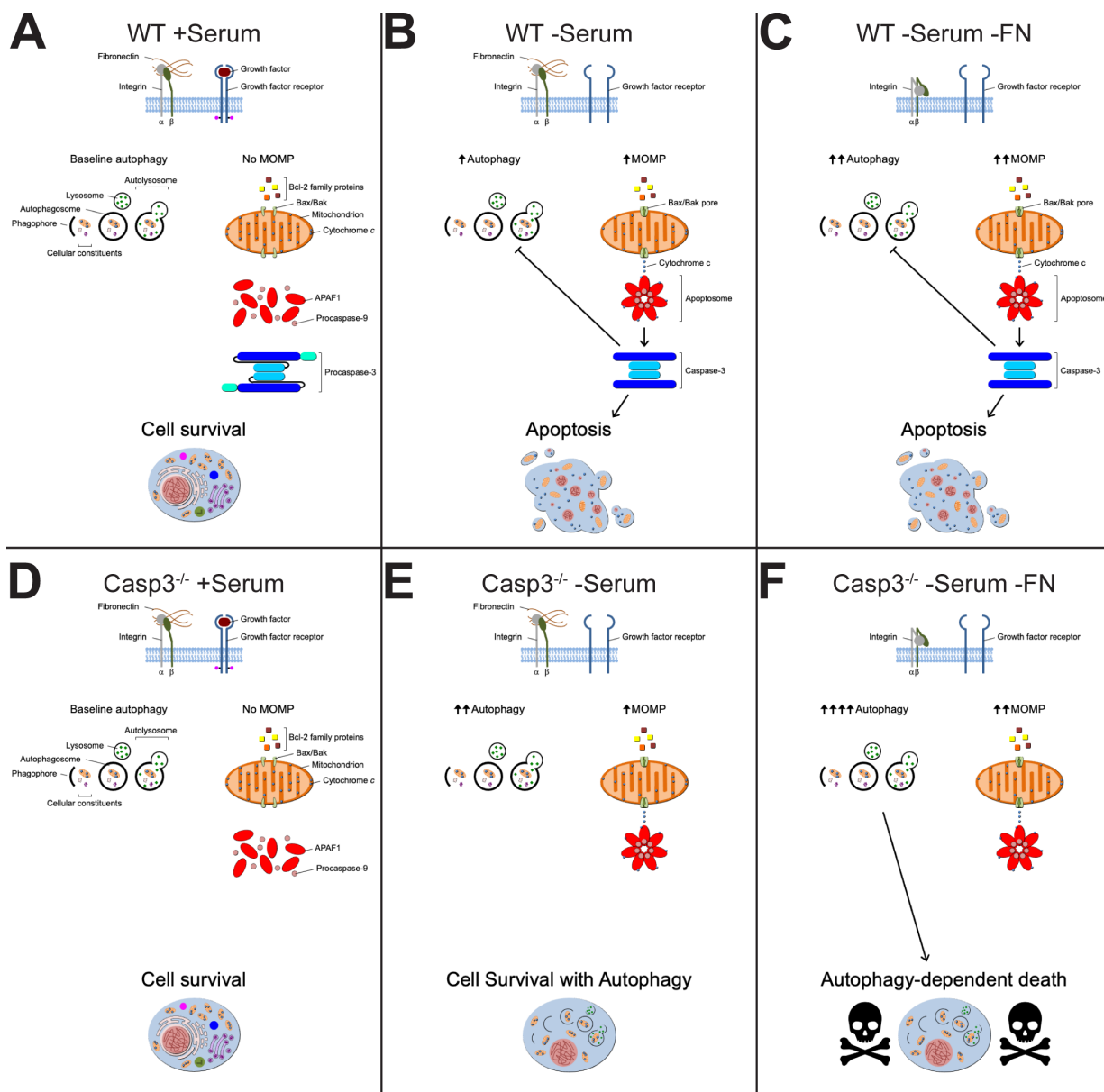
Fig. 7. Casp3-deficient MEFs require FN for protection against autophagy-dependent death following serum withdrawal. (A) WT MEFs grown in medium containing serum have both FN and growth factors for integrins and growth factor receptors to bind to, respectively. Under these conditions, cells have baseline autophagy and no MOMP takes place. (B) Serum withdrawal induces both autophagy and MOMP in WT MEFs. MOMP allows release of cytochrome c from mitochondria, which leads to activation of caspase-3. Once activated, caspase-3 both inhibits autophagy and completes apoptosis. (C) Serum

withdrawal in the absence of FN results in increased autophagy and MOMP in the WT MEF population. Higher amounts of MOMP allows release of more cytochrome *c*, and thus more caspase-3 activation. Elevated levels of active caspase-3 still inhibit autophagy and results in more apoptotic death within the WT MEF population. (D) Casp3-deficient MEFs grown in medium containing serum also have both FN and growth factors for integrins and growth factor receptors to bind to, respectively. Under these conditions, Casp3-deficient MEFs also have baseline autophagy, while no MOMP takes place. (E) In Casp3-deficient MEFs, serum withdrawal induces increased autophagy compared to WT MEFs, but the same amount of MOMP. Caspase-3 is not present to inhibit autophagy or complete apoptosis, and cells survive. (F) In the absence of FN, serum withdrawal induces still more autophagy, as well as increased MOMP in Casp3-deficient MEFs. Cells die in an autophagy-dependent, non-apoptotic fashion.
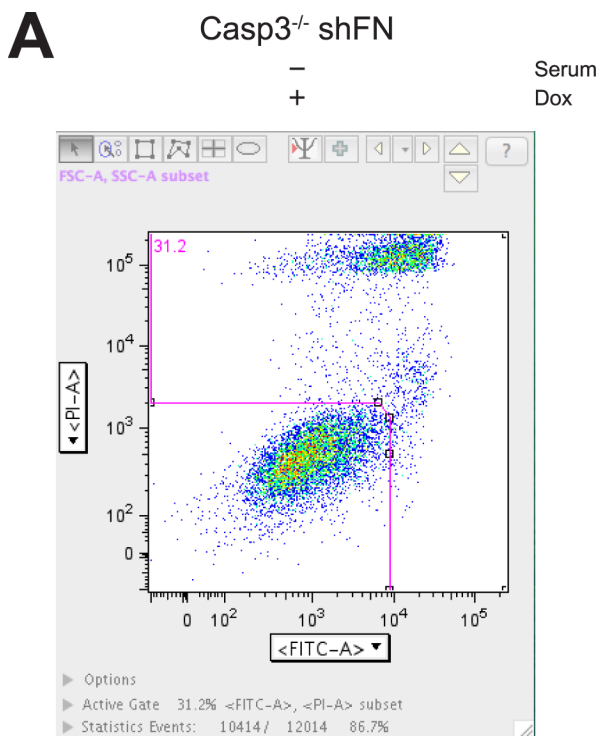
A Casp3^{-/-} shFN

Fig. S1. Representative flow cytometry plot of cell death experiment. (A) Casp3^{-/-} shFN MEFs were seeded in medium without serum, in the presence of Dox (5μg/ml) and incubated for 24hr. Cell death was analyzed via annexin V-PI staining and flow cytometry with the dead cells defined as those in the gate (Annexin V- and/or PI-positive)
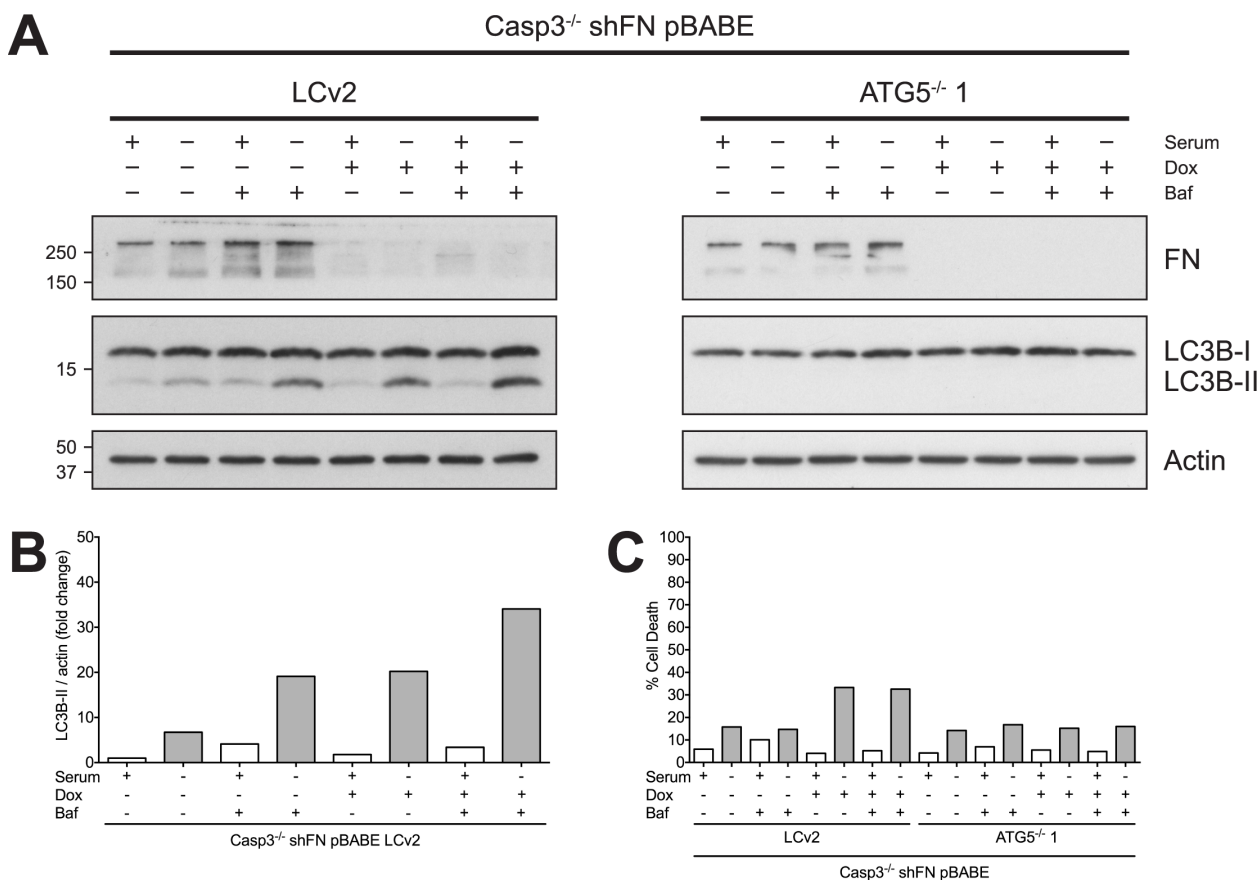
Fig. S2. Inhibition of autophagic flux with Bafilomycin A1 results in increased LC3B-II accumulation following serum withdrawal. (A) Casp3^{-/-} shFN pBABE LCv2 and Casp3^{-/-} shFN pBABE ATG5^{-/-} 1 MEFs were seeded in medium with or without serum, in the absence or presence of Dox (5μg/ml) and incubated for 24hr. Baf (100nM) was added to medium for final 4hr of serum withdrawal where indicated. Cell lysates were analyzed via western blot. (B) Quantification of LC3B-II in Casp3^{-/-} shFN pBABE LCv2 MEFs in panel A. (C) Cell death was analyzed via annexin V-PI staining and flow cytometry.
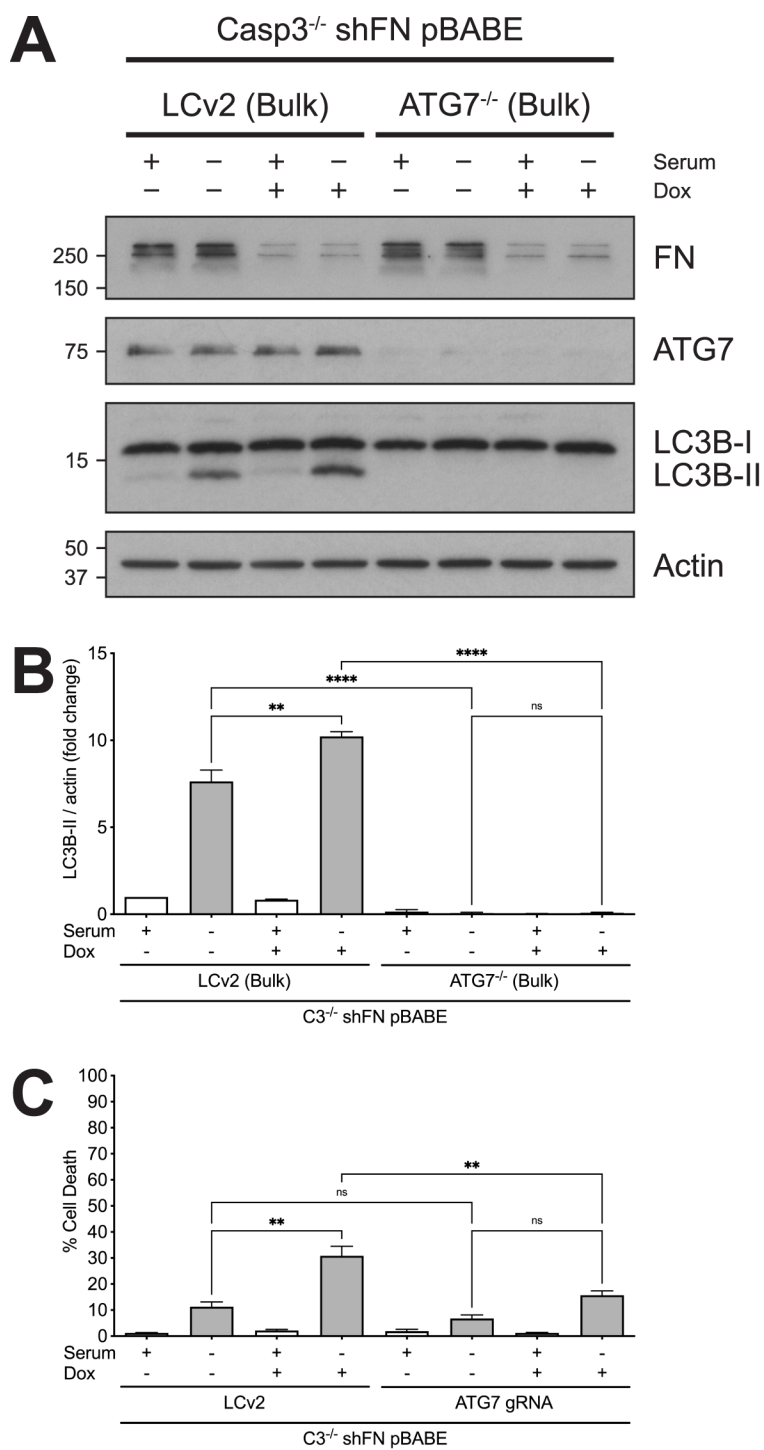
Fig. S3. ATG7 knockout inhibits serum withdrawal-induced death in Casp3-deficient

MEFs. (A) A bulk population of cells with functional ATG7 (Casp3$^{-/-}$ shFN pBABE LCv2

Bulk) and a bulk population of cells with ATG7 knockout (Casp3$^{-/-}$ shFN pBABE ATG7$^{-/-}$ Bulk) were seeded in medium with or without serum, in the absence or presence of Dox (5µg/ml), and incubated for 24hr. Cell lysates were analyzed via western blot. (B) Quantification of LC3B-II in Casp3$^{-/-}$ shFN pBABE LCv2 Bulk and C3$^{-/-}$ shFN pBABE ATG7$^{-/-}$ Bulk MEFs in panel A. (D) Cell death was analyzed via annexin V-PI staining and flow cytometry. Data are represented as mean ± s.e.m. All data are from at least three independent experiments. Ordinary one-way ANOVA: F = 214.1, p < 0.0001; Šidák's multiple comparisons: **p = 0.0036, ****p < 0.0001.
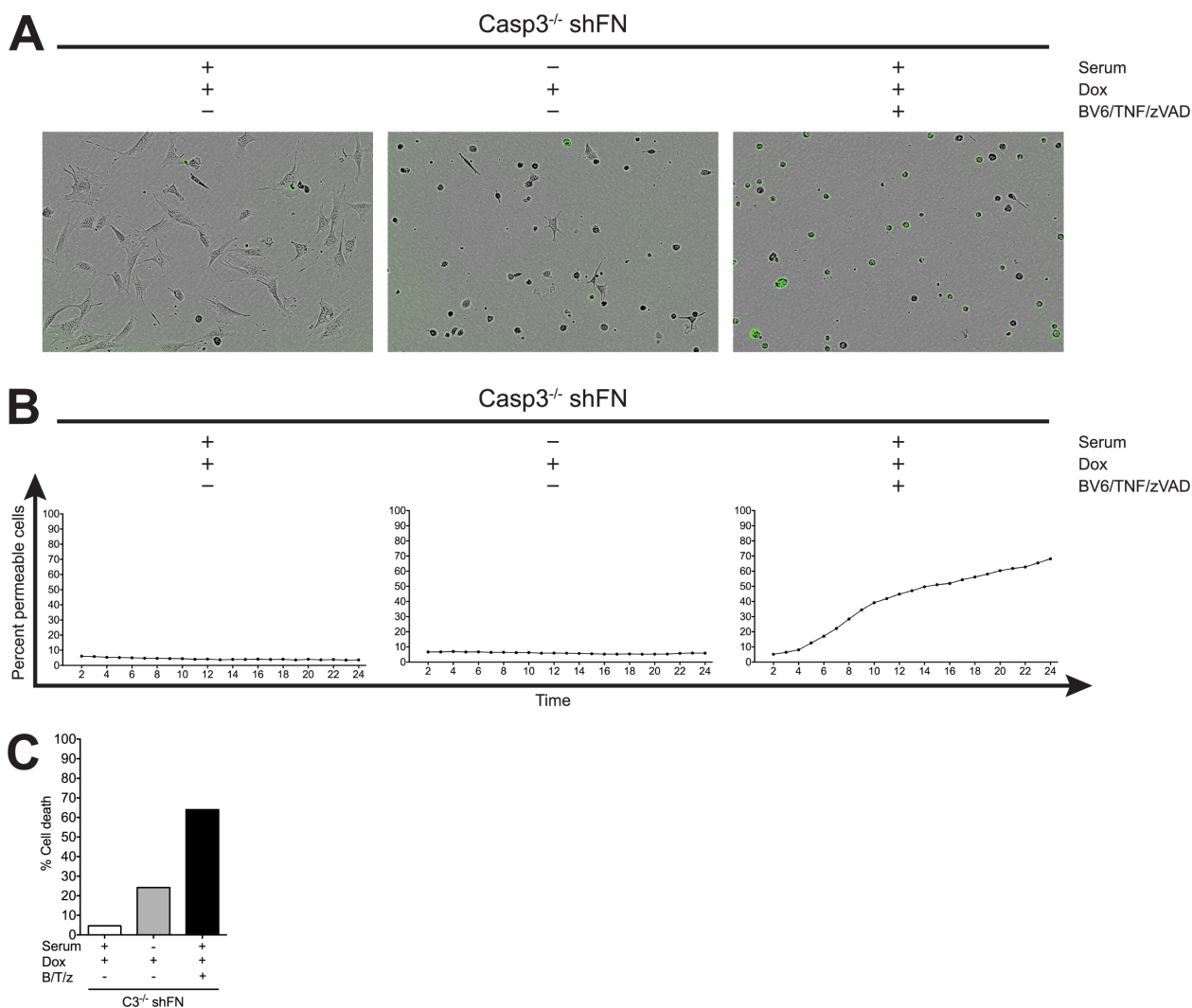
Fig. S4. Casp3-deficient MEFs die in a non-necroptotic fashion following serum withdrawal in the absence of FN. (A) Casp3^{-/-} shFN MEFs were seeded in medium with or without serum, in the presence of Dox (5μg/ml), in the absence or presence of a necroptosis-inducing cocktail [BV6 (0.5μM), TNF (25ng/ml), zVAD (25 μM)], and incubated for 24hr. The cell-impermeant dye Sytox green was included in all conditions. Necroptosis was analyzed via bright field and fluorescence imaging. (B) The percentage of Sytox green-permeable cells was plotted over time. (C) Cell death was analyzed via annexin V-PI staining and flow cytometry.

IV. Discussion

A. Implications of studies

Balance between cell survival and cell death is crucial to the maintenance of healthy tissues and organs. Cells can die via a variety of cellular programs. Understanding of cell death programs sheds light on diseases in which they are nonfunctional or partially functional. Crucially this opens avenues for potential therapies to those diseases. In our studies of caspase-3-deficient fibroblasts, we demonstrated that these cells require fibronectin for protection against autophagy-dependent death due to serum withdrawal. Previous work using these cells investigated changes in apoptosis. Our work, on the other hand, has focused on a non-apoptotic role of caspase-3, specifically its function as a negative regulator of fibronectin secretion. Extensive crosstalk between cell survival and cell death exists. It's possible that autophagy serves as a potential back up mechanism for cells deficient in apoptosis that need to die. This could prove important to diseases with aberrant cell death programs, such as cancer. Resisting cell death is well established as one of the hallmarks of cancer (Hanahan and Weinberg, 2011). If a cell with a nonfunctional apoptotic program were allowed to survive death signals, that cell might become a problem with regards to organismal homeostasis. That cell might continue to grow and divide, possibly picking up genomic instability leading to tumorigenesis. Autophagy-dependent death may function as a failsafe or back up mechanism to prevent tumorigenesis from occurring.

Apoptosis and autophagy have a complex relationship (Maiuri et al., 2007;Eisenberg-Lerner et al., 2009;Fuchs and Steller, 2015;Tsapras and Nezis, 2017). The two molecular pathways can be triggered by the same stimuli, share individual components, and are capable of interacting in several distinct ways (Maiuri et al.,

2007;Eisenberg-Lerner et al., 2009;Fuchs and Steller, 2015;Song et al., 2017;Tsapras and Nezis, 2017), including in collaboration (Espert et al., 2006;Ravikumar et al., 2006;Scott et al., 2007;Pan et al., 2020), as well as in opposition to one another (Boya et al., 2005;Yousefi et al., 2006;Zhu et al., 2010;Tiwari et al., 2011;Pagliarini et al., 2012;Fitzwalter et al., 2018). Crucially, despite the fact that autophagy usually functions as a cytoprotective mechanism (Komatsu et al., 2006;Colell et al., 2007;Sun et al., 2013), it can also cause cell death under certain conditions, including when a cell is incapable of undergoing apoptosis (Shimizu et al., 2004;Yu et al., 2004;Lum et al., 2005;Pattingre et al., 2005;Yu et al., 2006;Lamy et al., 2013;Kim et al., 2018;Denton and Kumar, 2019;Nassour et al., 2019;Zhou et al., 2019). For example, when MEFs lacking the proteins Bax and Bak were treated with etoposide, they were found to die via a non-apoptotic program that is dependent upon autophagic proteins (Shimizu et al., 2004). Furthermore, bone marrow-derived IL-3-dependent Bax/Bak-deficient mouse cells activate autophagy and ultimately succumb to cell death, when withdrawn from IL-3 (Lum et al., 2005). Additionally, autophagic cell death was induced by zVAD in L929 cells when caspase-8 expression was decreased (Yu et al., 2004). It is crucial to note that these previous studies that looked at autophagy-dependent death in the absence of apoptosis blocked MOMP or events upstream of MOMP, while our manipulations were post-MOMP. In these studies, we demonstrate that cells lacking Casp3 become dependent on FN for survival following serum withdrawal, and cells undergo non-apoptotic, autophagy-dependent death. In this particular instance autophagy and apoptosis are working against each other—caspase-3 limits autophagy in WT MEFs, so that when the apoptotic machinery is functioning autophagy is "turned off." In Casp3-deficient MEFs autophagy is functioning as a

cytoprotective mechanism. It is only when Casp3-deficient MEFs do not have fibronectin to bind to that autophagy becomes excessive and cells actually die from this over-active prosurvival pathway.

This work makes an important contribution to understanding how autophagy-dependent cell death is regulated by a fibronectin-dependent mechanism. Prior to these findings, no work had been done relating autophagy-dependent death to cell adhesion. This new knowledge opens up new possibilities in the understanding of certain diseases, including cancer, and applications for therapy. Numerous cancer therapies induce autophagy (Bursch et al., 1996;Kanzawa et al., 2004;Opipari et al., 2004;Natsumeda et al., 2011). When administered low doses of estrogen agonists, MCF-7 breast cancer cells, one of the few cancer cells lacking caspase-3, were shown to have extensive autophagosome formation and die by a non-apoptotic mechanism (Bursch et al., 1996). Targeting cancer cells via promotion of autophagy has been suggested as a therapeutic approach (Levy et al., 2017;Levy and Thorburn, 2020). Many clinical trials have investigated cancer therapies that induce autophagy (Wu et al., 2005;Farag et al., 2009;Nahta and O'Regan, 2010;Rothbart et al., 2010). However, the vast majority of those trials did not involve intentional enhancement of autophagy, nor attempt to determine if autophagy is increased by treatment (Levy and Thorburn, 2011). Most previous investigation focused on autophagy-based therapies has involved inhibiting it (Levy et al., 2017;Levy and Thorburn, 2020). Our findings suggest that research focused on autophagy-based cancer therapies that enhance autophagy may be further warranted. Additionally, there are implications to metastasis, specifically to the ability of cells to survive traveling through the blood stream with no prosurvival signaling from fibronectin-integrin interactions. Given our work

showing that Casp3-deficient MEFs cannot survive serum withdrawal without fibronectin, perhaps cells circulating tumor cells (CTCs) would be vulnerable to an autophagy-inducing therapy. One study found that melanoma cells in lymph experience less oxidative stress and form more metastases than melanoma cells in blood(Ubellacker et al., 2020). Exposure to the lymphatic environment was shown to protect melanoma cells from ferroptosis and increase their ability to survive during subsequent metastasis through blood (Ubellacker et al., 2020). One might wonder if the lymphatic environment might influence autophagy and possibly autophagy-dependent cell death.

B. Opportunities for further research

Our studies demonstrated that fibronectin secretion is regulated by procaspase-3. Our data suggests procaspase-3 plays a role in ER/Golgi transport or vesicle trafficking. However, we never formally demonstrated whether secretion of other extracellular matrix proteins, or cell surface expression of additional adhesion molecules also contributes to this phenotype.

One major caveat to our studies is the use of only a single cell type, namely mouse embryonic fibroblasts. We attempted to apply our studies to one other cell line, but met with little success. Specifically, we attempted to perform serum withdrawal experiments on MCF7 cells. The MCF7 cell line is one of the very few cancer cell lines that lacks caspase-3. Given its central role in apoptosis, one might expect caspase-3 to be frequently lost in cancer. In fact, this is not the case, and caspase-3 is rarely lost in cancer. We used the parental MCF7 cell line, and a daughter cell line that we introduced caspase-3. We ran into difficulties because MCF7 cells lacking caspase-3 died due to serum withdrawal, and

the introduction of caspase-3 did little to change the amount of cell death. This indicates that a death program other than autophagy-dependent death was triggered in those cells. Future research should include an additional cell line that lacks caspase-3. This cell line may have to be generated from a parental cell line that expresses caspase-3.

Another limitation of the current studies is that they are performed only *in vitro*. We hypothesize that the role of autophagy in caspase-3-deficient cells may have implications with regards to cancer. To effectively test this hypothesis, experiments must be performed at the organismal level and not just cells in culture. Future studies should include *in vivo* experiments in murine systems and, if successful, ultimately in human participants.

Despite the limitations of these studies, our findings make some important contributions to the overall understanding of cell death mechanisms. We show that inhibiting apoptosis downstream of MOMP can lead to a program switch to autophagy-dependent death. Additionally, we show that there is a definitive link between fibronectin-mediated adhesion and autophagy-dependent death in the absence of apoptosis.

References

Altman, J.K., Szilard, A., Goussetis, D.J., Sassano, A., Colamonici, M., Gounaris, E., Frankfurt, O., Giles, F.J., Eklund, E.A., Beauchamp, E.M., and Platanias, L.C. (2014). Autophagy is a survival mechanism of acute myelogenous leukemia precursors during dual mTORC2/mTORC1 targeting. *Clin Cancer Res* 20**,** 2400-2409.

Amaravadi, R., Kimmelman, A.C., and White, E. (2016). Recent insights into the function of autophagy in cancer. *Genes Dev* 30**,** 1913-1930.

Aram, L., Yacobi-Sharon, K., and Arama, E. (2017). CDPs: caspase-dependent non-lethal cellular processes. *Cell Death Differ* 24**,** 1307-1310.

Arama, E., Agapite, J., and Steller, H. (2003). Caspase activity and a specific cytochrome C are required for sperm differentiation in Drosophila. *Dev Cell* 4**,** 687-697.

Axe, E.L., Walker, S.A., Manifava, M., Chandra, P., Roderick, H.L., Habermann, A., Griffiths, G., and Ktistakis, N.T. (2008). Autophagosome formation from membrane compartments enriched in phosphatidylinositol 3-phosphate and dynamically connected to the endoplasmic reticulum. *J Cell Biol* 182**,** 685-701.

Baehrecke, E.H. (2005). Autophagy: dual roles in life and death? *Nat Rev Mol Cell Biol* 6**,** 505-510.

Ballestrem, C., Wehrle-Haller, B., Hinz, B., and Imhof, B.A. (2000). Actin-dependent Lamellipodia Formation and Microtubule-dependent Tail Retraction Control-directed Cell Migration.

Bao, Q., and Shi, Y. (2007). Apoptosome: a platform for the activation of initiator caspases. *Cell Death Differ* 14**,** 56-65.

Basu, S., Rajakaruna, S., and Menko, A.S. (2012). "Insulin-like growth factor receptor-1 and nuclear factor kappaB are crucial survival signals that regulate caspase-3-mediated lens epithelial cell differentiation initiation," in *J Biol Chem*. (United States), 8384-8397.

Belaid, A., Cerezo, M., Chargui, A., Corcelle-Termeau, E., Pedeutour, F., Giuliano, S., Ilie, M., Rubera, I., Tauc, M., Barale, S., Bertolotto, C., Brest, P., Vouret-Craviari, V., Klionsky, D.J., Carle, G.F., Hofman, P., and Mograbi, B. (2013). Autophagy plays a critical role in the degradation of active RHOA, the control of cell cytokinesis, and genomic stability. *Cancer Res* 73**,** 4311-4322.

Beningo, K.A., Dembo, M., Kaverina, I., Small, J.V., and Wang, Y.L. (2001). Nascent focal adhesions are responsible for the generation of strong propulsive forces in migrating fibroblasts. *J Cell Biol* 153**,** 881-888.

Bialik, S., and Dasari, S.K. (2018). Autophagy-dependent cell death - where, how and why a cell eats itself to death. 131.

Boatright, K.M., Renatus, M., Scott, F.L., Sperandio, S., Shin, H., Pedersen, I.M., Ricci, J.E., Edris, W.A., Sutherlin, D.P., Green, D.R., and Salvesen, G.S. (2003). A unified model for apical caspase activation. *Mol Cell* 11**,** 529-541.

Boya, P., González-Polo, R.A., Casares, N., Perfettini, J.L., Dessen, P., Larochette, N., Métivier, D., Meley, D., Souquere, S., Yoshimori, T., Pierron, G., Codogno, P., and Kroemer, G. (2005). Inhibition of macroautophagy triggers apoptosis. *Mol Cell Biol* 25**,** 1025-1040.

Brentnall, M., Rodriguez-Menocal, L., De Guevara, R.L., Cepero, E., and Boise, L.H. (2013). Caspase-9, caspase-3 and caspase-7 have distinct roles during intrinsic apoptosis. *BMC Cell Biol* 14**,** 32.

Brentnall, M., Weir, D.B., Rongvaux, A., Marcus, A.I., and Boise, L.H. (2014). Procaspase-3 regulates fibronectin secretion and influences adhesion, migration and survival independently of catalytic function. *J Cell Sci* 127**,** 2217-2226.

Brooks, P.C., Klemke, R.L., Schon, S., Lewis, J.M., Schwartz, M.A., and Cheresh, D.A. (1997). Insulin-like growth factor receptor cooperates with integrin alpha v beta 5 to promote tumor cell dissemination in vivo. *J Clin Invest* 99**,** 1390-1398.

Bursch, W., Ellinger, A., Kienzl, H., Török, L., Pandey, S., Sikorska, M., Walker, R., and Hermann, R.S. (1996). Active cell death induced by the anti-estrogens tamoxifen and ICI 164 384 in human mammary carcinoma cells (MCF-7) in culture: the role of autophagy. *Carcinogenesis* 17**,** 1595-1607.

Cerretti, D.P., Kozlosky, C.J., Mosley, B., Nelson, N., Van Ness, K., Greenstreet, T.A., March, C.J., Kronheim, S.R., Druck, T., Cannizzaro, L.A., and Et Al. (1992). Molecular cloning of the interleukin-1 beta converting enzyme. *Science* 256**,** 97-100.

Chen, N., and Debnath, J. (2013). IκB kinase complex (IKK) triggers detachment-induced autophagy in mammary epithelial cells independently of the PI3K-AKT-MTORC1 pathway. *Autophagy* 9**,** 1214-1227.

Chen, S.Y., Chiu, L.Y., Maa, M.C., Wang, J.S., Chien, C.L., and Lin, W.W. (2011). zVAD-induced autophagic cell death requires c-Src-dependent ERK and JNK activation and reactive oxygen species generation. *Autophagy* 7**,** 217-228.

Cheng, Y.J., Lee, C.H., Lin, Y.P., Huang, J.Y., Su, C.C., Chang, W.T., and Yang, B.C. (2008). Caspase-3 enhances lung metastasis and cell migration in a protease-independent mechanism through the ERK pathway. *Int J Cancer* 123**,** 1278-1285.

Chera, S., Ghila, L., Dobretz, K., Wenger, Y., Bauer, C., Buzgariu, W., Martinou, J.C., and Galliot, B. (2009). "Apoptotic cells provide an unexpected source of Wnt3 signaling to drive hydra head regeneration," in *Dev Cell*. (United States), 279-289.

Chipuk, J.E., Moldoveanu, T., Llambi, F., Parsons, M.J., and Green, D.R. (2010). The BCL-2 family reunion. *Mol Cell* 37**,** 299-310.

Cho, D.H., Jo, Y.K., Hwang, J.J., Lee, Y.M., Roh, S.A., and Kim, J.C. (2009). Caspase-mediated cleavage of ATG6/Beclin-1 links apoptosis to autophagy in HeLa cells. *Cancer Lett* 274**,** 95-100.

Clarke, P.G. (1990). Developmental cell death: morphological diversity and multiple mechanisms. *Anat Embryol (Berl)* 181**,** 195-213.

Clarke, P.G., and Clarke, S. (1996). Nineteenth century research on naturally occurring cell death and related phenomena. *Anat Embryol (Berl)* 193**,** 81-99.

Colell, A., Ricci, J.E., Tait, S., Milasta, S., Maurer, U., Bouchier-Hayes, L., Fitzgerald, P., Guio-Carrion, A., Waterhouse, N.J., Li, C.W., Mari, B., Barbry, P., Newmeyer, D.D., Beere, H.M., and Green, D.R. (2007). GAPDH and autophagy preserve survival after apoptotic cytochrome c release in the absence of caspase activation. *Cell* 129**,** 983-997.

Cornelis, S., Bruynooghe, Y., Van Loo, G., Saelens, X., Vandenabeele, P., and Beyaert, R. (2005). Apoptosis of hematopoietic cells induced by growth factor withdrawal

is associated with caspase-9 mediated cleavage of Raf-1. *Oncogene* 24**,** 1552-1562.

Creagh, E.M., and Martin, S.J. (2001). Caspases: cellular demolition experts. *Biochem Soc Trans* 29**,** 696-702.

Czabotar, P.E., Lessene, G., Strasser, A., and Adams, J.M. (2014). Control of apoptosis by the BCL-2 protein family: implications for physiology and therapy. *Nat Rev Mol Cell Biol* 15**,** 49-63.

D'amelio, M., Cavallucci, V., and Cecconi, F. (2010). Neuronal caspase-3 signaling: not only cell death. *Cell Death Differ* 17**,** 1104-1114.

Danial, N.N., Gramm, C.F., Scorrano, L., Zhang, C.Y., Krauss, S., Ranger, A.M., Datta, S.R., Greenberg, M.E., Licklider, L.J., Lowell, B.B., Gygi, S.P., and Korsmeyer, S.J. (2003). BAD and glucokinase reside in a mitochondrial complex that integrates glycolysis. *Nature* 424**,** 952-956.

Danial, N.N., and Korsmeyer, S.J. (2004). Cell death: critical control points. *Cell* 116**,** 205-219.

Danial, N.N., Walensky, L.D., Zhang, C.Y., Choi, C.S., Fisher, J.K., Molina, A.J., Datta, S.R., Pitter, K.L., Bird, G.H., Wikstrom, J.D., Deeney, J.T., Robertson, K., Morash, J., Kulkarni, A., Neschen, S., Kim, S., Greenberg, M.E., Corkey, B.E., Shirihai, O.S., Shulman, G.I., Lowell, B.B., and Korsmeyer, S.J. (2008). Dual role of proapoptotic BAD in insulin secretion and beta cell survival. *Nat Med* 14**,** 144-153.

Debnath, J., Baehrecke, E.H., and Kroemer, G. (2005). Does autophagy contribute to cell death? *Autophagy* 1**,** 66-74.

Degenhardt, K., Mathew, R., Beaudoin, B., Bray, K., Anderson, D., Chen, G., Mukherjee, C., Shi, Y., Gélinas, C., Fan, Y., Nelson, D.A., Jin, S., and White, E. (2006). Autophagy promotes tumor cell survival and restricts necrosis, inflammation, and tumorigenesis. *Cancer Cell* 10**,** 51-64.

Degterev, A., Boyce, M., and Yuan, J. (2003). A decade of caspases. *Oncogene* 22**,** 8543-8567.

Denton, D., and Kumar, S. (2019). Autophagy-dependent cell death. *Cell Death Differ* 26**,** 605-616.

Dix, M.M., Simon, G.M., and Cravatt, B.F. (2008). Global mapping of the topography and magnitude of proteolytic events in apoptosis. *Cell* 134**,** 679-691.

Dorstyn, L., Akey, C.W., and Kumar, S. (2018). New insights into apoptosome structure and function. *Cell Death Differ* 25**,** 1194-1208.

Dou, Z., Xu, C., Donahue, G., Shimi, T., Pan, J.A., Zhu, J., Ivanov, A., Capell, B.C., Drake, A.M., Shah, P.P., Catanzaro, J.M., Ricketts, M.D., Lamark, T., Adam, S.A., Marmorstein, R., Zong, W.X., Johansen, T., Goldman, R.D., Adams, P.D., and Berger, S.L. (2015). Autophagy mediates degradation of nuclear lamina. *Nature* 527**,** 105-109.

Earnshaw, W.C., Martins, L.M., and Kaufmann, S.H. (1999). Mammalian caspases: structure, activation, substrates, and functions during apoptosis. *Annu Rev Biochem* 68**,** 383-424.

Eisenberg-Lerner, A., Bialik, S., Simon, H.U., and Kimchi, A. (2009). Life and death partners: apoptosis, autophagy and the cross-talk between them. *Cell Death Differ* 16**,** 966-975.

Elliott, M.R., and Ravichandran, K.S. (2016). The Dynamics of Apoptotic Cell Clearance. *Dev Cell* 38**,** 147-160.

Ellis, H.M., and Horvitz, H.R. (1986). Genetic control of programmed cell death in the nematode C. elegans. *Cell* 44**,** 817-829.

Elmore, S. (2007). Apoptosis: a review of programmed cell death. *Toxicol Pathol* 35**,** 495-516.

Enari, M., Sakahira, H., Yokoyama, H., Okawa, K., Iwamatsu, A., and Nagata, S. (1998). A caspase-activated DNase that degrades DNA during apoptosis, and its inhibitor ICAD. *Nature* 391**,** 43-50.

Espert, L., Denizot, M., Grimaldi, M., Robert-Hebmann, V., Gay, B., Varbanov, M., Codogno, P., and Biard-Piechaczyk, M. (2006). Autophagy is involved in T cell death after binding of HIV-1 envelope proteins to CXCR4. *J Clin Invest* 116**,** 2161-2172.

Eum, K.H., and Lee, M. (2011). Crosstalk between autophagy and apoptosis in the regulation of paclitaxel-induced cell death in v-Ha-ras-transformed fibroblasts. *Mol Cell Biochem* 348**,** 61-68.

Farag, S.S., Zhang, S., Jansak, B.S., Wang, X., Kraut, E., Chan, K., Dancey, J.E., and Grever, M.R. (2009). Phase II trial of temsirolimus in patients with relapsed or refractory multiple myeloma. *Leuk Res* 33**,** 1475-1480.

Fink, S.L., and Cookson, B.T. (2005). Apoptosis, pyroptosis, and necrosis: mechanistic description of dead and dying eukaryotic cells. *Infect Immun* 73**,** 1907-1916.

Finlay, D., and Vuori, K. (2007). Novel noncatalytic role for caspase-8 in promoting SRC-mediated adhesion and Erk signaling in neuroblastoma cells. *Cancer Res* 67**,** 11704-11711.

Fitzwalter, B.E., Towers, C.G., Sullivan, K.D., Andrysik, Z., Hoh, M., Ludwig, M., O'prey, J., Ryan, K.M., Espinosa, J.M., Morgan, M.J., and Thorburn, A. (2018). Autophagy Inhibition Mediates Apoptosis Sensitization in Cancer Therapy by Relieving FOXO3a Turnover. *Dev Cell* 44**,** 555-565.e553.

Fuchs, Y., and Steller, H. (2011). Programmed cell death in animal development and disease. *Cell* 147**,** 742-758.

Fuchs, Y., and Steller, H. (2015). Live to die another way: modes of programmed cell death and the signals emanating from dying cells. *Nat Rev Mol Cell Biol* 16**,** 329-344.

Fuentes-Prior, P., and Salvesen, G.S. (2004). The protein structures that shape caspase activity, specificity, activation and inhibition. *Biochem J* 384**,** 201-232.

Fujita, J., Crane, A.M., Souza, M.K., Dejosez, M., Kyba, M., Flavell, R.A., Thomson, J.A., and Zwaka, T.P. (2008). Caspase activity mediates the differentiation of embryonic stem cells. *Cell Stem Cell* 2**,** 595-601.

Fung, C., Lock, R., Gao, S., Salas, E., and Debnath, J. (2008). Induction of autophagy during extracellular matrix detachment promotes cell survival. *Mol Biol Cell* 19**,** 797-806.

Galluzzi, L., Baehrecke, E.H., Ballabio, A., Boya, P., Bravo-San Pedro, J.M., Cecconi, F., Choi, A.M., Chu, C.T., Codogno, P., Colombo, M.I., Cuervo, A.M., Debnath, J., Deretic, V., Dikic, I., Eskelinen, E.L., Fimia, G.M., Fulda, S., Gewirtz, D.A., Green, D.R., Hansen, M., Harper, J.W., Jäättelä, M., Johansen, T., Juhasz, G., Kimmelman, A.C., Kraft, C., Ktistakis, N.T., Kumar, S., Levine, B., Lopez-Otin,

C., Madeo, F., Martens, S., Martinez, J., Melendez, A., Mizushima, N., Münz, C., Murphy, L.O., Penninger, J.M., Piacentini, M., Reggiori, F., Rubinsztein, D.C., Ryan, K.M., Santambrogio, L., Scorrano, L., Simon, A.K., Simon, H.U., Simonsen, A., Tavernarakis, N., Tooze, S.A., Yoshimori, T., Yuan, J., Yue, Z., Zhong, Q., and Kroemer, G. (2017a). Molecular definitions of autophagy and related processes. *Embo j* 36**,** 1811-1836.

Galluzzi, L., Bravo-San Pedro, J.M., Levine, B., Green, D.R., and Kroemer, G. (2017b). Pharmacological modulation of autophagy: therapeutic potential and persisting obstacles. *Nat Rev Drug Discov* 16**,** 487-511.

Galluzzi, L., and Green, D.R. (2019). Autophagy-Independent Functions of the Autophagy Machinery. *Cell* 177**,** 1682-1699.

Galluzzi, L., Vitale, I., Aaronson, S.A., Abrams, J.M., Adam, D., Agostinis, P., Alnemri, E.S., Altucci, L., Amelio, I., Andrews, D.W., Annicchiarico-Petruzzelli, M., Antonov, A.V., Arama, E., Baehrecke, E.H., Barlev, N.A., Bazan, N.G., Bernassola, F., Bertrand, M.J.M., Bianchi, K., Blagosklonny, M.V., Blomgren, K., Borner, C., Boya, P., Brenner, C., Campanella, M., Candi, E., Carmona-Gutierrez, D., Cecconi, F., Chan, F.K., Chandel, N.S., Cheng, E.H., Chipuk, J.E., Cidlowski, J.A., Ciechanover, A., Cohen, G.M., Conrad, M., Cubillos-Ruiz, J.R., Czabotar, P.E., D'angiolella, V., Dawson, T.M., Dawson, V.L., De Laurenzi, V., De Maria, R., Debatin, K.M., Deberardinis, R.J., Deshmukh, M., Di Daniele, N., Di Virgilio, F., Dixit, V.M., Dixon, S.J., Duckett, C.S., Dynlacht, B.D., El-Deiry, W.S., Elrod, J.W., Fimia, G.M., Fulda, S., Garcia-Saez, A.J., Garg, A.D., Garrido, C., Gavathiotis, E., Golstein, P., Gottlieb, E., Green, D.R., Greene, L.A., Gronemeyer, H., Gross, A., Hajnoczky, G., Hardwick, J.M., Harris, I.S., Hengartner, M.O., Hetz, C., Ichijo, H., Jaattela, M., Joseph, B., Jost, P.J., Juin, P.P., Kaiser, W.J., Karin, M., Kaufmann, T., Kepp, O., Kimchi, A., Kitsis, R.N., Klionsky, D.J., Knight, R.A., Kumar, S., Lee, S.W., Lemasters, J.J., Levine, B., Linkermann, A., Lipton, S.A., Lockshin, R.A., Lopez-Otin, C., Lowe, S.W., Luedde, T., Lugli, E., Macfarlane, M., Madeo, F., Malewicz, M., Malorni, W., Manic, G., et al. (2018). Molecular mechanisms of cell death: recommendations of the Nomenclature Committee on Cell Death 2018. *Cell Death Differ* 25**,** 486-541.

Gao, M., Monian, P., Pan, Q., Zhang, W., Xiang, J., and Jiang, X. (2016). Ferroptosis is an autophagic cell death process. *Cell Res* 26**,** 1021-1032.

Gardel, M.L., Schneider, I.C., Yvonne Aratyn-Schaus, and Waterman, C.M. (2010). Mechanical Integration of Actin and Adhesion Dynamics in Cell Migration. *http://dx.doi.org/10.1146/annurev.cellbio.011209.122036*.

Ghavami, S., Hashemi, M., Ande, S.R., Yeganeh, B., Xiao, W., Eshraghi, M., Bus, C.J., Kadkhoda, K., Wiechec, E., Halayko, A.J., and Los, M. (2009). Apoptosis and cancer: mutations within caspase genes. *J Med Genet* 46**,** 497-510.

Green, D.R., and Levine, B. (2014). To be or not to be? How selective autophagy and cell death govern cell fate. *Cell* 157**,** 65-75.

Green, D.R., and Llambi, F. (2015). Cell Death Signaling. *Cold Spring Harb Perspect Biol* 7.

Gross, A., and Katz, S.G. (2017). Non-apoptotic functions of BCL-2 family proteins. *Cell Death Differ* 24**,** 1348-1358.

Gumbiner, B.M. (1996). "Cell adhesion: the molecular basis of tissue architecture and morphogenesis," in *Cell*. (United States), 345-357.

Gump, J.M., Staskiewicz, L., Morgan, M.J., Bamberg, A., Riches, D.W., and Thorburn, A. (2014). Autophagy variation within a cell population determines cell fate through selective degradation of Fap-1. *Nat Cell Biol* 16**,** 47-54.

Hailey, D.W., Rambold, A.S., Satpute-Krishnan, P., Mitra, K., Sougrat, R., Kim, P.K., and Lippincott-Schwartz, J. (2010). Mitochondria supply membranes for autophagosome biogenesis during starvation. *Cell* 141**,** 656-667.

Hanahan, D., and Weinberg, R.A. (2011). Hallmarks of cancer: the next generation. *Cell* 144**,** 646-674.

He, W., Wang, Q., Srinivasan, B., Xu, J., Padilla, M.T., Li, Z., Wang, X., Liu, Y., Gou, X., Shen, H.M., Xing, C., and Lin, Y. (2014). A JNK-mediated autophagy pathway that triggers c-IAP degradation and necroptosis for anticancer chemotherapy. *Oncogene* 33**,** 3004-3013.

Hengartner, M.O. (2000). The biochemistry of apoptosis. *Nature* 407**,** 770-776.

Hengartner, M.O., Ellis, R.E., and Horvitz, H.R. (1992). Caenorhabditis elegans gene ced-9 protects cells from programmed cell death. *Nature* 356**,** 494-499.

Hengartner, M.O., and Horvitz, H.R. (1994). Programmed cell death in Caenorhabditis elegans. *Curr Opin Genet Dev* 4**,** 581-586.

Henry, C.M., and Martin, S.J. (2017). Caspase-8 Acts in a Non-enzymatic Role as a Scaffold for Assembly of a Pro-inflammatory "FADDosome" Complex upon TRAIL Stimulation. *Mol Cell* 65**,** 715-729.e715.

Horton, E.R., Byron, A., Askari, J.A., Ng, D.H.J., Millon-Frémillon, A., Robertson, J., Koper, E.J., Paul, N.R., Warwood, S., Knight, D., Humphries, J.D., and Humphries, M.J. (2015). Definition of a consensus integrin adhesome and its dynamics during adhesion complex assembly and disassembly. *Nat Cell Biol* 17**,** 1577-1587.

Hou, W., Xie, Y., Song, X., Sun, X., Lotze, M.T., Zeh, H.J., 3rd, Kang, R., and Tang, D. (2016). Autophagy promotes ferroptosis by degradation of ferritin. *Autophagy* 12**,** 1425-1428.

Humphries, M.J. (2009). Cell adhesion assays. *Methods Mol Biol* 522**,** 203-210.

Ishizaki, Y., Cheng, L., Mudge, A.W., and Raff, M.C. (1995). Programmed cell death by default in embryonic cells, fibroblasts, and cancer cells. *Mol Biol Cell* 6**,** 1443-1458.

Ishizaki, Y., Jacobson, M.D., and Raff, M.C. (1998). A role for caspases in lens fiber differentiation. *J Cell Biol* 140**,** 153-158.

Jäger, R., and Zwacka, R.M. (2010a). The enigmatic roles of caspases in tumor development. *Cancers (Basel)* 2**,** 1952-1979.

Jäger, R., and Zwacka, R.M. (2010b). The Enigmatic Roles of Caspases in Tumor Development. *Cancers* 2**,** 1952-1979.

Jänicke, R.U., Ng, P., Sprengart, M.L., and Porter, A.G. (1998). Caspase-3 is required for alpha-fodrin cleavage but dispensable for cleavage of other death substrates in apoptosis. *J Biol Chem* 273**,** 15540-15545.

Janzen, V., Fleming, H.E., Riedt, T., Karlsson, G., Riese, M.J., Lo Celso, C., Reynolds, G., Milne, C.D., Paige, C.J., Karlsson, S., Woo, M., and Scadden, D.T. (2008).

Hematopoietic stem cell responsiveness to exogenous signals is limited by caspase-3. *Cell Stem Cell* 2**,** 584-594.

Jiang, X., and Wang, X. (2004). Cytochrome C-mediated apoptosis. *Annu Rev Biochem* 73**,** 87-106.

Johansson, S., Svineng, G., Wennerberg, K., Armulik, A., and Lohikangas, L. (1997). Fibronectin-integrin interactions. *Front Biosci* 2**,** d126-146.

Johnson, B.W., and Boise, L.H. (1999). Bcl-2 and caspase inhibition cooperate to inhibit tumor necrosis factor-alpha-induced cell death in a Bcl-2 cleavage-independent fashion. *J Biol Chem* 274**,** 18552-18558.

Julien, O., and Wells, J.A. (2017). Caspases and their substrates. *Cell Death Differ* 24**,** 1380-1389.

Kabeya, Y., Mizushima, N., Ueno, T., Yamamoto, A., Kirisako, T., Noda, T., Kominami, E., Ohsumi, Y., and Yoshimori, T. (2000). LC3, a mammalian homologue of yeast Apg8p, is localized in autophagosome membranes after processing. *Embo j* 19**,** 5720-5728.

Kabeya, Y., Mizushima, N., Yamamoto, A., Oshitani-Okamoto, S., Ohsumi, Y., and Yoshimori, T. (2004). LC3, GABARAP and GATE16 localize to autophagosomal membrane depending on form-II formation. *J Cell Sci* 117**,** 2805-2812.

Kaiser, W.J., Upton, J.W., Long, A.B., Livingston-Rosanoff, D., Daley-Bauer, L.P., Hakem, R., Caspary, T., and Mocarski, E.S. (2011). RIP3 mediates the embryonic lethality of caspase-8-deficient mice. *Nature* 471**,** 368-372.

Kale, J., Osterlund, E.J., and Andrews, D.W. (2018). BCL-2 family proteins: changing partners in the dance towards death. *Cell Death Differ* 25**,** 65-80.

Kalkavan, H., and Green, D.R. (2018). MOMP, cell suicide as a BCL-2 family business. *Cell Death Differ* 25**,** 46-55.

Kamber Kaya, H.E., Ditzel, M., Meier, P., and Bergmann, A. (2017). An inhibitory mono-ubiquitylation of the Drosophila initiator caspase Dronc functions in both apoptotic and non-apoptotic pathways. *PLoS Genet* 13**,** e1006438.

Kang, M.R., Kim, M.S., Oh, J.E., Kim, Y.R., Song, S.Y., Kim, S.S., Ahn, C.H., Yoo, N.J., and Lee, S.H. (2009). Frameshift mutations of autophagy-related genes ATG2B, ATG5, ATG9B and ATG12 in gastric and colorectal cancers with microsatellite instability. *J Pathol* 217**,** 702-706.

Kanzawa, T., Germano, I.M., Komata, T., Ito, H., Kondo, Y., and Kondo, S. (2004). Role of autophagy in temozolomide-induced cytotoxicity for malignant glioma cells. *Cell Death Differ* 11**,** 448-457.

Karantza-Wadsworth, V., Patel, S., Kravchuk, O., Chen, G., Mathew, R., Jin, S., and White, E. (2007). Autophagy mitigates metabolic stress and genome damage in mammary tumorigenesis. *Genes Dev* 21**,** 1621-1635.

Kaushik, S., and Cuervo, A.M. (2012). Chaperone-mediated autophagy: a unique way to enter the lysosome world. *Trends Cell Biol* 22**,** 407-417.

Kaushik, S., and Cuervo, A.M. (2018). The coming of age of chaperone-mediated autophagy. *Nat Rev Mol Cell Biol* 19**,** 365-381.

Kechagia, J.Z., and Ivaska, J. (2019). Integrins as biomechanical sensors of the microenvironment. 20**,** 457-473.

Keller, M., Rüegg, A., Werner, S., and Beer, H.D. (2008). Active caspase-1 is a regulator of unconventional protein secretion. *Cell* 132**,** 818-831.

Kerr, J.F., Wyllie, A.H., and Currie, A.R. (1972). Apoptosis: a basic biological phenomenon with wide-ranging implications in tissue kinetics. *Br J Cancer* 26**,** 239-257.

Kesavardhana, S., Malireddi, R.K.S., and Kanneganti, T.D. (2020). Caspases in Cell Death, Inflammation, and Pyroptosis. *Annu Rev Immunol* 38**,** 567-595.

Kim, T.W., Lee, S.Y., Kim, M., Cheon, C., and Ko, S.G. (2018). Kaempferol induces autophagic cell death via IRE1-JNK-CHOP pathway and inhibition of G9a in gastric cancer cells. *Cell Death Dis* 9**,** 875.

Klionsky, D.J. (2008). Autophagy revisited: a conversation with Christian de Duve. *Autophagy* 4**,** 740-743.

Klionsky, D.J., Abdel-Aziz, A.K., Abdelfatah, S., Abdellatif, M., Abdoli, A., Abel, S., Abeliovich, H., Abildgaard, M.H., Abudu, Y.P., Acevedo-Arozena, A., Adamopoulos, I.E., Adeli, K., Adolph, T.E., Adornetto, A., Aflaki, E., Agam, G., Agarwal, A., Aggarwal, B.B., Agnello, M., Agostinis, P., Agrewala, J.N., Agrotis, A., Aguilar, P.V., Ahmad, S.T., Ahmed, Z.M., Ahumada-Castro, U., Aits, S., Aizawa, S., Akkoc, Y., Akoumianaki, T., Akpinar, H.A., Al-Abd, A.M., Al-Akra, L., Al-Gharaibeh, A., Alaoui-Jamali, M.A., Alberti, S., Alcocer-Gómez, E., Alessandri, C., Ali, M., Alim Al-Bari, M.A., Aliwaini, S., Alizadeh, J., Almacellas, E., Almasan, A., Alonso, A., Alonso, G.D., Altan-Bonnet, N., Altieri, D.C., Álvarez É, M.C., Alves, S., Alves Da Costa, C., Alzaharna, M.M., Amadio, M., Amantini, C., Amaral, C., Ambrosio, S., Amer, A.O., Ammanathan, V., An, Z., Andersen, S.U., Andrabi, S.A., Andrade-Silva, M., Andres, A.M., Angelini, S., Ann, D., Anozie, U.C., Ansari, M.Y., Antas, P., Antebi, A., Antón, Z., Anwar, T., Apetoh, L., Apostolova, N., Araki, T., Araki, Y., Arasaki, K., Araújo, W.L., Araya, J., Arden, C., Arévalo, M.A., Arguelles, S., Arias, E., Arikkath, J., Arimoto, H., Ariosa, A.R., Armstrong-James, D., Arnauné-Pelloquin, L., Aroca, A., Arroyo, D.S., Arsov, I., Artero, R., Asaro, D.M.L., Aschner, M., Ashrafizadeh, M., Ashur-Fabian, O., Atanasov, A.G., Au, A.K., Auberger, P., Auner, H.W., Aurelian, L., et al. (2021). Guidelines for the use and interpretation of assays for monitoring autophagy (4th edition)(1). *Autophagy* 17**,** 1-382.

Klionsky, D.J., Abdelmohsen, K., Abe, A., Abedin, M.J., Abeliovich, H., Acevedo Arozena, A., Adachi, H., Adams, C.M., Adams, P.D., Adeli, K., Adhihetty, P.J., Adler, S.G., Agam, G., Agarwal, R., Aghi, M.K., Agnello, M., Agostinis, P., Aguilar, P.V., Aguirre-Ghiso, J., Airoldi, E.M., Ait-Si-Ali, S., Akematsu, T., Akporiaye, E.T., Al-Rubeai, M., Albaiceta, G.M., Albanese, C., Albani, D., Albert, M.L., Aldudo, J., Algül, H., Alirezaei, M., Alloza, I., Almasan, A., Almonte-Beceril, M., Alnemri, E.S., Alonso, C., Altan-Bonnet, N., Altieri, D.C., Alvarez, S., Alvarez-Erviti, L., Alves, S., Amadoro, G., Amano, A., Amantini, C., Ambrosio, S., Amelio, I., Amer, A.O., Amessou, M., Amon, A., An, Z., Anania, F.A., Andersen, S.U., Andley, U.P., Andreadi, C.K., Andrieu-Abadie, N., Anel, A., Ann, D.K., Anoopkumar-Dukie, S., Antonioli, M., Aoki, H., Apostolova, N., Aquila, S., Aquilano, K., Araki, K., Arama, E., Aranda, A., Araya, J., Arcaro, A., Arias, E., Arimoto, H., Ariosa, A.R., Armstrong, J.L., Arnould, T., Arsov, I., Asanuma, K., Askanas, V., Asselin, E., Atarashi, R., Atherton, S.S., Atkin, J.D., Attardi, L.D., Auberger, P., Auburger, G., Aurelian, L., Autelli, R., Avagliano, L., Avantaggiati, M.L., Avrahami, L., Awale, S., Azad, N., Bachetti, T., Backer,

J.M., Bae, D.H., Bae, J.S., Bae, O.N., Bae, S.H., Baehrecke, E.H., Baek, S.H., Baghdiguian, S., Bagniewska-Zadworna, A., et al. (2016). Guidelines for the use and interpretation of assays for monitoring autophagy (3rd edition). *Autophagy* 12**,** 1-222.

Klionsky, D.J., and Emr, S.D. (2000). Autophagy as a regulated pathway of cellular degradation. *Science* 290**,** 1717-1721.

Kluck, R.M., Ellerby, L.M., Ellerby, H.M., Naiem, S., Yaffe, M.P., Margoliash, E., Bredesen, D., Mauk, A.G., Sherman, F., and Newmeyer, D.D. (2000). Determinants of Cytochrome c Pro-apoptotic Activity.

Komatsu, M., Waguri, S., Chiba, T., Murata, S., Iwata, J., Tanida, I., Ueno, T., Koike, M., Uchiyama, Y., Kominami, E., and Tanaka, K. (2006). Loss of autophagy in the central nervous system causes neurodegeneration in mice. *Nature* 441**,** 880-884.

Korsmeyer, S.J., Wei, M.C., Saito, M., Weiler, S., Oh, K.J., and Schlesinger, P.H. (2000). Pro-apoptotic cascade activates BID, which oligomerizes BAK or BAX into pores that result in the release of cytochrome c. *Cell Death Differ* 7**,** 1166-1173.

Kothakota, S., Azuma, T., Reinhard, C., Klippel, A., Tang, J., Chu, K., Mcgarry, T.J., Kirschner, M.W., Koths, K., Kwiatkowski, D.J., and Williams, L.T. (1997). Caspase-3-generated fragment of gelsolin: effector of morphological change in apoptosis. *Science* 278**,** 294-298.

Krishan, A. (1975). Rapid flow cytofluorometric analysis of mammalian cell cycle by propidium iodide staining. *J Cell Biol* 66**,** 188-193.

Kroemer, G., Mariño, G., and Levine, B. (2010). Autophagy and the integrated stress response. *Mol Cell* 40**,** 280-293.

Kumar, S. (2007). Caspase function in programmed cell death. *Cell Death Differ* 14**,** 32-43.

Kun, Z., Hanqing, G., Hailing, T., Yuan, Y., Jun, Z., Lingxia, Z., Kun, H., and Xin, Z. (2017). Gastrin Enhances Autophagy and Promotes Gastric Carcinoma Proliferation via Inducing AMPKα. *Oncol Res* 25**,** 1399-1407.

Kuwana, T., Bouchier-Hayes, L., Chipuk, J.E., Bonzon, C., Sullivan, B.A., Green, D.R., and Newmeyer, D.D. (2005). BH3 domains of BH3-only proteins differentially regulate Bax-mediated mitochondrial membrane permeabilization both directly and indirectly. *Mol Cell* 17**,** 525-535.

Lakhani, S.A., Masud, A., Kuida, K., Porter, G.A., Jr., Booth, C.J., Mehal, W.Z., Inayat, I., and Flavell, R.A. (2006). Caspases 3 and 7: key mediators of mitochondrial events of apoptosis. *Science* 311**,** 847-851.

Lamkanfi, M., Declercq, W., Kalai, M., Saelens, X., and Vandenabeele, P. (2002). Alice in caspase land. A phylogenetic analysis of caspases from worm to man. *Cell Death Differ* 9**,** 358-361.

Lamy, L., Ngo, V.N., Emre, N.C., Shaffer, A.L., 3rd, Yang, Y., Tian, E., Nair, V., Kruhlak, M.J., Zingone, A., Landgren, O., and Staudt, L.M. (2013). Control of autophagic cell death by caspase-10 in multiple myeloma. *Cancer Cell* 23**,** 435-449.

Larsen, B.D., Rampalli, S., Burns, L.E., Brunette, S., Dilworth, F.J., and Megeney, L.A. (2010). "Caspase 3/caspase-activated DNase promote cell differentiation by

inducing DNA strand breaks," in *Proc Natl Acad Sci U S A*. (United States), 4230-4235.

Le Rhun, Y., Kirkland, J.B., and Shah, G.M. (1998). Cellular responses to DNA damage in the absence of Poly(ADP-ribose) polymerase. *Biochem Biophys Res Commun* 245**,** 1-10.

Lebovitz, C.B., Robertson, A.G., Goya, R., Jones, S.J., Morin, R.D., Marra, M.A., and Gorski, S.M. (2015). Cross-cancer profiling of molecular alterations within the human autophagy interaction network. *Autophagy* 11**,** 1668-1687.

Letai, A., Bassik, M.C., Walensky, L.D., Sorcinelli, M.D., Weiler, S., and Korsmeyer, S.J. (2002). Distinct BH3 domains either sensitize or activate mitochondrial apoptosis, serving as prototype cancer therapeutics. *Cancer Cell* 2**,** 183-192.

Levine, B., and Kroemer, G. (2008). Autophagy in the pathogenesis of disease. *Cell* 132**,** 27-42.

Levine, B., and Kroemer, G. (2019). Biological Functions of Autophagy Genes: A Disease Perspective. *Cell* 176**,** 11-42.

Levy, J.M.M., and Thorburn, A. (2011). Targeting autophagy during cancer therapy to improve clinical outcomes. *Pharmacol Ther* 131**,** 130-141.

Levy, J.M.M., and Thorburn, A. (2020). Autophagy in cancer: moving from understanding mechanism to improving therapy responses in patients. *Cell Death Differ* 27**,** 843-857.

Levy, J.M.M., Towers, C.G., and Thorburn, A. (2017). Targeting autophagy in cancer. *Nat Rev Cancer* 17**,** 528-542.

Li, F., Huang, Q., Chen, J., Peng, Y., Roop, D.R., Bedford, J.S., and Li, C.Y. (2010). Apoptotic cells activate the "phoenix rising" pathway to promote wound healing and tissue regeneration. *Sci Signal* 3**,** ra13.

Li, J., Brieher, W.M., Scimone, M.L., Kang, S.J., Zhu, H., Yin, H., Von Andrian, U.H., Mitchison, T., and Yuan, J. (2007). Caspase-11 regulates cell migration by promoting Aip1-Cofilin-mediated actin depolymerization. *Nat Cell Biol* 9**,** 276-286.

Li, J., and Yuan, J. (2008). Caspases in apoptosis and beyond. *Oncogene* 27**,** 6194-6206.

Li, P., Nijhawan, D., Budihardjo, I., Srinivasula, S.M., Ahmad, M., Alnemri, E.S., and Wang, X. (1997). Cytochrome c and dATP-dependent formation of Apaf-1/caspase-9 complex initiates an apoptotic protease cascade. *Cell* 91**,** 479-489.

Liang, C.C., Park, A.Y., and Guan, J.L. (2007). "In vitro scratch assay: a convenient and inexpensive method for analysis of cell migration in vitro," in *Nat Protoc*. (England), 329-333.

Liang, X.H., Jackson, S., Seaman, M., Brown, K., Kempkes, B., Hibshoosh, H., and Levine, B. (1999). Induction of autophagy and inhibition of tumorigenesis by beclin 1. *Nature* 402**,** 672-676.

Liu, Y., and Levine, B. (2015). Autosis and autophagic cell death: the dark side of autophagy. *Cell Death Differ* 22**,** 367-376.

Liu, Y., Shoji-Kawata, S., Sumpter, R.M., Jr., Wei, Y., Ginet, V., Zhang, L., Posner, B., Tran, K.A., Green, D.R., Xavier, R.J., Shaw, S.Y., Clarke, P.G., Puyal, J., and Levine, B. (2013). Autosis is a Na+,K+-ATPase-regulated form of cell death triggered by autophagy-inducing peptides, starvation, and hypoxia-ischemia. *Proc Natl Acad Sci U S A* 110**,** 20364-20371.

Lockshin, R.A. (1969). Programmed cell death. Activation of lysis by a mechanism involving the synthesis of protein. *J Insect Physiol* 15**,** 1505-1516.

Lockshin, R.A., and Williams, C.M. (1964). Programmed cell death. II. Endocrine potentiation of the breakdown of the intersegmental muscles of silkmoths. *J Insect Physiol* 10**,** 643-649.

Lum, J.J., Bauer, D.E., Kong, M., Harris, M.H., Li, C., Lindsten, T., and Thompson, C.B. (2005). Growth factor regulation of autophagy and cell survival in the absence of apoptosis. *Cell* 120**,** 237-248.

Luo, S., and Rubinsztein, D.C. (2007). Atg5 and Bcl-2 provide novel insights into the interplay between apoptosis and autophagy. *Cell Death Differ* 14**,** 1247-1250.

Luthi, A.U., and Martin, S.J. (2007). The CASBAH: a searchable database of caspase substrates. *Cell Death Differ* 14**,** 641-650.

Mahrus, S., Trinidad, J.C., Barkan, D.T., Sali, A., Burlingame, A.L., and Wells, J.A. (2008). Global sequencing of proteolytic cleavage sites in apoptosis by specific labeling of protein N termini. *Cell* 134**,** 866-876.

Maiuri, M.C., Zalckvar, E., Kimchi, A., and Kroemer, G. (2007). Self-eating and self-killing: crosstalk between autophagy and apoptosis. *Nat Rev Mol Cell Biol* 8**,** 741-752.

Maria B. Witte, M., and Adrian Barbul, M., Facs (1997). GENERAL PRINCIPLES OF WOUNDHEALING. 77**,** 509–528.

Masui, A., Hamada, M., Kameyama, H., Wakabayashi, K., Takasu, A., Imai, T., Iwai, S., and Yura, Y. (2016). Autophagy as a Survival Mechanism for Squamous Cell Carcinoma Cells in Endonuclease G-Mediated Apoptosis. *PLoS One* 11**,** e0162786.

Matthias Krause, Erik W. Dent, James E. Bear, Joseph J. Loureiro, A., and Gertler, F.B. (2003). ENA/VASP PROTEINS: Regulators of the Actin Cytoskeleton and Cell Migration. *http://dx.doi.org/10.1146/annurev.cellbio.19.050103.103356*.

Mattila, E., Pellinen, T., Nevo, J., Vuoriluoto, K., Arjonen, A., and Ivaska, J. (2005). Negative regulation of EGFR signalling through integrin-alpha1beta1-mediated activation of protein tyrosine phosphatase TCPTP. *Nat Cell Biol* 7**,** 78-85.

Mcilwain, D.R., Berger, T., and Mak, T.W. (2015). Caspase functions in cell death and disease. *Cold Spring Harb Perspect Biol* 7.

Mizushima, N. (2007). Autophagy: process and function. *Genes Dev* 21**,** 2861-2873.

Mizushima, N., and Komatsu, M. (2011). Autophagy: renovation of cells and tissues. *Cell* 147**,** 728-741.

Morales, A.A., Gutman, D., Lee, K.P., and Boise, L.H. (2008). BH3-only proteins Noxa, Bmf, and Bim are necessary for arsenic trioxide-induced cell death in myeloma. *Blood* 111**,** 5152-5162.

Mukherjee, A., and Williams, D.W. (2017). More alive than dead: non-apoptotic roles for caspases in neuronal development, plasticity and disease. *Cell Death Differ* 24**,** 1411-1421.

Munoz, J., Zhou, Y., and Jarrett, H.W. (2010). LG4-5 domains of laminin-211 binds alpha-dystroglycan to allow myotube attachment. *J Cell Physiol* 222**,** 111-119.

Nahta, R., and O'regan, R.M. (2010). Evolving strategies for overcoming resistance to HER2-directed therapy: targeting the PI3K/Akt/mTOR pathway. *Clin Breast Cancer* 10 Suppl 3**,** S72-78.

Nassour, J., Radford, R., Correia, A., Fusté, J.M., Schoell, B., Jauch, A., Shaw, R.J., and Karlseder, J. (2019). Autophagic cell death restricts chromosomal instability during replicative crisis. *Nature* 565**,** 659-663.

Natsumeda, M., Aoki, H., Miyahara, H., Yajima, N., Uzuka, T., Toyoshima, Y., Kakita, A., Takahashi, H., and Fujii, Y. (2011). Induction of autophagy in temozolomide treated malignant gliomas. *Neuropathology* 31**,** 486-493.

Nicholson, D.W., Ali, A., Thornberry, N.A., Vaillancourt, J.P., Ding, C.K., Gallant, M., Gareau, Y., Griffin, P.R., Labelle, M., Lazebnik, Y.A., and Et Al. (1995). Identification and inhibition of the ICE/CED-3 protease necessary for mammalian apoptosis. *Nature* 376**,** 37-43.

Nirmala, J.G., and Lopus, M. (2020). Cell death mechanisms in eukaryotes. 36**,** 145-164.

Noda, N.N., and Inagaki, F. (2015). Mechanisms of Autophagy. *Annu Rev Biophys* 44**,** 101-122.

Norman, J.M., Cohen, G.M., and Bampton, E.T. (2010). The in vitro cleavage of the hAtg proteins by cell death proteases. *Autophagy* 6**,** 1042-1056.

O'donovan, N., Crown, J., Stunell, H., Hill, A.D., Mcdermott, E., O'higgins, N., and Duffy, M.J. (2003). Caspase 3 in breast cancer. *Clin Cancer Res* 9**,** 738-742.

Opipari, A.W., Jr., Tan, L., Boitano, A.E., Sorenson, D.R., Aurora, A., and Liu, J.R. (2004). Resveratrol-induced autophagocytosis in ovarian cancer cells. *Cancer Res* 64**,** 696-703.

Otomo, C., Metlagel, Z., Takaesu, G., and Otomo, T. (2013). Structure of the human ATG12~ATG5 conjugate required for LC3 lipidation in autophagy. *Nat Struct Mol Biol* 20**,** 59-66.

Pagliarini, V., Wirawan, E., Romagnoli, A., Ciccosanti, F., Lisi, G., Lippens, S., Cecconi, F., Fimia, G.M., Vandenabeele, P., Corazzari, M., and Piacentini, M. (2012). Proteolysis of Ambra1 during apoptosis has a role in the inhibition of the autophagic pro-survival response. *Cell Death Differ* 19**,** 1495-1504.

Pan, M., Yin, Y., Wang, X., Wang, Q., and Zhang, L. (2020). Mice deficient in UXT exhibit retinitis pigmentosa-like features via aberrant autophagy activation. 1-16.

Pankov, R., and Yamada, K.M. (2002a). Fibronectin at a glance. *J Cell Sci* 115**,** 3861-3863.

Pankov, R., and Yamada, K.M. (2002b). Fibronectin at a glance.

Patel, V., Balakrishnan, K., Keating, M.J., Wierda, W.G., and Gandhi, V. (2015). Expression of executioner procaspases and their activation by a procaspase-activating compound in chronic lymphocytic leukemia cells. *Blood* 125**,** 1126-1136.

Pattingre, S., Tassa, A., Qu, X., Garuti, R., Liang, X.H., Mizushima, N., Packer, M., Schneider, M.D., and Levine, B. (2005). Bcl-2 antiapoptotic proteins inhibit Beclin 1-dependent autophagy. *Cell* 122**,** 927-939.

Pihán, P., Carreras-Sureda, A., and Hetz, C. (2017). BCL-2 family: integrating stress responses at the ER to control cell demise. *Cell Death Differ* 24**,** 1478-1487.

Plow, E.F., Haas, T.A., Zhang, L., Loftus, J., and Smith, J.W. (2000). Ligand binding to integrins. *J Biol Chem* 275**,** 21785-21788.

Ponder, K.G., and Boise, L.H. (2019). The prodomain of caspase-3 regulates its own removal and caspase activation. *Cell Death Discov* 5**,** 56.

Pop, C., Timmer, J., Sperandio, S., and Salvesen, G.S. (2006). The apoptosome activates caspase-9 by dimerization. *Mol Cell* 22**,** 269-275.

Qu, X., Yu, J., Bhagat, G., Furuya, N., Hibshoosh, H., Troxel, A., Rosen, J., Eskelinen, E.L., Mizushima, N., Ohsumi, Y., Cattoretti, G., and Levine, B. (2003). Promotion of tumorigenesis by heterozygous disruption of the beclin 1 autophagy gene. *J Clin Invest* 112**,** 1809-1820.

Ravikumar, B., Berger, Z., Vacher, C., O'kane, C.J., and Rubinsztein, D.C. (2006). Rapamycin pre-treatment protects against apoptosis. *Hum Mol Genet* 15**,** 1209-1216.

Ravikumar, B., Moreau, K., Jahreiss, L., Puri, C., and Rubinsztein, D.C. (2010). Plasma membrane contributes to the formation of pre-autophagosomal structures. *Nat Cell Biol* 12**,** 747-757.

Reed, J.C., and Tomaselli, K.J. (2000). Drug discovery opportunities from apoptosis research. *Curr Opin Biotechnol* 11**,** 586-592.

Renatus, M., Stennicke, H.R., Scott, F.L., Liddington, R.C., and Salvesen, G.S. (2001). Dimer formation drives the activation of the cell death protease caspase 9. *Proc Natl Acad Sci U S A* 98**,** 14250-14255.

Ridley, A.J., Schwartz, M.A., Burridge, K., Firtel, R.A., Ginsberg, M.H., Borisy, G., Parsons, J.T., and Horwitz, A.R. (2003). Cell migration: integrating signals from front to back. *Science* 302**,** 1704-1709.

Riedl, S.J., and Salvesen, G.S. (2007). The apoptosome: signalling platform of cell death. *Nat Rev Mol Cell Biol* 8**,** 405-413.

Rodriguez, J., and Lazebnik, Y. (1999). Caspase-9 and APAF-1 form an active holoenzyme. *Genes Dev* 13**,** 3179-3184.

Roos, W.P., Thomas, A.D., and Kaina, B. (2016). DNA damage and the balance between survival and death in cancer biology. *Nat Rev Cancer* 16**,** 20-33.

Rosenfeldt, M.T., O'prey, J., Morton, J.P., Nixon, C., Mackay, G., Mrowinska, A., Au, A., Rai, T.S., Zheng, L., Ridgway, R., Adams, P.D., Anderson, K.I., Gottlieb, E., Sansom, O.J., and Ryan, K.M. (2013). p53 status determines the role of autophagy in pancreatic tumour development. *Nature* 504**,** 296-300.

Rothbart, S.B., Racanelli, A.C., and Moran, R.G. (2010). Pemetrexed indirectly activates the metabolic kinase AMPK in human carcinomas. *Cancer Res* 70**,** 10299-10309.

Ryan, J., Montero, J., Rocco, J., and Letai, A. (2016). iBH3: simple, fixable BH3 profiling to determine apoptotic priming in primary tissue by flow cytometry. 397**,** 671-678.

Sahu, R., Kaushik, S., Clement, C.C., Cannizzo, E.S., Scharf, B., Follenzi, A., Potolicchio, I., Nieves, E., Cuervo, A.M., and Santambrogio, L. (2011). Microautophagy of cytosolic proteins by late endosomes. *Dev Cell* 20**,** 131-139.

Salvesen, G.S., and Ashkenazi, A. (2011). Snapshot: caspases. *Cell* 147**,** 476-476.e471.

Saunders, J.W., Jr. (1966). Death in embryonic systems. *Science* 154**,** 604-612.

Scharner, D., Rössig, L., Carmona, G., Chavakis, E., Urbich, C., Fischer, A., Kang, T.B., Wallach, D., Chiang, Y.J., Deribe, Y.L., Dikic, I., Zeiher, A.M., and Dimmeler, S. (2009). Caspase-8 is involved in neovascularization-promoting progenitor cell functions. *Arterioscler Thromb Vasc Biol* 29**,** 571-578.

Schneller, M., Vuori, K., and Ruoslahti, E. (1997). Alphavbeta3 integrin associates with activated insulin and PDGFbeta receptors and potentiates the biological activity of PDGF. *Embo j* 16**,** 5600-5607.

Schuck, S. (2020). Microautophagy - distinct molecular mechanisms handle cargoes of many sizes. *J Cell Sci* 133.

Scott, R.C., Juhász, G., and Neufeld, T.P. (2007). Direct induction of autophagy by Atg1 inhibits cell growth and induces apoptotic cell death. *Curr Biol* 17**,** 1-11.

Sebbagh, M., Renvoizé, C., Hamelin, J., Riché, N., Bertoglio, J., and Bréard, J. (2001). Caspase-3-mediated cleavage of ROCK I induces MLC phosphorylation and apoptotic membrane blebbing. *Nat Cell Biol* 3**,** 346-352.

Senft, J., Helfer, B., and Frisch, S.M. (2007). Caspase-8 interacts with the p85 subunit of phosphatidylinositol 3-kinase to regulate cell adhesion and motility. *Cancer Res* 67**,** 11505-11509.

Shalini, S., Dorstyn, L., Dawar, S., and Kumar, S. (2015). Old, new and emerging functions of caspases. *Cell Death Differ* 22**,** 526-539.

Shao, Y., Gao, Z., Marks, P.A., and Jiang, X. (2004). Apoptotic and autophagic cell death induced by histone deacetylase inhibitors. *Proc Natl Acad Sci U S A* 101**,** 18030-18035.

Shi, Y. (2002). Mechanisms of caspase activation and inhibition during apoptosis. *Mol Cell* 9**,** 459-470.

Shimizu, S., Kanaseki, T., Mizushima, N., Mizuta, T., Arakawa-Kobayashi, S., Thompson, C.B., and Tsujimoto, Y. (2004). Role of Bcl-2 family proteins in a non-apoptotic programmed cell death dependent on autophagy genes. *Nat Cell Biol* 6**,** 1221-1228.

Shimizu, S., Konishi, A., Nishida, Y., Mizuta, T., Nishina, H., Yamamoto, A., and Tsujimoto, Y. (2010). Involvement of JNK in the regulation of autophagic cell death. *Oncogene* 29**,** 2070-2082.

Singh, R., Letai, A., and Sarosiek, K. (2019). Regulation of apoptosis in health and disease: the balancing act of BCL-2 family proteins. 20**,** 175-193.

Slee, E.A., Harte, M.T., Kluck, R.M., Wolf, B.B., Casiano, C.A., Newmeyer, D.D., Wang, H.G., Reed, J.C., Nicholson, D.W., Alnemri, E.S., Green, D.R., and Martin, S.J. (1999). Ordering the cytochrome c-initiated caspase cascade: hierarchical activation of caspases-2, -3, -6, -7, -8, and -10 in a caspase-9-dependent manner. *J Cell Biol* 144**,** 281-292.

Song, S., Tan, J., Miao, Y., Li, M., and Zhang, Q. (2017). Crosstalk of autophagy and apoptosis: Involvement of the dual role of autophagy under ER stress. 232**,** 2977-2984.

Srinivasula, S.M., Ahmad, M., Fernandes-Alnemri, T., and Alnemri, E.S. (1998). Autoactivation of procaspase-9 by Apaf-1-mediated oligomerization. *Mol Cell* 1**,** 949-957.

Stennicke, H.R., Deveraux, Q.L., Humke, E.W., Reed, J.C., Dixit, V.M., and Salvesen, G.S. (1999). Caspase-9 can be activated without proteolytic processing. *J Biol Chem* 274**,** 8359-8362.

Stolz, A., Ernst, A., and Dikic, I. (2014). Cargo recognition and trafficking in selective autophagy. *Nat Cell Biol* 16**,** 495-501.

Sun, Q., Gao, W., Loughran, P., Shapiro, R., Fan, J., Billiar, T.R., and Scott, M.J. (2013). Caspase 1 activation is protective against hepatocyte cell death by up-regulating beclin 1 protein and mitochondrial autophagy in the setting of redox stress. *J Biol Chem* 288**,** 15947-15958.

Tait, S.W., and Green, D.R. (2010). Mitochondria and cell death: outer membrane permeabilization and beyond. *Nat Rev Mol Cell Biol* 11**,** 621-632.

Takamura, A., Komatsu, M., Hara, T., Sakamoto, A., Kishi, C., Waguri, S., Eishi, Y., Hino, O., Tanaka, K., and Mizushima, N. (2011). Autophagy-deficient mice develop multiple liver tumors. *Genes Dev* 25**,** 795-800.

Tang, D., Kang, R., Berghe, T.V., Vandenabeele, P., and Kroemer, G. (2019). The molecular machinery of regulated cell death. 29**,** 347-364.

Tata, J.R. (1966). Requirement for RNA and protein synthesis for induced regression of the tadpole tail in organ culture. *Dev Biol* 13**,** 77-94.

Taylor, R.C., Cullen, S.P., and Martin, S.J. (2008). Apoptosis: controlled demolition at the cellular level. *Nat Rev Mol Cell Biol* 9**,** 231-241.

Tewari, M., Quan, L.T., O'rourke, K., Desnoyers, S., Zeng, Z., Beidler, D.R., Poirier, G.G., Salvesen, G.S., and Dixit, V.M. (1995). Yama/CPP32 beta, a mammalian homolog of CED-3, is a CrmA-inhibitable protease that cleaves the death substrate poly(ADP-ribose) polymerase. *Cell* 81**,** 801-809.

Thornberry, N.A., Bull, H.G., Calaycay, J.R., Chapman, K.T., Howard, A.D., Kostura, M.J., Miller, D.K., Molineaux, S.M., Weidner, J.R., Aunins, J., and Et Al. (1992). A novel heterodimeric cysteine protease is required for interleukin-1 beta processing in monocytes. *Nature* 356**,** 768-774.

Tiwari, M., Lopez-Cruzan, M., Morgan, W.W., and Herman, B. (2011). Loss of caspase-2-dependent apoptosis induces autophagy after mitochondrial oxidative stress in primary cultures of young adult cortical neurons. *J Biol Chem* 286**,** 8493-8506.

Totsukawa, G., Wu, Y., Sasaki, Y., Hartshorne, D.J., Yamakita, Y., Yamashiro, S., and Matsumura, F. (2004). "Distinct roles of MLCK and ROCK in the regulation of membrane protrusions and focal adhesion dynamics during cell migration of fibroblasts," in *J Cell Biol*. (United States: The Rockefeller University Press), 427-439.

Tsapras, P., and Nezis, I.P. (2017). Caspase involvement in autophagy. *Cell Death Differ* 24**,** 1369-1379.

Tseng, A.S., Adams, D.S., Qiu, D., Koustubhan, P., and Levin, M. (2007). "Apoptosis is required during early stages of tail regeneration in Xenopus laevis," in *Dev Biol*. (United States), 62-69.

Ubellacker, J.M., Tasdogan, A., Ramesh, V., Shen, B., Mitchell, E.C., Martin-Sandoval, M.S., Gu, Z., Mccormick, M.L., Durham, A.B., Spitz, D.R., Zhao, Z., Mathews, T.P., and Morrison, S.J. (2020). Lymph protects metastasizing melanoma cells from ferroptosis. *Nature* 585**,** 113-118.

Unsain, N., and Barker, P.A. (2015). New Views on the Misconstrued: Executioner Caspases and Their Diverse Non-apoptotic Roles. *Neuron* 88**,** 461-474.

Uttenweiler, A., and Mayer, A. (2008). Microautophagy in the yeast Saccharomyces cerevisiae. *Methods Mol Biol* 445**,** 245-259.

Van Opdenbosch, N., and Lamkanfi, M. (2019). Caspases in Cell Death, Inflammation, and Disease. *Immunity* 50**,** 1352-1364.

Vlahakis, A., and Debnath, J. (2017). The Interconnections between Autophagy and Integrin-Mediated Cell Adhesion. *J Mol Biol* 429**,** 515-530.

Walsh, J.G., Cullen, S.P., Sheridan, C., Lüthi, A.U., Gerner, C., and Martin, S.J. (2008). Executioner caspase-3 and caspase-7 are functionally distinct proteases. *Proc Natl Acad Sci U S A* 105**,** 12815-12819.

Wang, Y., Zhang, N., Zhang, L., Li, R., Fu, W., Ma, K., Li, X., Wang, L., Wang, J., Zhang, H., Gu, W., Zhu, W.G., and Zhao, Y. (2016). Autophagy Regulates Chromatin Ubiquitination in DNA Damage Response through Elimination of SQSTM1/p62. *Mol Cell* 63**,** 34-48.

Wei, M.C., Zong, W.X., Cheng, E.H., Lindsten, T., Panoutsakopoulou, V., Ross, A.J., Roth, K.A., Macgregor, G.R., Thompson, C.B., and Korsmeyer, S.J. (2001). Proapoptotic BAX and BAK: a requisite gateway to mitochondrial dysfunction and death. *Science* 292**,** 727-730.

Williams, D.W., Kondo, S., Krzyzanowska, A., Hiromi, Y., and Truman, J.W. (2006). "Local caspase activity directs engulfment of dendrites during pruning," in *Nat Neurosci*. (United States), 1234-1236.

Woo, M., Hakem, R., Soengas, M.S., Duncan, G.S., Shahinian, A., Kägi, D., Hakem, A., Mccurrach, M., Khoo, W., Kaufman, S.A., Senaldi, G., Howard, T., Lowe, S.W., and Mak, T.W. (1998). Essential contribution of caspase 3/CPP32 to apoptosis and its associated nuclear changes. *Genes Dev* 12**,** 806-819.

Wu, L., Birle, D.C., and Tannock, I.F. (2005). Effects of the mammalian target of rapamycin inhibitor CCI-779 used alone or with chemotherapy on human prostate cancer cells and xenografts. *Cancer Res* 65**,** 2825-2831.

Wyllie, A.H. (1980). Glucocorticoid-induced thymocyte apoptosis is associated with endogenous endonuclease activation. *Nature* 284**,** 555-556.

Xue, D., Shaham, S., and Horvitz, H.R. (1996). The Caenorhabditis elegans cell-death protein CED-3 is a cysteine protease with substrate specificities similar to those of the human CPP32 protease. *Genes Dev* 10**,** 1073-1083.

Yang, Y., and Klionsky, D.J. (2020). Autophagy and disease: unanswered questions. *Cell Death Differ* 27**,** 858-871.

Yi, C.H., and Yuan, J. (2009). The Jekyll and Hyde functions of caspases. *Dev Cell* 16**,** 21-34.

Yoo, N.J., Kim, H.S., Kim, S.Y., Park, W.S., Kim, S.H., Lee, J.Y., and Lee, S.H. (2002). Stomach cancer highly expresses both initiator and effector caspases; an immunohistochemical study. *Apmis* 110**,** 825-832.

Youle, R.J., and Strasser, A. (2008). The BCL-2 protein family: opposing activities that mediate cell death. *Nat Rev Mol Cell Biol* 9**,** 47-59.

Yousefi, S., Perozzo, R., Schmid, I., Ziemiecki, A., Schaffner, T., Scapozza, L., Brunner, T., and Simon, H.U. (2006). Calpain-mediated cleavage of Atg5 switches autophagy to apoptosis. *Nat Cell Biol* 8**,** 1124-1132.

Yu, L., Alva, A., Su, H., Dutt, P., Freundt, E., Welsh, S., Baehrecke, E.H., and Lenardo, M.J. (2004). Regulation of an ATG7-beclin 1 program of autophagic cell death by caspase-8. *Science* 304**,** 1500-1502.

Yu, L., Wan, F., Dutta, S., Welsh, S., Liu, Z., Freundt, E., Baehrecke, E.H., and Lenardo, M. (2006). Autophagic programmed cell death by selective catalase degradation. *Proc Natl Acad Sci U S A* 103**,** 4952-4957.

Yu, T., Wang, X., Purring-Koch, C., Wei, Y., and Mclendon, G.L. (2001). A Mutational Epitope for Cytochrome c Binding to the Apoptosis Protease Activation Factor-1.

Yuan, J., and Horvitz, H.R. (1992). The Caenorhabditis elegans cell death gene ced-4 encodes a novel protein and is expressed during the period of extensive programmed cell death. *Development* 116**,** 309-320.

Yuan, J., Shaham, S., Ledoux, S., Ellis, H.M., and Horvitz, H.R. (1993). The C. elegans cell death gene ced-3 encodes a protein similar to mammalian interleukin-1 beta-converting enzyme. *Cell* 75**,** 641-652.

Zhou, B., Liu, J., Kang, R., Klionsky, D.J., Kroemer, G., and Tang, D. (2019). Ferroptosis is a type of autophagy-dependent cell death. *Semin Cancer Biol*.

Zhu, Y., Zhao, L., Liu, L., Gao, P., Tian, W., Wang, X., Jin, H., Xu, H., and Chen, Q. (2010). Beclin 1 cleavage by caspase-3 inactivates autophagy and promotes apoptosis. *Protein Cell* 1**,** 468-477.

Zou, H., Henzel, W.J., Liu, X., Lutschg, A., and Wang, X. (1997). Apaf-1, a human protein homologous to C. elegans CED-4, participates in cytochrome c-dependent activation of caspase-3. *Cell* 90**,** 405-413.